INTER-INDIVIDUAL VARIABILITY IN DNA DAMAGE AND EPIGENETIC EFFECTS IN RESPONSE TO 1,3-BUTADIENE

A Dissertation

by

LAUREN ANNE LEWIS

Submitted to the Office of Graduate and Professional Studies of
Texas A&M University
in partial fulfillment of the requirements for the degree of

DOCTOR OF PHILOSOPHY

Chair of Committee,	Ivan Rusyn
Committee Members,	Candice Brinkmeyer-Langford
	Igor P. Pogribny
	David W. Threadgill
Head of Department,	Larry J. Suva

December 2019

Major Subject: Toxicology

Copyright 2019 Lauren Anne Lewis

ABSTRACT

Exposure to environmental and occupational chemicals can result in human disease which may be driven by genotoxicity and epigenetic alterations. In addition, genetic variants and sex-specific differences in epigenetic modifications and DNA damage may also influence chemical-induced adverse health effects. *Our overall objective is to investigate inter-individual variability in epigenetic alterations and DNA damage in response to 1,3-butadiene, a model genotoxic carcinogen and industrial toxicant.* Although genotoxicity is an established mechanism of 1,3-butadiene carcinogenesis, epigenetic effects such as DNA methylation and histone modifications have also been reported. Importantly, inter-strain differences exist in both 1,3-butadiene-induced DNA damage and epigenetic effects in mice. Recent studies indicate that the variation in epigenetic alterations may be a key driver of the inter-individual susceptibility to 1,3-butadiene genotoxicity. First, we characterized inter-individual differences in 1,3-butadiene-induced DNA damage and epigenetic effects using a population-based model of Collaborative Cross mouse strains. We observed strain- and tissue-dependent variability of 1,3-butadiene-induced epigenetic alterations which may influence individual and organ susceptibility to carcinogenesis. Genetic mapping identified several candidate genes that may play a role in individual differences in global histone modifications. Second, we investigated sex-specific effects in response to 1,3-butadiene. Strain- and tissue-specific differences in DNA damage and global epigenetic alterations were detected. Third, we evaluated the expression of microRNA in order to better understand the mechanisms by which 1,3-butadiene alters the epigenome as well as the transcriptome. We observed strain- and tissue-specific

expression profiles of microRNA. Furthermore, we identified microRNA as candidate master regulators of differential gene expression across strains and tissues. Overall, our work contributes to a better understanding of inter-individual variability in response to chemical exposure which is a critical need in hazard and risk assessment.

ACKNOWLEDGEMENTS

I would like to thank my advisor, Dr. Ivan Rusyn for letting me join his research group. Although I did not set out to be a toxicologist in the beginning of graduate school, I am very thankful that I found my way to his lab and the Texas A&M Interdisciplinary Faculty of Toxicology doctoral program. I am also very grateful for Drs. Igor Pogribny, Candice Brinkmeyer-Langford, and David Threadgill for serving on my dissertation committee and providing me with guidance on my doctoral research projects.

I would like to thank the past and present members of the Rusyn lab for their support. The "butadiene project" started many years before I joined the lab. My dissertation research was made possible because of the hard work of Dr. Grace Chappell, Dr. Tetyana Kobets, Bridget E. O'Brian, and Oksana Kosyk. I would also like to thank Drs. Joe Cichocki, Abhishek Venkatranam, Shinji Furuya, Hisataka "Taka" Fukushima, Yu-Syuan "Dave" Luo, and Courtney Sakolish. They were always willing to help with experiments, work through R scripts, break open file cabinets, or just make me an extremely strong cup of questionable coffee. I would also like to acknowledge Zunwei Chen for all of his help in the *in vitro* lab and for making Saturday assay days enjoyable.

I would like to acknowledge our coauthors Igor Pogribny, Natalia Y. Tretyakova, Oksana Kosyk, Dewakar Sangaraju, Wanda Bodnar, Barbara Borowa-Mazgaj, Aline de Conti, Grace Chappell, Yu-Syuan Luo, Kranti Konganti, Fred A. Wright, David W. Threadgill, Weihsueh A. Chiu, Jennifer Israel, Greg Keele, Bryan Quash, Gregory Crawford, and Terrence Furey. Without their contributions, this work would have not been possible. In addition, I am very grateful to Drs. Igor Pogribny, Aline de Conti, and Barbara

Borowa-Mazgaj for welcoming me into the Pogribny lab so I could learn and conduct global epigenetic experiments under their guidance.

CONTRIBUTORS AND FUNDING SOURCES

Contributors

This research was evaluated by a dissertation committee consisting of Professors Ivan Rusyn (advisor), Candice Brinkmeyer-Langford, Igor P. Pogribny, and David W. Threadgill.

The animal studies in this dissertation were conducted by former graduate students from the Rusyn lab at the University of North Carolina at Chapel Hill. Specifically, the animal studies in Chapter II and Chapter IV were organized by Dr. Grace A. Chappell. The animal study in Chapter III was facilitated by Bridget E. O'Brien. Oksana Kosyk, former manager of the Rusyn lab, was instrumental in all mouse studies conducted at the University of North Carolina at Chapel Hill.

In this dissertation, DNA adduct and DNA crosslink levels were measured in collaboration with Drs. Wanda Bodnar at the University of North Carolina at Chapel Hill and Natalia Tretykova at the University of Minnesota. In addition, global epigenetic experiments were conducted in collaboration with Dr. Igor P. Pogribny at the National Center for Toxicological Research. All other work completed for this dissertation was completed by the student independently.

Funding Sources

Graduate study was supported, in part, by grants from the National Institute of Environmental Health Sciences (R01 ES023195, R01 CA095039, P30 ES025128 and R01 ES029911). Supplemental training was made possible by awards from the Society of Toxicology and Texas A&M College of Veterinary Medicine and Biomedical Sciences.

NOMENCLATURE

ATAC-seq	Assay for Transposase Accessible Chromatin
IARC	International Agency for Research on Cancer
LINE	Long Interspersed Nuclear Element
miRNA	microRNA
mRNA	Messenger RNA
QTL mapping	Quantitative Trait Loci mapping
RNA-seq	RNA sequencing
SINE	Short Interspersed Nuclear Element
THB-Gua	N-7-(2,3,4-trihydroxybut-1-yl)-guanine

TABLE OF CONTENTS

Page

LIST OF FIGURES

Page

LIST OF TABLES

Page

CHAPTER I

INTRODUCTION: GENETIC AND EPIGENETIC DETERMINANTS OF INTER-INDIVIDUAL VARIABILITY IN RESPONSES TO TOXICANTS[1]

1.1 Overview

It is well established that genetic variability has a major impact on susceptibility to common diseases, responses to drugs and toxicants, and influences disease-related outcomes. The appreciation that epigenetic marks also vary across the population is growing with more data becoming available from studies in humans and model organisms. In addition, the links between genetic variability, toxicity outcomes and epigenetics are being actively explored. Recent studies demonstrate that gene-by-environment interactions involve both chromatin states and transcriptional regulation, and that epigenetics provides important mechanistic clues to connect expression-related quantitative trait loci (QTL) and disease outcomes. Furthermore, sex-specific differences in response to chemical exposure may also play a role in individual susceptibility to disease development. We propose that assessment of global epigenetic changes and levels of DNA adducts is necessary to sufficiently characterize epigenetic alterations and genotoxicity in the context of understanding the inter-individual variability in responses to toxicants.

[1]Text from sections 1.1 to 1.4 of this chapter is an Author's Original Manuscript reprinted with permission from an article published by Elsevier in Current Opinion in Toxicology on 12 September 2017, available online: https://doi.org/10.1016/j.cotox.2017.08.006

1.2 Genetic Variability

Estimation of the degree of inter-individual variability in the population is a required step in assessing the human health hazard posed by environmental chemicals. Indeed, the National Academies report *Science and Decisions* [1] called for the need to better "*account for differences among humans in cancer susceptibility other than from possible early-life susceptibility.*" Recent advances in the ability to conduct genome-wide association studies (GWAS) that identify quantitative trait loci (QTL) have enabled identification of genetic variants associated with important diseases [2]. It is clear that genetic variation influences the response of an individual to drugs and chemicals [3]. The blossoming field of personalized medicine now brings GWAS-enabled understanding of basic biology into clinical practice to determine how the knowledge of genetic variation can make therapies safer and more effective by tailoring selection and dosing of drugs for an individual patient [4].

GWAS that characterize effects of environmental toxicants on humans are usually based on epidemiological data, not controlled exposures [5]. This makes it a challenge to interpret findings from human cohorts exposed in the occupational or environmental settings. In addition, collection of tissues (with the exception of blood) from a wide variety of anatomical sites or developmental stages is not possible in humans that have been exposed to environmental toxicants. These limitations can be alleviated, at least partially, by the use of appropriate genetically-diverse laboratory animal-based model systems [6].

The mouse is a popular *in vivo* model for which genetic resources with publicly available genetic maps across dozens of strains are now available [7]. Mouse populations, such as the Collaborative Cross [8], provide an excellent testing system for evaluation of complexities in toxicokinetics and toxicodynamics [6, 9-11]. In the past decade, it has been demonstrated convincingly that genetic diversity in the mouse can be used to identify sensitive sub-populations using a mouse model of the human population approach [12-25]. Most of the genetic variability among mouse strains has been focused on SNPs; however, variation in structure of DNA regions affecting DNA sequence length and/or orientation that includes deletions, insertions, copy-number gains, inversions, and transposable elements, may also underpin susceptibility traits [26]. In addition, while inbred mouse strains are considered isogenic, intra-strain differences and their influence on experimental outcomes have been identified [27, 28].

While advances in sequencing technologies, statistical genetics analysis methods and clinical trial designs have shown promise for the discovery of variants associated with drug response, interpretation of both human and mouse GWAS through identifying causal variants is a challenge, and the translation of the findings to the clinic and/or regulatory actions is slow. On the one hand, it remains difficult to interpret the outcomes of GWAS and validate genes underlying QTLs with certainty, due in part to not knowing which organs, tissues, and/or cell types any particular QTL is having a significant functional effect. On the other hand, the GWAS-driven attempts to disentangle treatment responders from non-responders via genetic predictors in pharmacogenetics studies have not been uniformly successful [29].

1.3 Environmental agents cause toxicity through epigenetic mechanisms

Epigenetic reprogramming has been proposed as an integral part of the "genome instability" enabling characteristic of cancer cells [30] and it is well established that chemical carcinogens may affect the cellular epigenetic state [31]. Changes in DNA methylation, histone/chromatin remodeling, and altered expression of miRNAs represent the most frequently reported toxicant-induced alterations of the epigenome [32]. Because of the potential impact of these epigenotoxic effects on gene expression patterns and, consequently, on the toxicity phenotypes, epigenetic changes have been proposed as biomarkers of carcinogen exposure and effect [33, 34].

One of the first examples of the linkages between environment, epigenetics and phenotypes were studies of *in utero* exposure to environmental agents that can also disrupt the epigenome. The agouti mouse model was used to demonstrate that environmental factors may affect the fetal epigenome [35]. Using this mouse model, maternal exposure to the endocrine disruptor BPA causes loss of DNA methylation at key loci, resulting in a shift in coat color of offspring [36]. Normal methylation patterns can then be restored with maternal dietary supplementation using methyl donors like folic acid. Evidence shows along with DNA methylation, variable histone modifications affect the inter-individual epigenetic variation of this metastable epiallele [37].

Another prominent example of how environmental toxicants may have epigenetic effects are studies on the mechanism of carcinogenesis for metals [38]. Arsenic, a ubiquitous

environmental contaminant, disrupts the normal epigenome transforming the epigenetic landscape to reflect that of a cancer cell [39]. Exposure to metals like arsenic causes significant epigenetic modifications such as changes in global histone methylation levels [40]. After exposure to arsenic compounds, human lung carcinoma A549 cells showed an increase in global levels of H3K4me3 and H3K9me2 [41]. Similarly, human peripheral blood nuclear cells extracted from subjects exposed to high levels of arsenic in water had an increase in H3K9me2 levels [42].

Environmental contaminants can also alter gene expression by epigenetically reprogramming tissues. Neonatal BPA exposure increases H3K4me3 levels in promoters of genes associated with prostate cancer through activation of histone methyltransferase MLL1 [43]. Although there was no difference in basal expression of levels of BPA reprogrammed genes, once challenged with hormone treatment, there is enhanced gene-specific transcription. It is thought the change in levels of H3K4me3 primes these genes for an enhanced response. Additionally, evidence suggests that BPA exposure during prostate development could epigenetically reprogram the expression of *Scgb2a1* in the adult prostate [44].

Epigenetic changes may be a consequence of DNA damage [45], or may be part of the non-genotoxic mechanisms of carcinogenesis [46]. The interplay between chemical-induced DNA damage response and transcription, DNA replication, and repair has only recently been linked to chromatin dynamics, especially to histone modifications and post-repair chromatin restoration at the sites of DNA damage [47]. For example, a local response to DNA double-stranded breaks gives rise to chromatin condensation which spreads at

least over several Kb from the damage sites and can induce epigenetic silencing of the nearby genes [48]. In addition, it was shown that levels of the heterochromatin-associated histone modification H3K9me3 accounted for more than 40% of mutation rate variation, providing striking evidence that mutation rates in cancer genomes are related closely to chromatin organization [49]. Besides that, DNA repair can cause local chromatin state transitions eventually resulting in prolonged inactivation of transcription via not yet fully established gene silencing mechanisms. Modulation of the epigenetic status of damaged genes potentially expands the field of DNA damage into the sphere of regulation of gene expression [45]. While the interest in the role of epigenome in toxicity mechanisms is growing, the genotoxicity of chemicals has been more thoroughly studied and characterized, as evidenced by a systematic review of published studies of genotoxic carcinogens that investigated epigenetic endpoints [50].

DNA methylation is another key epigenetic mechanism, regulating both gene expression and chromatin stability. DNA methylation studies have been recently combined with RNA-seq and ChIP-seq to identify the role of the changes in the methylome in disease pathogenesis [51]. DNA methylation and genetic polymorphisms have important concomitant regulatory effects on transcription factor-driven gene expression [52]. Aberrant DNA methylation patterns due to exposure to environmental chemicals are also well-characterized. Exposure to benzene, metals, and traffic pollution are all examples of toxicants that can have an effect on DNA methylation [53-56].

1.4 Environmental effects on the epigenome in the context of genetic variability

There is now overwhelming evidence that connects genetic variability and epigenetic marks and that chemical exposures can exert toxicity through epigenetic mechanisms; yet less is known about how the effects on the epigenome may vary in the population. Intriguing novel insights into linkages between genotoxic and epigenetic mechanisms of carcinogenesis, and the role of genetic variability among individuals have been provided by studies of a classical genotoxic carcinogen 1,3-butadiene. It is a genotoxic chemical with DNA damaging effects that vary among genetically distinct individuals. 1,3-Butadiene is a major industrial chemical used in the production of synthetic rubbers and polymers. It is also a ubiquitous environmental contaminant that is found in cigarette smoke and automobile exhaust. IARC has classified 1,3-butadiene as a known human carcinogen [57]. It is well established that the mechanism of carcinogenicity is due to butadiene's reactive metabolites. These epoxides interact directly with DNA and form mutagenic DNA adducts. 1,3-Butadiene also elicits an epigenetic response, causing significant loss of global DNA methylation as well as a decrease in H3K9, H3K27, and H3K20 trimethylation in C57BL/6J mouse liver [58].

Using a mouse population-based model it was shown that inter-individual (*e.g.*, inter-strain) differences exist in both genotoxic and epigenotoxic effects of 1,3-butadiene exposure and that the chromatin remodeling response is at least one mechanism for the inter-strain differences in 1,3-butadiene-induced DNA damage [14]. Specifically, it was shown that 1,3-butadiene alters bulk chromatin histone mark levels resulting in strain-specific abundances of these marks. In particular, CAST/EiJ and C57BL/6J mice, two

genetically distinct strains, exhibited basal and treatment-induced differences in overall levels of these histone marks.

1.5 Environmental effects on the epigenome in the context of sex-specific differences

In general, sex-specific effects from environmental toxicant exposure are poorly characterized. This is supported by a recent systematic review of genotoxic human carcinogens that shows a deficiency in animal studies that examine sex-specific differences in epigenetic alterations caused by environmental agents[50]. Available studies focus on prenatal and *in utero* exposure to environmental chemicals[59].

1.6 Specific aims

In this dissertation, three specific aims were developed to characterize inter-individual variability in DNA damage and epigenetic effects in response to chemical exposure. In **specific aim 1**, we evaluate population variability in genotoxicity and global epigenetic alterations by using a population-based mouse model. **Specific aim 2** investigates sex-specific differences in DNA damage and epigenetic modifications. Lastly, **specific aim 3** characterizes strain- and tissue-specific expression of microRNA, an additional epigenetic endpoint, in response to chemical exposure.

<u>Specific aim 1:</u> To evaluate inter-individual differences in 1,3-butadiene-induced epigenetic alterations and DNA damage in a mouse population. *We hypothesized that DNA adducts and epigenetic effects will vary across strains.* In this aim, we used a panel

of recombinant mouse lines from the Collaborative Cross resource. We evaluated DNA damage by measuring DNA adduct levels and epigenetic effects by analyzing histone modifications and DNA methylation.

Specific aim 2: To investigate sex differences in genotoxic and epigenetic effects of 1,3-butadiene. *This aim will test the hypothesis that exposure to 1,3-butadiene will result in sex-specific effects in DNA damage and epigenetic modifications.* We used male and female C57BL/6J and CAST/EiJ mice to investigate epigenetic alterations by analyzing global histone modifications and DNA methylation changes.

Specific Aim 3: To characterize microRNA expression profiles in response to 1,3-butadiene exposure in mice. *We hypothesize that 1,3-butadiene-induced microRNA expression varies between strains and tissues.* To investigate strain-specific differences in microRNA expression in response to 1,3-butadiene exposure we will use male C57BL/6J and CAST/EiJ mice. We evaluated expression profiles in these two strains by Next Generation Sequencing technologies.

CHAPTER II

POPULATION-BASED ANALYSIS OF DNA DAMAGE AND EPIGENETIC EFFECTS OF 1,3-BUTADIENE IN THE MOUSE[2]

2.1 Introduction

Traditional toxicology studies in animals are conducted in a single strain and do not test for population variability, which is a critical need in human health risk assessment.[9] A mouse population-based approach provides data on the variability in responses to chemicals at the population level.[6] Indeed, studies that use multiple strains to model genetic diversity have successfully demonstrated the utility of the population-based approach for investigating inter-individual variability in toxicity and metabolism.[60-62]

In the past decade, several genetically diverse mouse reference populations were created, including the Collaborative Cross.[63, 64] The Collaborative Cross mouse genetic reference population is derived from eight founder strains and represents 90% of the genetic variation in laboratory mice.[65] This recombinant inbred panel of strains aims to replicate the genetic heterogeneity of the human population[66] and can be effectively used for quantitative trait loci (QTL) mapping because of their balanced allele frequencies.[8] Previous studies using Collaborative Cross mice have identified genetic determinants for disease susceptibility, biological pathways, and complex traits.[67-70]

An increasing number of toxicology studies are using the Collaborative Cross mouse population to evaluate inter-individual variability in susceptibility to toxicity.[10, 71-75] The population-wide approach allows for better understanding of gene×environment

[2]The text of this chapter is an Author's Original Manuscript reprinted with permission from an article published by the American Chemical Society in Chemical Research in Toxicology on 16 April 2019, available online: https://doi.org/10.1021/acs.chemrestox.9b00035

interactions; however, epigenetic determinants of inter-individual variability in responses to toxicants are yet to be explored.[76] For example, while it is well documented that strain differences exist in both genotoxic and epigenetic effects of a known human carcinogen 1,3-butadiene,[14, 77, 78] few strains have been examined and the genetic determinants of these differences are yet to be mapped. The importance of characterizing inter-individual variability for carcinogenic risks was highlighted by the National Academy of Sciences [1] *Science and Decisions* report, which noted that current practices in cancer risk assessment largely neglect the presence of population variability in susceptibility to cancer. Unlike for non-cancer effects, where notable progress has been made in addressing human variability both methodologically and in terms of data availability [60, 79], progress on addressing this gap for cancer effects has been lacking, partially due to lack of relevant data.

The goal of the present study was to investigate the extent and molecular drivers of inter-individual variability in DNA damage and global epigenetic effects of 1,3-butadiene across three tissues, two of which are targets of 1,3-butadiene-induced carcinogenicity. We hypothesized that tissue- and strain-specific epigenetic modifications affect inter-strain differences in DNA damage by 1,3-butadiene. We exposed mice from 20 strains of Collaborative Cross to clean air or 635 ppm 1,3-butadiene by inhalation for 2 weeks (6 hours/day, 5 days/week). Amount of *N*-7-(2,3,4-trihydroxybut-1-yl) guanine (THB-Gua) adducts, as well as changes in global cytosine DNA methylation and histone modifications were examined to evaluate inter-strain and tissue differences in both DNA damage and epigenetic effects. We then map the candidate susceptibility loci and quantify

the implications of these results for cancer risk assessment by calculating a chemical-specific adjustment factor to quantitatively address inter-individual differences in cancer susceptibility.

2.2 Materials and Methods

Animals and exposures. Adult male mice (8-12 weeks old) from 20 Collaborative Cross strains were acquired from the University of North Carolina Systems Genetics Core (Chapel Hill, NC). Mice were fed an NTP 2000 wafer diet (Zeigler Brothers, Inc., Gardens, PA) and water *ad libitum*. The housing room was maintained on a 12-h light – and dark cycle. Mice were allowed to acclimate for 14 days before study. Exposures consisted of filtered air or 1,3-butadiene 6/hr day, 5 days/week (Monday-Friday) for 2 consecutive weeks as detailed elsewhere.[58] One mouse from each strain was used for control or 1,3-butadiene exposed groups, a study design aimed to maximize the statistical power of the study by maximizing the number of strains tested.[80] While sex-specific differences in epigenetic effects of 1,3-butadiene have been recently shown,[81] this study was limited to the responses in male mice and further studies are needed to fully characterize sex-dependent genetic modifiers. Exposure concentration and protocol were selected based on the National Toxicology Program's carcinogenesis studies with 1,3-butadiene in mice.[82] Concentrations of 1,3-butadiene in exposure chambers were monitored at the beginning and end of each daily exposure period using gas chromatography and the average concentration of 1,3-butadiene in the exposure chamber was 635±77 ppm. Necropsies and tissue collections were performed within 2 h of the

cessation of exposure. Mice were euthanized by exsanguination following deep isoflurane anesthesia. Tissues and blood were removed, snap-frozen in liquid nitrogen, and stored at -80ºC. All experimental procedures involving animals were reviewed and approved by the Institutional Animal Care and Use Committee at the University of North Carolina at Chapel Hill.

Determination of N-7-(2,3,4-trihydroxybut-1-yl)-guanine (THB-Gua) adducts. Genomic DNA was isolated from flash-frozen liver, lung, and kidney using commercial kits (Qiagen, Germantown, MD) according to the manufacturer's instructions. Levels of THB-Gua were measured as described elsewhere.[83]

Methylated DNA immunoprecipitation qPCR analysis. Methylated DNA-immunoprecipitation (MeDIP) was conducted in tissues from control and 1,3-butadiene exposed mice using the MethylMiner Methylated DNA Enrichment Kit (Invitrogen, Carlsbad, CA). The methylation status of long interspersed nuclear elements 1 (LINE-1) and short interspersed nuclear elements B1 (SINE B1) was evaluated by qPCR using immunoprecipitated DNA or input DNA. The primer sequences are listed in Supporting Information Table S1.

Western blot analysis of histone modifications. The levels of trimethylation of histones H3 lysine 9 (H3K9me3), H3 lysine 27 (H3K27me3), and H4 lysine 20 (H4K20me3) and acetylation of histones H3 lysine 9 (H3K9ac), H3 lysine 27 (H3K27ac), and H4 lysine 16 (H4K16ac) were evaluated by western immunoblotting as previously described [58] in control and 1,3-butadiene exposed mice. The protein of interest was normalized to the relative intensity of the average relative intensity of two loading control samples run on

each gel. Antibodies and their dilutions are listed in Supporting Information, Table S2. IRDye 800CW–labeled anti-rabbit secondary antibodies (LI-COR Biosciences, Lincoln, NE) was used for visualization. Fluorescence was measured using the Odyssey CLx Infrared Imager and the images quantified using ImageStudio 4.0 software (LI-COR Biosciences). Equal sample loading was confirmed by normalizing relative intensity of the protein of interest to the average relative intensity of two control samples loaded on each gel.

Calculation of chemical-specific inter-individual variability factors based on inter-strain variability. The National Academy of Sciences [1] proposed adding incorporation of a human variability factor in cancer risk assessment to characterize the degree to which more sensitive individuals may be at higher risk of developing cancer. Here, we use inter-strain variability as a surrogate for human variability [21, 60]. The degree of inter-strain variability in genotoxic and epigenetic effects of 1,3-butadiene was estimated by decomposing the total observed variance across Collaborative Cross strains into two components: intrinsic inter-strain heterogeneity and intra-strain variability (e.g., variability due to environmental factors and measurement error) as described in detail in Ref. [75] and is briefly summarized as follows. Because one sample from each Collaborative Cross strain was available, the intra-strain variability was estimated from previously reported data on variation in these parameters and tissues for C57BL/6J [14] or CAST/EiJ [84] strains, as follows:

$\sigma^2_{\text{inter-strain}} = \sigma^2_{\text{total}} - \sigma^2_{\text{intra-strain}}$

σ^2_{total}= variance of log-transformed data across 20 CC mice

$\sigma^2_{intra\text{-}strain}$= variance of log-transformed data from C57BL/6J or CAST/EiJ mice

To quantitatively express the degree of inter-strain variability in the effects in each tissue, assuming a lognormal distribution for inter-individual variability, a human variability factor (HVF) was calculated as HVF= $e^{z^*\sigma}$, where z= Z statistics at the 95% cut-off, and σ represents the square root of inter-strain variance [1]. The HVF calculated in this manner therefore theoretically represents the factor by which the cancer risk or slope factor is greater in the 95th percentile of the population as compared to that for the median individual. Higher percentiles, such as the 99th percentile used by U.S. EPA for trichloroethylene and dichloromethane [85, 86] can be derived by using larger values of z, but were not derived here given the sample size of ~20.

Genome-wide quantitative trait locus (QTL) mapping. QTL mapping was conducted to identify potential loci driving differences in population variability in 1,3-butadiene-induced DNA damage and epigenetic alterations. We used the gQTL web application v1.4[87] with the following settings: auto transformation, MegaMUGA Build 37, and 1000 permutations. This approach uses genome scans with the classical Haley-Knott regression with a linear mixed model where the polygenic effect is captured in as random-effects. Statistical thresholds were determined by permutation analysis. Trait outliers were not removed. Phenotype data used for this analysis was DNA adduct levels and fold change for global epigenetic endpoints for each Collaborative Cross strain (Supporting Information, Table S3). A confidence interval based on the 1.5 LOD interval was used to mark the region likely containing the causative gene(s). This interval was compared to the annotated mouse genome to identify potential candidates. A list of candidate genes was

created by inputting the chromosome region for a significant QTL to the University of California-Santa Cruz genome browser.

Statistical Analyses. GraphPad Prism (La Jolla, CA) was used for statistical analysis of the phenotype data. Wilcoxon matched-pairs signed rank test was used to evaluate differences between control and 1,3-butadiene exposed samples. The F-test was used to compare variances. Significance was determined when $p<0.05$ for all tests performed. R software (version 3.4.3) was used to generate paired box plots (*ggplot2* package) and correlation matrices (*hmisc* package).

2.3 Results

Population variability of 1,3-butadiene-induced DNA damage

The metabolism of 1,3-butadiene results in formation of reactive epoxides which form a variety of DNA adducts, among which THB-Gua adducts are commonly used as a biomarker of 1,3-butadiene exposure.[88, 89] Therefore in the present study we evaluated THB-Gua adduct levels in lung, liver and kidney of Collaborative Cross mice. Adducts were undetectable in mice exposed to filtered air (data not shown). Figure 1A shows that THB-Gua adducts were present in all tissues in 1,3-butadiene-exposed mice, but the number of adducts varied several-fold in each tissue. Among the tissues, the liver had the highest population mean of adduct levels followed by the kidney and lung. It is noteworthy that THB-Gua adduct levels positively correlate among all tissues with the strongest correlation between lung and kidney (Figures 1B-D).

In concordance with previous reports, we observed inter-strain variability in adduct levels.[14, 77, 81] For example, strains CC031, CC038 and CC061 had the highest THB-Gua adduct levels across tissues (Supporting Information, Figure S1). In contrast, strains CC016 and CC023 presented intermediate levels, and CC002 and CC039 had the lowest amount of THB-Gua adduct levels across tissues. Within each tissue, the range of THB-Gua adduct levels varied by two- to six-fold across the population tested. Although some strains showed consistent responses to 1,3-butadiene-exposure across tissues, there were also strains that demonstrated tissue-specific responses.

Population variability in 1,3-butadiene-induced effects on global DNA methylation

Exposure to 1,3-butadiene disrupts the epigenome status,[58] an effect that is one of key characteristics of known human carcinogens.[31] In order to examine changes in cytosine DNA methylation patterns in response to 1,3-butadiene exposure, we evaluated the methylation status of LINE-1 and SINE B1 retrotransposons, commonly used indicators of global methylation status.[90] Figure 2 shows that there were no overall significant differences between control and 1,3-butadiene exposed mice across tissues. Previously reported DNA methylation data from a panel of inbred mouse strains showed that although inter-strain variability exists, the majority of strains did not present significant changes in the methylation status of LINE-1.[14] In the lung, methylation levels of LINE-1 positively correlated with methylation levels of SINE B1.

Even though there were no significant population 1,3-butadiene-induced effects on methylation of LINE-1 and SINE B1 elements, there was appreciable degree of inter-strain variability within each tissue. For example, in the lung, strains CC020, CC037, and

CC038 showed increases in DNA methylation levels in response to 1,3-butadiene exposure. In contrast, in the same tissue, strains CC016, CC023, and CC028 showed loss of DNA methylation and strain CC068 had less than 10% change in methylation levels for both SINE B1 and LINE-1. Similar trends were observed in the liver and kidney. Interestingly, in the kidney, there was no strain with less than 10% change in DNA methylation levels. Our results are in concordance with previous multi-strain studies which identified 1,3-butadiene-induced strain-specific effects in DNA methylation patterns.[14, 81] In the present study, strain responses also varied across tissues. For example, strains CC016 showed a loss of methylation in the lung and liver but an increase in methylation in the kidney. In previous studies, strain- and tissue-specific effects have also been identified. C57BL/6J mice demonstrated loss of methylation of SINE B1 in the liver whereas CAST/EiJ mice showed loss of methylation in the lung.[81]

Population variability in 1,3-butadiene-induced effects on histone modifications

Exposure to chemicals can disrupt chromatin structure, a process that is tightly controlled by post-translational modifications of various histones.[91, 92] Previous studies showed that 1,3-butadiene has effects on both histone modifications[14, 58] and the chromatin landscape.[77, 78] Figure 3 shows the effects on levels of H3K9me3, H3K27me3, H4K20me3, H3K9ac, H3K27ac, and H4K16ac across three tissues in control and 1,3-butadiene exposed mice. There were significant decreases in trimethylation of H3K9 and acetylation of H3K27 in the lung in response to 1,3-butadiene at the population level. In contrast, there were significant increases in trimethylation of H4K20 in the liver and H3K9 in the kidney. Figure 4 shows the fold change for each histone modification that had a

significant change in population mean in response to 1,3-butadiene exposure. While the overall population effects were less than 2-fold, inter-strain differences in chromatin responses were identified which is in concordance with previously reported results.[14]

Correlation analysis of DNA damage and epigenetic phenotypes

In order to investigate the associations among histone modifications, DNA methylation, and THB-Gua adduct levels, we performed rank (Spearman) correlation analyses. Figure 5A shows the global correlation matrix which includes phenotypes for all strains and tissues. This analysis shows that tissue-specific responses to 1,3-butadiene exposure are most evident, and in agreement with previous observations.[77, 81] As noted previously, levels of THB-Gua were most similar in the lung and kidney and significantly correlated in all three organs. Among the epigenetic alterations evaluated, the effect of 1,3-butadiene on cytosine DNA methylation and histone modifications was most prominent and concordant among the strains in the lung and liver, target organs for 1,3-butadiene carcinogenicity (Figures 5B and 5C). In the lung, this was evidenced by a positive correlation between LINE-1 and SINE B1 methylation, and trimethylation and acetylation of histones (Figures 5B). In the liver, there were positive correlations between the trimethylation of H4K20 and H3K27 and between the trimethylation of H3K27 and H3K9 (Figure 5C), well-established marks of heterochromatin.[93, 94] In contrast, correlations between epigenetic marks in the kidney, a non-target organ for 1,3-butadiene carcinogenicity, were less evident (Figure 5D).

It should be noted, that liver was the only organ to show a significant correlation between DNA damage and epigenetic effects. Specifically, we observed a negative

correlation between 1,3-butadiene-induced adduct levels and the extent SINE B1 methylation at the population level (Figure 5C). Similarly, at the individual mouse strain levels, CC001, CC061, and CC012 strains that exhibited the highest levels of THB-Gua were also characterized by lowest extent of SINE B1 methylation.

Quantifying the variability in tissue-specific DNA damage and epigenetic effects of 1,3-butadiene

Our study collected quantitative data on population variability in DNA damage and epigenetic effects of 1,3-butadiene across various tissues, information that can be used to calculate chemical-specific human variability factors that pertain to its cancer hazard (Table 1). Specifically, we selected three representative phenotypes for quantifying the variability in tissue-specific DNA damage and epigenetic effects of 1,3-butadiene. THB-Gua adducts were representative of genotoxic effects, methylation effects on LINE-1 of DNA methylation effects, and trimethylation of H3K9 of histone modification effects. These chemical-specific values represent the first attempt to incorporate chemical-specific data-informed susceptibility information beyond toxicokinetics in the cancer risk assessment of 1,3-butadiene.

The variance in THB-Gua adducts was similar across lung, liver and kidney, leading to HVF values of less than a factor of 2. Similar variability was observed for the effects on H3K9 trimethylation. However, a large degree of variability in global DNA methylation, as measured by methylation of LINE-1, was observed, leading to HVF values of about 3 to 8. Interestingly, the largest HVF value was for the kidney, which is not a target tissue for 1,3-butadiene-induced carcinogenicity. Focusing on the target tissues of

lung and liver, these results suggest that susceptible individuals at the 95th percentile may be at up to 4 times higher risk based on these early events alone.

QTL Mapping

In order to identify genomic regions associated with inter-strain differences in 1,3-butadiene-associated DNA damage and epigenetic effects, we performed QTL mapping using a model that considered each of the eight founder alleles separately[87] with data on DNA adduct levels and $\log_2$ fold change values for epigenetic phenotypes (DNA methylation and histone modifications) from each strain and tissue. The QTL mapping provides genomic intervals that are statistically associated with trait variances. These intervals are typically marked by a confidence interval. Genome wide-significant (95% confidence) or suggestive (80-95% confidence) loci were identified in the lung (Figures 6-8) and the boundaries and protein-coding genes in each locus are listed in Table 2. Genes residing within these intervals become candidates. By looking through genes residing within the intervals, those with credible linkages to histone modifications become high-quality candidates for the causative drivers of variation in histone modification.

H3K9me3 in the lung was significantly effected by 1,3-butadiene exposure at the population level and it also had one of the most prominent QTLs identified (Figure 6A). A 3.1 Mb locus (exceeding the suggestive genome-wide threshold of 85% confidence) for the effect of 1,3-butadiene on this histone mark is located on chromosome 6 (119.48-122.59 Mb; 6qF1 region) and had a LOD score of 10.52 (p=2.89e-08). We found that PWK/PhJ and 129S1/SvlmJ founder strain alleles had most pronounced effects on this QTL (Figure 6B). This locus contains 33 protein-coding genes (Figure 6C, Table 2).

H3K9ac in the lung was not significantly effected by 1,3-butadiene exposure on the population level, but it had the most significant (exceeding genome-wide threshold of 95% confidence) QTL (Figure 7A). An 8.2 Mb locus for the effect of 1,3-butadiene on this histone mark is located on chromosome 2 (33.32-41.50 Mb; 2qB region) and had a LOD score of 10.40 (p=3.75e-08). We observed that NOD/ShiLtJ founder allele had the most pronounced effect on this QTL (Figure 7B). This locus contains 49 protein-coding genes (Figure 7C, Table 2).

H4K16ac in the lung was also not significantly effected by 1,3-butadiene exposure on the population level, but it had a suggestive QTL (exceeding genome-wide threshold of 85% confidence) (Figure 8A). A 0.54 Mb locus for the effect of 1,3-butadiene on this histone mark is located on chromosome 14 (33.42-33.96 Mb; 14qB region) and had a LOD score of 9.04 (p=6.17e-07). We observed that CAST/EiJ founder allele had the most pronounced effect on this QTL (Figure 8B). This locus contains 5 protein-coding genes (Figure 8C, Table 2).

2.4 Discussion

1,3-Butadiene, a known human and rodent carcinogen, has been used as a model genotoxic toxicant for investigating the mechanistic links between the genome, epigenome, and DNA damage.[57, 77] 1,3-Butadiene is an industrial chemical that is also a ubiquitous environmental contaminant and an occupational health hazard. Metabolism of 1,3-butadiene results in formation of reactive epoxides which can form a number of mutagenic DNA adducts, and genotoxicity is considered to be a key event in 1,3-butadiene

carcinogenicity.[88] Although 1,3-butadiene-associated DNA damage has been reported in all species and tissues tested, only lung, liver and lymphoid organs are the target tissues for tumorigenesis in the mouse.[95] In humans, hemoglobin adducts and urinary butadiene-mercapturic acids serve as biomarkers for 1,3-butadiene exposure.[88, 96] Lymphocytes obtained from 1,3-butadiene exposed factory workers demonstrated genetic damage such as sister-chromatid exchanges and chromosomal aberrations.[97] Occupational human exposure to 1,3-butadiene is associated with an increase incidence of leukemia.[57]

In addition to genotoxicity, exposure to 1,3-butadiene results in epigenetic effects, including effects of histones,[58, 81, 84] chromatin remodeling,[77, 78] and alterations in cytosine DNA methylation.[14, 58] Strain-dependent tissue-specific epigenetic variability in these effects was demonstrated using inbred mouse strains.[14, 77, 78, 81] The effects on chromatin states and cytosine DNA methylation have been identified as a potential mechanism for the tissue-specific carcinogenicity of 1,3-butadiene.[50, 98] This suggests that variation in epigenetic alterations could influence the inter-individual susceptibility to 1,3-butadiene genotoxicity. In this study, using a much larger mouse population, a compendium of Collaborative Cross mouse strains, we demonstrate that 1,3-butadiene-induced THB-Gua adducts and epigenetic alterations in lung, liver, and kidney of exposed mice greatly vary among organs and strains. Butadiene is carcinogenic in mice at doses as low as 6.25 ppm and it has been tested in doses of up to 8,000 ppm;[99] thus, our selection of exposure concentration that is well within the range of carcinogenic doses is based on both prior studies by others,[83, 100] and our own work demonstrating robust and strain-specific differences in genotoxic, epigenetic and transcriptional responses.[14, 58, 78, 84] We found that

tissue-specific levels of THB-Gua adducts were highly correlated. These data are of significance because while THB-Gua is widely used as a biomarker of effect in studies of 1,3-butadiene, it was not known how well tissue extrapolations can be made.[88]

It is also well-recognized that epigenetic alterations are as important for the carcinogenic process as those that are characterized as genotoxicity[31, 50] and that cross-talk between these two key characteristics of known human carcinogens exists.[101] Some epigenetic changes may drive the development of cancer, while others may be accompanying epigenetic events. Therefore, it is important to identify the epigenetic changes that are driving the development of the chemical-induced carcinogenic process. In this respect, a marked decrease in trimethylation of histone H3K9 in the lung, as well as demethylation of SINE B1 in the liver that tightly correlated with the formation of THB-Gua adducts in the liver and other tissues, are of potential significance.

With respect to the population-based effects on DNA methylation, we note that our data in 20 CC lines demonstrates discordant strain-specific effects and the lack of the overall effect of 1,3-butadiene on global changes in DNA methylation. This observation is concordant with that reported in 7 inbred mouse lines[14], and further reinforces the need to employ population-based models in toxicological studies to account for population-wide differences in effects.[6, 60] Furthermore, the lack of population-wide effects does not negate a potential role for DNA methylation effects in relation to the overall strain-specific mechanisms. For example, we note that SINE retrotransposons are some of the most abundant transposable elements dispersed throughout the mammalian genome. It is estimated that 5% of the mouse genome and 11% of human genome consists of SINE

retrotransposons, respectively.[102] Activation of expression of these transposable elements may lead to genetic instability, and cytosine DNA methylation plays a fundamental role in their transcriptional silencing and protecting of genome.[103] The results of numerous studies have demonstrated that prolonged exposure to genotoxic chemical carcinogens may result in a loss of SINE methylation and their transcriptional activation.[14, 81, 84] In light of this, an inverse correlation between the levels of THB-Gua adducts and SINE B1 methylation in the liver found in this study provides a mechanistic insight for 1,3-butadiene induced carcinogenesis. Still, future studies on the locus-specific methylation patterns are needed to fully address the role of DNA methylation in susceptibility to butadiene-associated carcinogenesis, especially in light of recent reports that tissue variation in cancer risk correlates with the degree of aberrant CpG island DNA methylation in normal cells.[104]

Even though the population size of the Collaborative Cross mice used in this study was relatively small in terms of mapping needs, haplotype-associated mapping yielded several candidate loci and genes for the observed epigenetic effects of 1,3-butadiene. Complex long-term exposure studies in multiple strains are difficult to conduct in large populations, a known challenge to the adoption of the population-wide studies in toxicology.[61] Still, candidate genes that are identified through genomic mapping studies can afford additional strength to the mechanistic linkages between exposures and effects. In this study, we aimed to determine whether inter-strain variation in genes that have been linked to chromatin dynamics may explain the inter-individual variability in 1,3-butadiene-induced changes in chromatin structure.

Histone H3K9me3 plays a central role in the formation of heterochromatin and the maintenance of genomic stability and chromatin integrity.[105] Therefore, a loss of histone H3K9 trimethylation may compromise genomic stability and integrity, a key event in the carcinogenic process.[30] Indeed, several reports demonstrated a link between demethylation of histone H3K9me3 and carcinogenesis.[106, 107] In the lung, we identified a QTL associated with the effects on histone H3K9me3. The Collaborative Cross population demonstrated a significant decrease in H3K9me3 in response to 1,3-butadiene exposure with a two and a half fold difference across strains. In this genomic region, we identified a lysine-specific demethylase gene, *KDM5A* (also known as *JARID1A* or *RBP2*). Although it is well-established that KDM5A removes methyl groups from di- and trimethylated H3K4, there is evidence of chromatin crosstalk, which refers to histone methyltransferases binding to non-target substrates. KDM5A contains three plant homeodomains (PHD) fingers which are considered chromatin recruitment modules that bind methyl-lysine residues. In yeast, PHD3 has been shown to bind to histone H3K9me3.[108] KDM5C and LID, homologs of KDM5A, have also demonstrated affinity toward H3K9me3.[109, 110]

We also identified a significant QTL for histone H4K16ac in the lung. H4K16ac is involved with genomic stability and chromatin organization.[111] A loss of histone H4K16ac has been proposed as a marker of carcinogenesis.[112] Although there were no significant changes in the population mean of H4K16ac in response to 1,3-butadiene exposure, it is important to note that a fourfold difference between lowest and highest levels among strains. We identified *MAPK8* (also known as *JNK1*) as a candidate gene based on evidence that MAPK8 phosphorylates SIRT1, an NAD-dependent deacetylase

that targets H4K16.[113] Previously, *SIRT1* expression was shown to be upregulated across tissues in 1,3-butadiene exposed C57BL6/J mice, which may contribute to sensitivity to 1,3-butadiene effects.[84]

Similar to histone H4K16ac, we identified a suggestive QTL that may be associated with 1,3-butadiene-mediated effects on histone H3K9ac in the lung. There were no significant changes in H3K9ac identified at the population level; however, among strains, there was a threefold difference in 1,3-butadiene-induced effects on this histone mark. There are two candidate genes related to chromatin biology in the QTL identified. The first candidate gene, *CRB2*, is a recruitment protein that binds to H4K20me2 which is critical for repair of double strand breaks [114]. Loss of methylation reduces CRB2 recruitment which consequently decreases cell survival after genotoxic exposure [115]. The second gene of potential interest is *NEK6*, a kinase linked to mitotic regulation [116]. In human cells, NEK6 has demonstrated the ability to phosphorylate histones 1 and 3 [117].

In addition to using the population-based data for further elucidation of the tissue-specific epigenetic effects of 1,3-butadiene, these data can be used to quantify the variability and enable the greater translation and the application in health risk assessment. Thus, we derived chemical-specific human variability factors for the effects of 1,3-butadiene on DNA damage and epigenetic markers in three tissues. We reason that these quantitative estimates can be considered in addressing human variability in future cancer assessments of 1,3-butadiene. Interestingly, we found the 1,3-butadiene-specific adjustment factors for DNA damage effects based on our data to be modest, less than a factor of 2. Variation in global DNA methylation was greater, but the largest HVF derived

was for this endpoint in the kidney, which is not a target tissue of 1,3-butadiene carcinogenicity. This result needs to be considered in light of the fact that the overall population-level change in kidney methylation is small (1.19-fold relative to control), suggesting that the "typical" individual may be minimally affected with only a small proportion of individuals more highly affected. Because genotoxicity is well accepted as a key event in the mechanism of 1,3-butadiene carcinogenicity, the HVF based on adducts probably represents a lower bound on the degree of variability in cancer susceptibility; however, questions remain as to how directly variation in epigenetic effects correlate with variation in cancer risks [50]. Additionally, it is possible that variation in downstream carcinogenic processes will also contribute to overall variation in cancer risk. Nonetheless, our results represent a key milestone in the use of a population-based model to characterize cancer susceptibility experimentally and provide data that may be directly useable in future re-evaluations of cancer risks of 1,3-butadiene exposure.

Overall, we conclude that by using the Collaborative Cross mouse model, we were able to investigate population variability in epigenetic and genotoxic effects in response to a model genotoxic chemical 1,3-butadiene. We identified tissue-specific epigenetic modifications which provide mechanistic insight to carcinogenesis in 1,3-butadiene target organs. Furthermore, we observed strain-specific epigenetic alterations which may play a role in individual susceptibility to DNA damage. Genetic mapping identified four candidate genes that may be driving underlying differences in chromatin remodeling for H3K9me3, H3K9ac, and H4K16ac. Furthermore, we calculated chemical-specific adjustment factors for DNA damage and epigenetic effects of 1,3-butadiene to provide

quantitative estimates that may be used in evaluation of inter-individual differences in cancer susceptibility for this chemical. Together, these findings demonstrate that population-based studies provide a model for uncovering the underlying mechanisms through which genetic variability and lay a foundation for future investigations into the degree and mechanisms of susceptibility to carcinogenic risks, addressing a critical gap in existing cancer risk assessments.

Acknowledgements

This work was supported, in part, by grants from the National Institute of Environmental Health Sciences (R01 ES023195 and R01 ES029911).

Table 2.1 Quantitation of inter-strain variability in genotoxic and epigenetic effects of 1,3-butadiene.

	THB-Gua Adducts ($\times 10^8$ Nucleotides)			LINE-1 (Fold-change relative to control)			H3K9me3 (Fold-change relative to control)		
	Lung	Liver	Kidney	Lung	Liver	Kidney	Lung	Liver	Kidney
GM	135	175	136	0.902	0.950	1.19	0.879	1.08	1.12
GSD	1.45	1.23	1.29	2.42	1.81	3.50	1.28	1.33	1.20
σ^2_{total}	0.152	0.044	0.088	1.02	0.592	1.91	0.072	0.097	0.051
$\sigma^2_{intra\text{-}strain}$	0.012	0.002	0.024	0.240	0.240	0.341	0.011	0.014	0.018
$\sigma^2_{inter\text{-}strain}$	0.139	0.042	0.064	0.781	0.352	1.57	0.060	0.083	0.033
HVF	1.85	1.40	1.52	4.28	2.65	7.87	1.50	1.61	1.35

GM=geometric mean; GSD= geometric standard deviation; σ^2_{total}= variance of log-transformed data from this study; $\sigma^2_{intra\text{-}strain}$=variance of log-transformed data from corresponding reference; $\sigma^2_{inter\text{-}strain} = \sigma^2_{total} - \sigma^2_{intra\text{-}strain}$; HVF = Chemical-specific human variability factor at 95th percentile.

Table 2.2 Quantitative Trait Loci mapping using log_2 fold change values for each phenotype identified loci on chromosomes 2, 6 and 14. Genes found in these regions are listed by genomic position.

Phenotype	Significant locus	Protein-coding genes in the locus
H3K9me3 [Lung]	Chr6: 119.48-122.59 Mb LOD=10.52 p=2.89e-08	*Fbxl14, Erc1, Rad52, Wnk1, Ninj2, B4galnt3, Ccdc77,* ***Kdm5a****, Il17ra, Tmem121b, Hdhd5, Cecr2, Slc25a18, Atp6v1e1, Bcl2l13, Bid, Mical3, Pex26, Tuba8, Usp18, Slc6a13, Slc6a12, lqsec3, A2m, Mug1, Mug2, Klrg1, M6pr, Phc1, Rimklb, Mfap5, Aicda, Apobec1*
H3K9ac [Lung]	Chr2: 33.32-41.50 Mb LOD=10.40 p=3.75e-08	*Ralgps1, Zbtb34, Zbtb43, Lmx1b, Mvb12b, Pbx3, Mapkap1, Gapvd1, Hspa5, Rabepk, Fbxw2, Psmd5, Cutal, Phf19, Traf1, Hc, Cntrl, Rab14, Gsn, Stom, Ggta1, Dab2ip, Ttll11, Ndufa8, Morn5, Lhx6, Rbm18, Mrrf, Ptgs1, Pdcl, Rc3h2, Zbtb26, Zbtb6, Rabgap1, Gpr21, Strbp,* ***Crb2****, Dennd1a, Lhx2,* ***Nek6****, Psmb7, Nr5a1, Nr6a1, Wdr38, Rpl35, Arpc5l, Golga1, Scai, Ppp6c, Lrp1b*
H4K16ac [Lung]	Chr14: 33.61-33.77 Mb LOD=9.04 p=6.17e-07	***Mapk8****, Ptpn20, Gdf10, Gdf2, Rbp3*

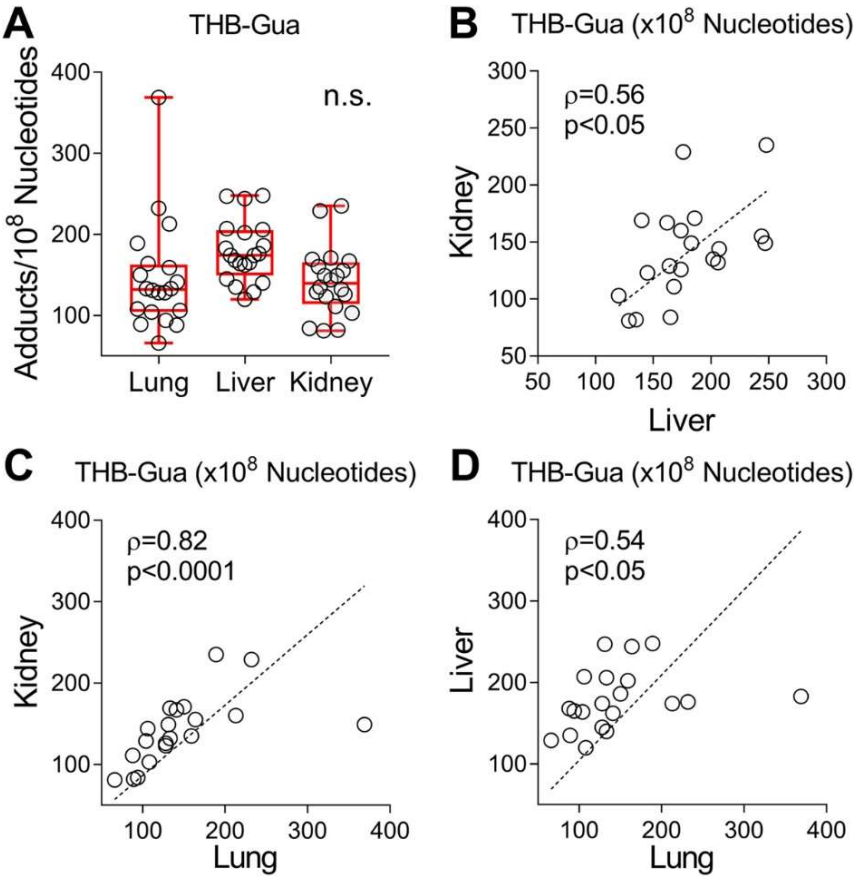

Figure 2.1 Population variability in genotoxicity of 1,3-butadiene across mouse tissues. Strain variability in levels of THB-Gua adducts in lung, liver, and kidney of mice exposed to 625 ppm of 1,3-butadiene for 2 weeks. The box shows the 1st and 3rd quartile ranges, the horizontal line represents the median, and the whiskers represent the min and max values. Each circle represents data for a CC strain. (B-D) Pairwise inter-tissue correlation in THB-Gua adducts in the populations of CC strains is shown as scatter plots. Trend lines and corresponding ρ (Spearman correlation) and p values are shown in each panel. Each circle represents data for a CC strain.

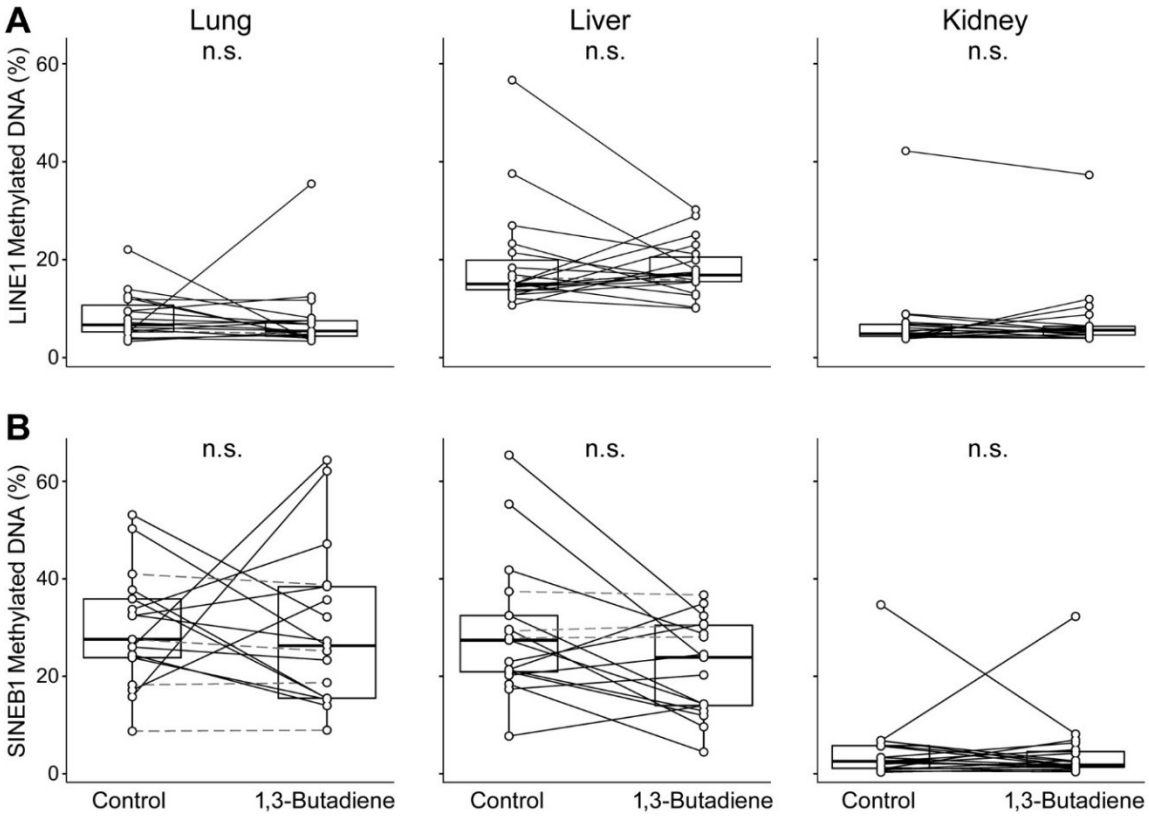

Figure 2.2 Population variability in global DNA methylation associated with exposure to 1,3-butadiene across mouse tissues. The results are presented as box and whisker plots for control (left) and 1,3-butadiene exposed mice (right) for LINE-1 (A) and SINEB1 (B) in the lung-left panel, liver-middle panel, and kidney-right panel. The box shows the 1st and 3rd quartile ranges and the whiskers represent the standard errors of the population mean. Each circle represents a mouse in the control or 1,3-butadiene exposed group. Lines connect the data for animals of the same strain. The dashed gray line represents less than 10% change from control to 1,3-butadiene exposed mouse.

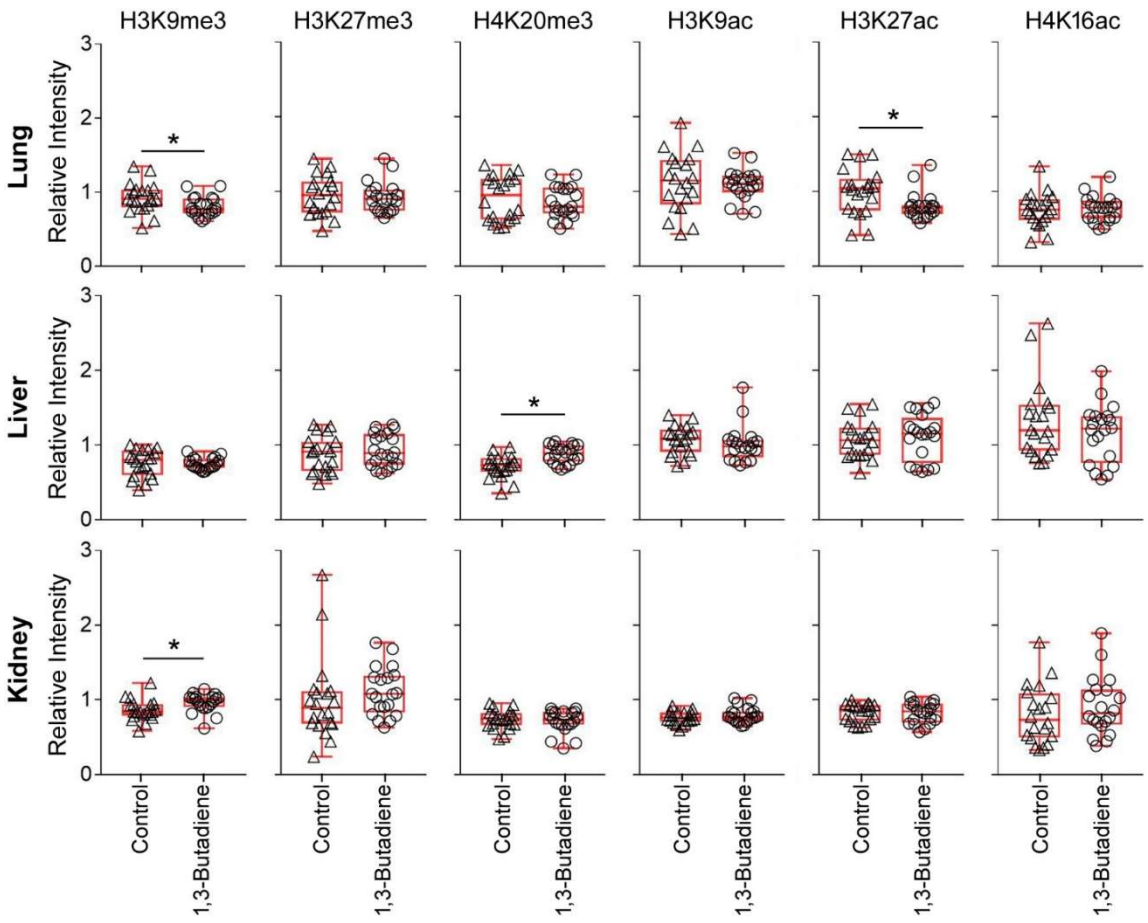

Figure 2.3 Population variability in histone modifications associated with exposure to 1,3-butadiene across mouse tissues. The results are presented as box and whisker plots for control (left box plot in each panel, triangles) and 1,3-butadiene exposed mice (right box plot in each panel, circles). The box shows the 1st and 3rd quartile ranges and the whiskers represent the min and max values. Results are expressed as the relative intensity for each sample (see Methods for normalization procedure). Asterisks (*) denote significant ($p<0.05$) difference from control group.

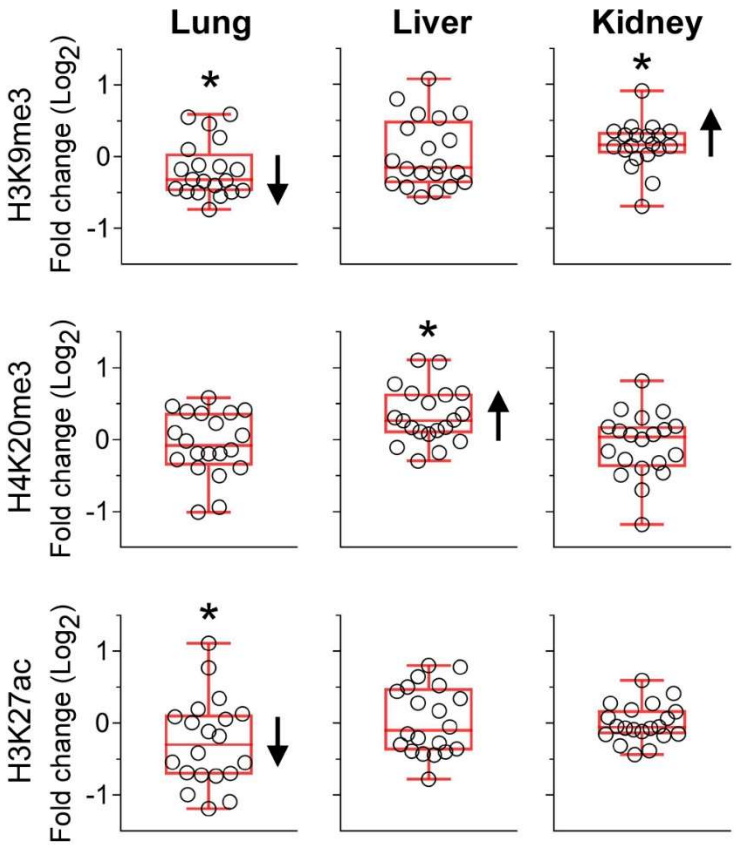

Figure 2.4 Effect levels on histone modifications with significant population variability associated with exposure to 1,3-butadiene across mouse tissues. Histone marks (H3K9me3-top panel, H4K20me3-middle, H3K27ac-bottom) that exhibited significant differences between population means of control and 1,3-butadiene exposed mice are shown. Each circle represents the log2 of fold change value for each strain and tissue (lung-left panel, liver-middle, kidney-right). Asterisks (*) denote significant ($p<0.05$) differences from control group.

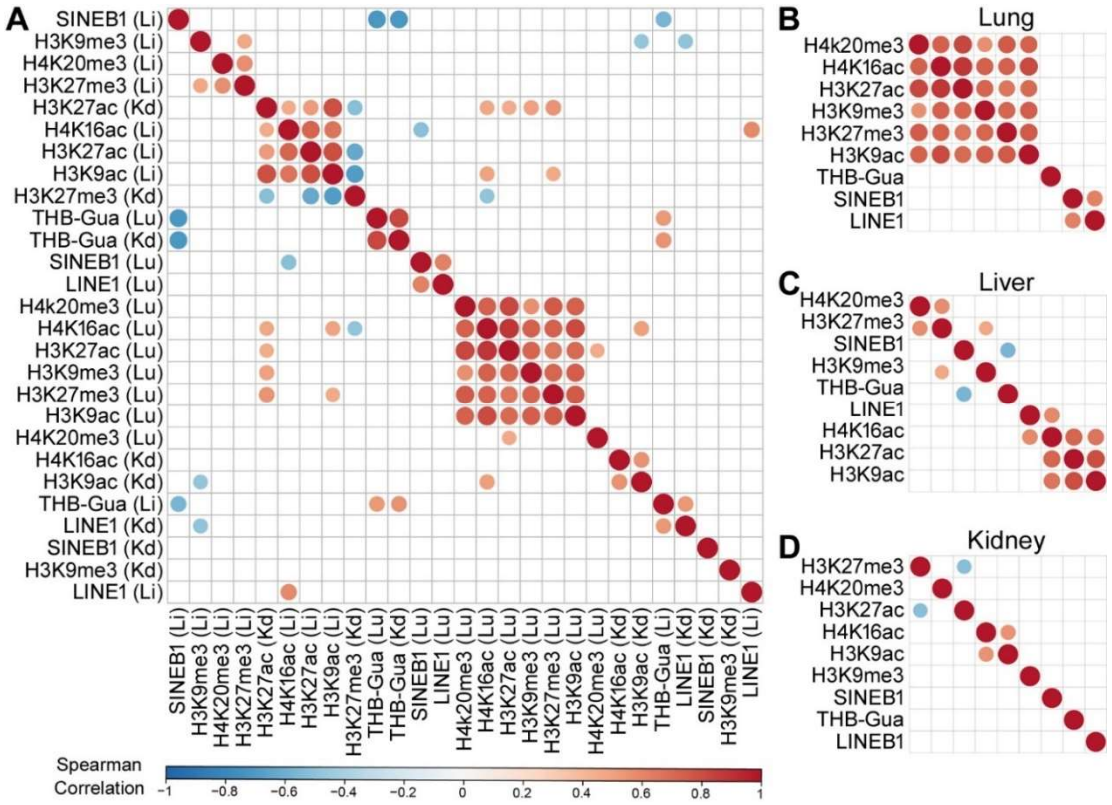

Figure 2.5 Correlation of genotoxic and epigenetic effects of 1,3-butadiene across mouse strains and tissues. Pairwise rank (Spearman) correlation analysis results where values used for DNA methylation and histone modifications were $\log_2$ (fold change relative to control)-transformed. (A) A correlation matrix of the phenotypes in all tissues of 20 CC strains. (B-D) Correlation matrices within each tissue. The x-axis labels (left to right) are identical to the y-axis labels (top to bottom). Each circle represents a significant correlation ($p < 0.05$) that was positive (red) or negative (blue).

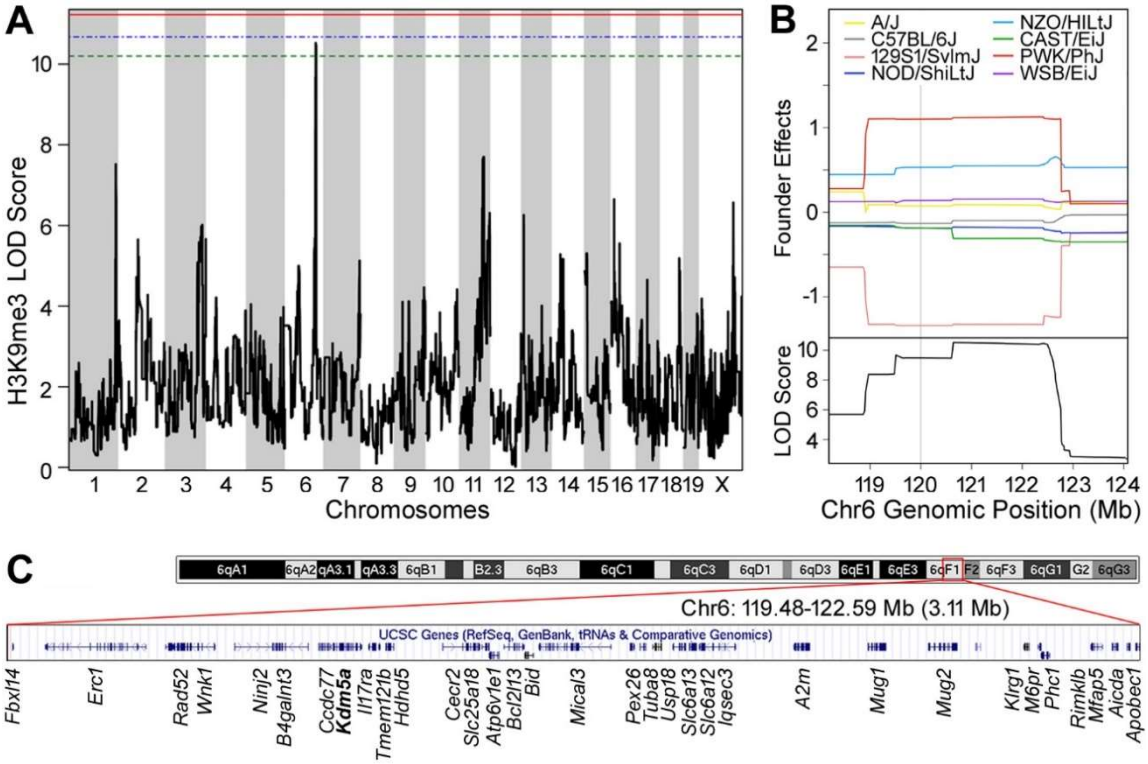

Figure 2.6 QTL mapping of H3K9me3. Values used for H3K9me3 were $\log_2$ (fold change relative to control)-transformed. Panel (A) shows the logarithmic odds ratio (LOD) scores across chromosomes 1 through X. The green, blue, and red lines represent the permutation-based significance thresholds of 85%, 90%, and 95% respectively (n=1000 permutations). Panel (B) shows the effects of the CC founder strain alleles on chromosome 6 (top) and a zoom-in on the chromosome region with a corresponding significant LOD score. Panel (C) shows the UCSC genes that are located on chromosome 6 [6qF1] in the region between 119.48-122.59 Mb.

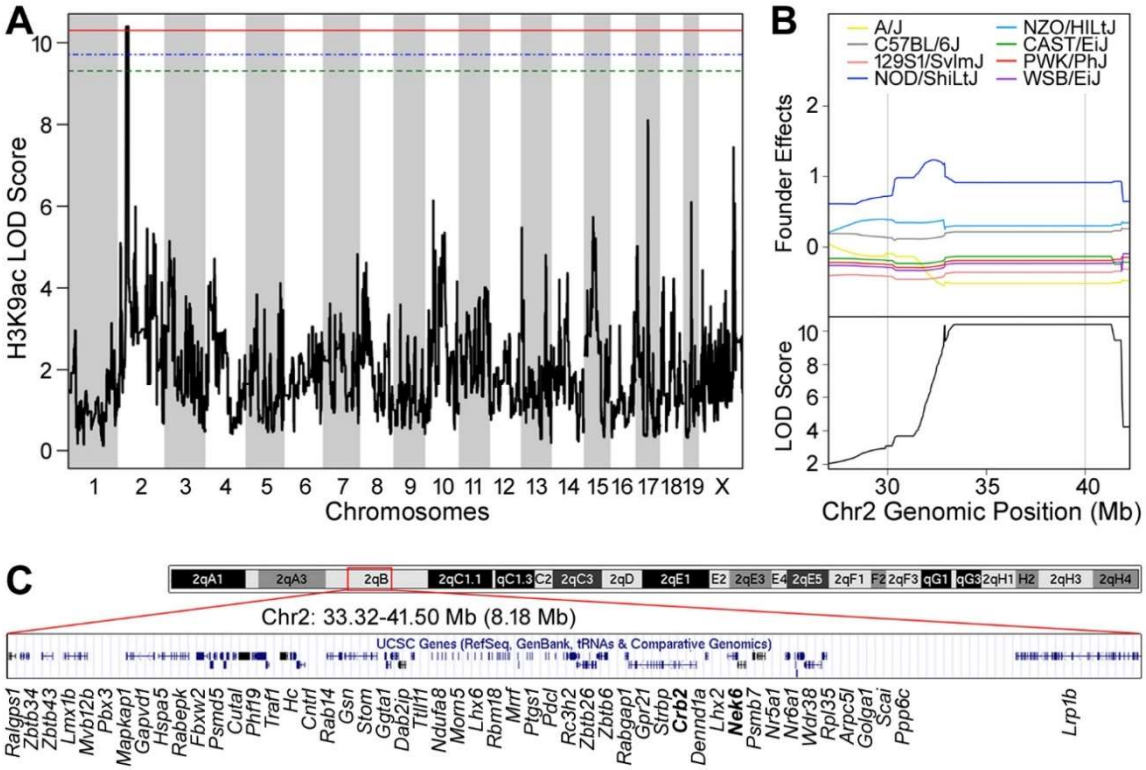

Figure 2.7 QTL mapping of H3K9ac. Values used for H3K9ac were log2 (fold change relative to control)-transformed. Panel (A) shows the logarithmic odds ratio (LOD) scores across chromosomes 1 through X. The green, blue, and red lines represent the permutation-based significance thresholds of 85%, 90%, and 95% respectively (n=1000 permutations). Panel (B) shows the effects of the CC founder strain alleles on chromosome 2 (top) and a zoom-in on the chromosome region with a corresponding significant LOD score. Panel (C) shows the UCSC genes that are located on chromosome 2 [2qB] in the region between 33.32-41.50 Mb.

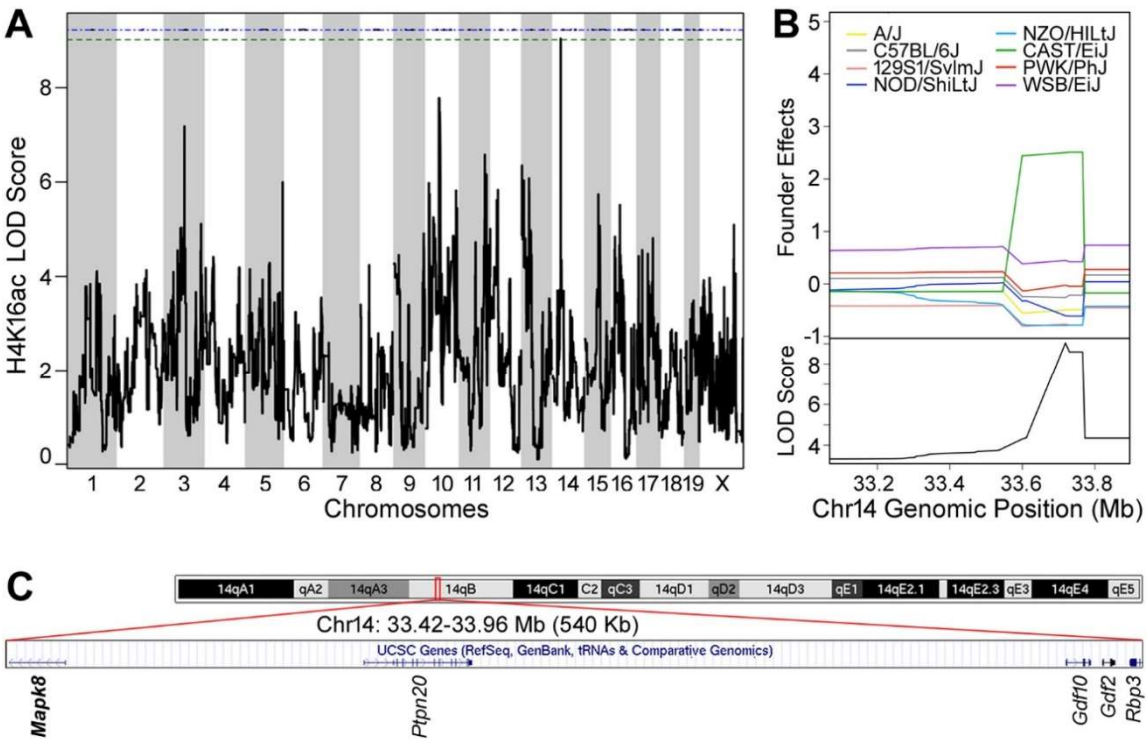

Figure 2.8 QTL mapping of H4K16ac. Values used for H4K16ac were $\log_2$ (fold change relative to control)-transformed. Panel (A) shows the logarithmic odds ratio (LOD) scores across chromosomes 1 through X. The green, and blue lines represent the permutation-based significance thresholds of 85% and 90% respectively (n=1000 permutations). Panel (B) shows the effects of the CC founder strain alleles on chromosome 14 (top) and a zoom-in on the chromosome region with a corresponding significant LOD score. Panel (C) shows the UCSC genes that are located on chromosome 14 [14qB] in the region between 33.42-33.96 Mb.

CHAPTER III

SEX-SPECIFIC DIFFERENCES IN GENOTOXIC AND EPIGENETIC EFFECTS OF 1,3-BUTADIENE AMONG MOUSE TISSUES[3]

3.1 Introduction

Accumulating evidence suggests that environmental chemicals may alter the epigenome by disrupting cytosine DNA methylation patterns, chromatin structure and expression of noncoding RNAs [50, 91, 118]. Epigenetic reprogramming has been linked to genomic instability, a hallmark of cancer [30], and induction of epigenetic alterations is one of key mechanistic characteristics of known human carcinogens [31]. Epigenetic alterations may be a result of DNA damage or non-genotoxic effects of chemicals [45]. However, even though there is an increasing interest in investigating the relationships between the states of the epigenome and chemical-induced adverse health effects [50, 119], few studies have considered sex-specific differences in epigenetic effects of chemicals, most of these were focused on prenatal or early life exposures [59, 120, 121].

It is well acknowledged that sex is an important biological variable that now is required to be included into research designs, analyses, and reporting in vertebrate animal and human studies [122]. Therefore, we aimed to study a chemical with well-known sex-specific differences in adverse health effects and determine whether its effects on epigenetic phenotypes are also sex-dependent. Specifically, we selected 1,3-butadiene, an industrial and environmental toxicant that is classified as a known human carcinogen [123].

[3]The text of this chapter is an Author's Original Manuscript reprinted with permission from an article published by Springer Nature in Archives of Toxicology, Volume 93, on 10 December 2019, available online: https://doi.org/10.1007/s00204-018-2374-x

In humans, exposure to 1,3-butadiene is associated with cancer in the haematolymphatic organs [124]. In mice, liver, lung, and lymphoid tissues are the primary sites of 1,3-butadiene-induced carcinogenesis [125]

Sex-specific differences in 1,3-butadiene-induced genotoxicity and carcinogenicity have been established in rodents and humans. Significant differences between male and female mice were reported in the levels of 1,3-butadiene DNA damage in the liver [126]. Sex-specific differences have also been identified in the occurrence of 1,3-butadiene-induced *Hprt* gene mutations, with female rodents exhibiting a greater susceptibility [127]. In human studies, female factory workers exposed to 1,3-butadiene had lower globin adduct levels when compared to male workers, but not other markers of genotoxicity, possibly because of the sex-specific differences in toxicokinetics of 1,3-butadiene [128]. With respect to tumor development, tumor sites also vary between males and females in studies of rats and mice [125, 129]. Furthermore, female mice form tumors at lower concentrations of 1,3-butadiene than male mice, further implicating sex-specific mechanisms as drivers of susceptibility to 1,3-butadiene-induced carcinogenesis [125].

Epigenetic effects of 1,3-butadiene are well established and have been studied in multiple tissues of male mice [14, 77, 78]. These studies demonstrated that there are organ- and strain-dependent effects. Variability in 1,3-butadiene-induced chromatin alterations represents one possible mechanism for strain-specific differences in DNA damage [77, 78]. Two inbred mouse strains, C57BL/6J and CAST/EiJ, have been extensively studied based on their sensitivity and resistance to 1,3-butadiene-induced DNA damage [14]. In addition, inter-strain variability has also been identified in 1,3-butadiene-induced mitochondrial

dysfunction using the Collaborative Cross mouse population model [73]. With respect to carcinogenesis-related genetic and epigenetic effects of 1,3-butadiene in mice, it was found that while exposure-induced DNA adducts are present in lung, liver, and kidney [77], epigenetic alterations [84] and tumor formation are restricted to the liver and lung [82, 125]. Tissue-specific epigenetic effects may provide mechanistic clues with respect to why certain organs are resistant to carcinogenesis even though they harbor appreciable genetic damage from 1,3-butadiene. In this study, we investigated sex-specific differences in DNA damage and epigenetic effects in response to 1,3-butadiene exposure in various organs in two inbred mouse strains. Overall, our results demonstrate that there are sex-specific differences in epigenetic modifications among mouse tissues and that these differences may play a role in cancer susceptibility in response to 1,3-butadiene exposures.

3.2 Methods

Animals and exposures

Male and female CAST/EiJ and C57BL/6J mice (Jackson Laboratory, Bar Harbor, ME; 9-13 weeks old) were housed in sterilized cages in a temperature-controlled (24°C) room with a 12/12-h light/dark cycle. Mice had *ad libitum* access to purified water and NIH-31 pelleted diet (Purina Mills, Gray Summit, MO). These strains were selected based on previous results which indicated that C57BL/6J male mice are more susceptible to 1,3-butadiene-induced DNA damage and epigenetic effects compared to CAST/EiJ male mice, which are considered more resistant [14]. Mice were allowed to acclimatize for 2 weeks and then were randomly assigned into control or 1,3-butadiene treatment groups.

Subsequently mice were exposed to filtered air or 425 ppm 1,3-butadiene 6 hr/day, 5 days/week (Monday-Friday) for two consecutive weeks, a study dosing and duration based on previous studies of 1,3-butadiene genotoxicity[88]. The average concentration of 1,3-butadiene in the exposure chamber in this study was 425.8+/-162.0 ppm. An in life portion of the study and tissue collection were previously described [84] and were approved by the Institutional Animal Care and Use Committee at the University of North Carolina at Chapel Hill.

Determination of N7-guanine adducts and bis-N7-guanine crosslinks

Genomic DNA was isolated from flash-frozen liver, lung and kidney using a Qiagen DNeasy Blood & Tissue Kit (Qiagen, Germantown, MD) according to the manufacturer's instructions. Levels of *N*-7-(2,3,4-trihydroxybut-1-yl)-guanine (THB-Gua) and 1,4-bis-(guan-7-yl)-2,3-butanediol crosslinks (bis-N7G-BD) in DNA were evaluated as described elsewhere [126, 130].

Quantitative reverse-transcription polymerase chain reaction (qRT-PCR)

Total RNA was extracted with an RNeasy kit (Qiagen) from flash-frozen samples of the liver, lung and kidney. The High Capacity cDNA Reverse Transcriptase Kit (Applied Biosystems, Carlsbad, CA) was used to synthesize cDNA. Treatment-induced effects on gene expression for *Mpg*, *Mgmt, Xrcc1*, *Dnmt1*, *Dnmt3a*, and *Dnmt3b* were assessed by qRT-PCR. Detailed information on mouse-specific primer sequences and catalogue numbers is provided in Supplemental Table 1. Reactions were performed with two to four replicates in a 96-well plate using the 7900HT Fast Real-Time PCR system (Applied Biosystems). The housekeeping gene *Gusb1* was used as a reference control.

DNA methylation of repetitive sequences

The McrBC-methylation sensitive quantitative PCR (qPCR) assay was used to determine the methylation status of short interspersed nucleotide elements B1 and B2 (SINEB1 and SINEB2) retrotransposons and minor and major satellites repetitive sequences in liver, lung, and kidney, as described in Martens et al [131]. Genomic DNA was digested overnight with the restriction enzyme McrBC (New England Bio Labs, Beverly, MA) and subsequently analyzed with qPCR on the 7900 Real Time PCR System (Applied Biosystems).

Western blot analysis of histone modifications

Total histones were extracted as described elsewhere [132]. Briefly, tissue samples were lysed with lysis buffer, incubated for one hour on ice, and centrifuged at 14,000×g for 10 minutes at 4°C. The supernatant was removed and mixed with 10 volumes of acetone for an overnight incubation. The precipitates were air-dried then dissolved in water. The levels of trimethylation of histones H3 lysine 9 (H3K9me3), H3 lysine 27 (H3K27me3), and H4 lysine 20 (H4K20me3) were evaluated by western immunoblotting using corresponding antibodies (Upstate, Charlottesville, VA) in the livers and kidneys of control and 1,3-butadiene-exposed mice as described elsewhere [132]. Equal sample loading was confirmed by immunostaining against total H3 and H4.

Statistical Analyses

Results are presented as mean +/- SD. GraphPad Prism was used for statistical analysis of data. The student's *t* test was used to evaluate differences between samples.

Spearman correlation coefficients were used to evaluate correlations between phenotypes. Significance was determined when $p<0.05$ for all tests performed.

3.3 Results

Sex-specific differences in 1,3-butadiene-induced DNA damage and repair

Metabolism of 1,3-butadiene yields a number of DNA-reactive moieties that form DNA adducts and cross-links in cultured cell, mice, rats, and humans [88, 129]. In the present study, we investigated THB-Gua adducts and *bis*-N7G crosslinks as markers of 1,3-butadiene-induced genotoxicity across several tissues in male and female mice. Figure 1 shows that THB-Gua adducts and *bis*-N7G crosslinks were present in all 1,3-butadiene-exposed mice. We include previously reported C57BL/6J male mice *bis*-N7G crosslinks results [84] for comparison. In C57BL/6J male mice, adduct levels were similar to those previously reported at a comparable 1,3-butadiene dose [84]. Both guanine monoadducts and DNA-DNA crosslinks were 5-20% lower in female mice than in male mice across all tissues in C57BL/6J strain. Our data are also concordant with major differences in the susceptibility to 1,3-butadiene-induced DNA damage between CAST/EiJ and C57BL/6J male mice [14]. Specifically, CAST/EiJ mice had three- to four-fold lower adduct and crosslink levels compared to C57BL/6J mice. No differences between male and female mice in adduct and crosslink levels were observed in CAST/EiJ strain. Among all tissues, in both strains and sexes, the lung had the highest levels of DNA damage, followed by the kidney and liver.

To further investigate sex-specific differences in DNA damage, we evaluated the expression of DNA repair genes that are involved in the base excision repair pathway (*Mpg* and *Xrcc1*) and removal of O^6-methyl guanine (*Mgmt*). Figure 2 shows sex-specific changes in DNA repair enzyme expression across liver, lung, and kidney. In C57BL/6J mice, there was a marked increase in expression of *Mgmt* in 1,3-butadiene-exposed female mice in the kidney, while in the liver, both *Mgmt* and *Mpg* expression was significantly decreased after exposure. In CAST/EiJ mice, *Mpg* was induced in the liver of female mice and *Xrcc1* was significantly decreased in the liver of female mice and the lung of male mice.

Sex-specific alterations in 1,3-butadiene-induced cytosine DNA methylation patterns

Increasing evidence suggests that disruption of cytosine DNA methylation patterns can play a role in disease [133]. Repetitive elements that are a major component of the genome [131] are usually methylated in somatic cells [134] and can serve as indicators of global DNA methylation status [90]. To investigate sex-specific cytosine DNA methylation changes in response to 1,3-butadiene exposure, the methylation status of SINEB1 and SINEB2 retrotransposons, as well as major and minor satellites, was assessed in control and 1,3-butadiene-treated mice across tissues. It is known that 1,3-butadiene exposure resulted in strain-dependent changes in DNA methylation patterns, where CAST/EiJ remained unaffected while C57BL/6J male mice exhibited DNA hypomethylation in the liver [14]. Previously reported DNA methylation data from male C57BL/6J mice [84] was used here to compare to the new data for C57BL/6J female mice and male and female CAST/EiJ mice. Figure 3 shows sex-specific DNA methylation changes of SINEB1, SINEB2

retrotransposons and major and minor satellites in response to 1,3-butadiene exposure. In male C57BL/6J mice, exposure to 1,3-butadiene was associated with loss of cytosine DNA methylation in the liver, whereas in female mice significant loss of cytosine DNA methylation was observed in the lung. No treatment-related cytosine DNA methylation changes were found in the kidney in male and female C57BL/6J mice. In contrast, exposure of CAST/EiJ mice to 1,3-butadiene resulted in 2- to 4-fold increase in repetitive element cytosine DNA methylation in the liver and lung in female mice, whereas only minor and sporadic DNA hypomethylation changes were found in the liver, lung, and kidney of male CAST/EiJ mice.

To provide mechanistic insight into 1,3-butadiene-associated sex-specific differences in DNA methylation, the expression of DNA methyltransferase genes were investigated. Figure 4 shows that overall there were few effects on expression of *Dnmt1*, *Dnmt3a*, or *Dnmt3b* in 1,3-butadiene-exposed mice in the liver, lung, and kidney. Specifically, in C57BL/6J mice, there was a decrease in expression in *Dnmt1* and *Dnmt3a* in the liver in both male and female mice, albeit this effect was significant only in male mice. In CAST/EiJ mice, a significant decrease in expression of *Dnmt3a* was observed in the liver in both male and female mice. In the lungs, a significant decrease in expression of *Dnmt3a* and *Dnmt3b* was observed in male mice only.

Sex-specific differences in 1,3-butadiene-induced histone modifications

Disruption of the chromatin structure has been associated with chemical carcinogen exposure [14, 91, 135]. In the present study, histone modifications that are related to chromatin assembly and transcription repression were investigated. Figure 5 shows the levels of

H3K9me3, H3K27me3, and H4K20me3 in the liver and kidney. In male C57BL/6J mice, effects of 1,3-butadiene on post-translational histone modifications were concordant with previously reported findings, which showed a significant increase in trimethylation of histones H3K9, H3K27 and H4K20 in the kidney [84]. In female C57BL/6J mice, significant increases in trimethylation of H3K27 and H4K20 were also observed in the kidney. A significant increase in H3K27ac was only observed in the liver of C57BL/6J male mice. In CAST/EiJ strain, 1,3-butadiene-exposed male mice exhibited significant increases in histone H3K9, H3K27, and H4K20 trimethylation in the liver, concordant with previous report [14]. In contrast, there was a significant decrease in trimethylation of histone H4K20 in the kidney of male CAST/EiJ mice and decrease in trimethylation of histones H3K9 and H3K27 in in the kidney of female mice. We also evaluated histone methyltransferase genes; however, there were no significant changes (data not shown).

3.4 Discussion

This study used 1,3-butadiene as a model genotoxic environmental chemical to investigate sex-specific differences in genotoxic and epigenetic effects. Exposure to 1,3-butadiene has been previously associated with the formation of DNA monoadducts and DNA-DNA crosslinks [136], as well as changes in DNA methylation and chromatin structure [14]. Our results indicate that 1,3-butadiene-induced DNA damage and epigenome disruption are sex-dependent. In addition, these observed sex-specific 1,3-butadiene-effects are strain-specific.

It is well established that exposure to 1,3-butadiene results in the formation of DNA monoadducts and interstrand crosslinks as supported by animal and human studies [88]. Similar to previous findings, we observed that 1,3-butadiene-induced DNA damage was highest in the lung, followed by the kidney, and liver. Our results also are in accord with previously identified inter-strain differences in DNA adduct formation between male CAST/EiJ and C57BL/6J mice [14, 77]. We found significant sex-specific differences in both monoadducts and interstrand crosslinks only in the lung of C57BL/6J mice. Sex-specific differences in 1,3-butadiene genotoxicity are well-documented. Female rats and mice have twice the DNA-DNA crosslink formation in the liver compared to male rats and mice [126]. Additionally, female rats and mice have a higher incidence of *Hprt* mutations [127]. Human molecular epidemiology studies reported similar or lower globin adduct levels in 1,3-butadiene-exposed female factory workers compared to male workers [128]. Our results also report levels of DNA damage in C57BL/6J mice that are concordant with findings in humans. Sex-specific differences in THB-G adduct levels have not been previously reported; however, in the present study we observed significant differences between C57BL/6J male and female mice [88]. The interplay between strain and sex may influence susceptibility to DNA damage. Strain- and sex-specific molecular events including upregulation of DNA repair enzymes and chromatin remodeling could be responsible for the observed significant differences in DNA adduct and crosslink formation between C57BL/6J male and female mice.

Investigating the expression of DNA repair enzymes may explain the variability in DNA damage observed between strains and sexes [137]. Interestingly, the effect of

exposure to 1,3-butadiene on DNA repair gene expression in the base and nucleotide excision pathways was rather muted overall. However, we observed up to an 8-fold induction of *Mgmt* in kidneys of female mice of C57BL/6J strain, which may be a result of their sensitivity to the adverse effects of 1,3-butadiene in comparison to other mouse strains [14]. C57BL/6J male mice also demonstrate an increase in expression in the lung, which could be in response to the higher incidence of DNA adduct and crosslink formation. While 1,3-butadiene is not known to form O^6-alkylguanine adducts, DNA cross-links at the O^6 position of guanine generated by butadiene present in tobacco smoke have been reported [138]. In addition, human MGMT could play a role in repair of these crosslinks [139]. Sex-specific differences in DNA repair gene expression have been identified in acute low-dose exposure to radiation, which induced a significant upregulation of *Mgmt* in female mice [140]. In addition, up-regulation of *Mgmt*, as observed in C57BL/6J female mice in the kidney, has been associated with resistance to carcinogenesis [141].

Chemical exposure can also result in disruption of global DNA methylation [33]. Sex-dependent changes in DNA methylation have been reported. For example, exposure to radiation and arsenic led to loss of methylation, however it was more evident in females compared to males [142, 143]. Exposure to 1,3-butadiene is associated with strain- and tissue-specific changes in DNA methylation, with varying degrees of cytosine DNA hypomethylation or no effect [14, 84].

In the present study we found a sex- and strain-dependent hypomethylation of major repetitive elements in the liver in male C57BL/6J mice and in the lung in female

C57BL/6J mice, two target organs for 1,3-butadiene-induced carcinogenesis in mice. In contrast, no treatment-related cytosine DNA methylation changes were found in the kidney, a non-target organ, in male and female C57BL/6J mice, even though the level of 1,3-butadiene-induced genotoxic alterations in the kidney of C57BL/6J mice was greater than in the liver. These findings provide a strong support of the importance of epigenetic alterations, in addition to genotoxic alterations, in the mechanism of chemical carcinogenesis. Additionally, the results of the present study corresponded to growing evidence of the ability of genotoxic carcinogens to induce non-genotoxic genomic alterations, e.g. transcriptomic and epigenomic, in target organ only. Specifically, it has been demonstrated that *in vivo* or *in vitro* exposure to the model genotoxic carcinogen benzo[*a*]pyrene resulted in the induction of both genotoxic and non-genotoxic alterations in target, but not in non-target organs [144, 145].

In order to uncover the underlying mechanisms of 1,3-butadiene-induced DNA methylation effects, we investigated the expression of DNA methyltransferases, which control the status of cytosine DNA methylation. Surprisingly, we found only slight down-regulation of *Dnmt1* and *Dnmt3a* in the livers of male C57BL/6J, indicating that inhibition of DNA methyltransferases is not the main factor that caused cytosine DNA hypomethylation in 1,3-butadiene-carcinogenesis target organs in C57BL/6J mice. It is well-known that the accurate status of the DNA methylome is maintained by the following factors; proper functioning of DNA methylation and demethylation pathways, DNA integrity, and one-carbon metabolism, which provides methyl groups for all cellular methylation reaction [146]. Our data indicate that neither inhibition of DNA

methyltransferases, nor 1,3-butadiene-induced genotoxic alterations, except in the lung of female mice, could explain the loss of cytosine DNA methylation in the liver and lung of C57BL/6J mice. This indicates that disruption of other molecular pathways such as mitochondrial dysfunction [73] and 1,3-butadiene-induced oxidative stress [147, 148], known factors that cause cytosine DNA hypomethylation [149], or alterations in one-carbon metabolism and tricarboxylic acid cycle, may cause loss of DNA methylation in the liver and lung of C57BL/6J mice.

Another interesting finding in our study is increased cytosine DNA methylation in the lung and liver in 1,3-butadiene-exposed CAST/EiJ female mice and no methylation changes in these organs in male mice. This may be attributed, at least in part, to substantially lower levels of 1,3-butadiene-induced DNA adducts and crosslinks in CAST/EiJ mice as compared to C57BL/6J mice. Although hypermethylation has been implicated in carcinogenesis [150], evidence suggests that increased levels of cytosine DNA methylation at repetitive elements could also provide protection against DNA damage [151]. Hypermethylation has also been proposed as a protective epigenetic mechanism against repeat expansion-associated pathologies [134, 152]. An additional mechanism that may prevent the loss of cytosine DNA methylation in target organs is formation of compact chromatin in response to chemical exposure. Indeed, we observed an increase in trimethylation of histones H3K9, H3K27, and H4K20 in the liver of male CAST/EiJ mice. This finding reinforces previously reported observations with exposure to a higher dose of 1,3-butadiene [14].

In summary, this study focused on identifying sex-specific differences in DNA damage and global epigenetics. Our results demonstrate that although DNA damage was present in all tissues, changes in DNA methylation and histone modification patterns varied between strains, sexes, and tissues. The present study demonstrates the existence of sex-specific differences in response to 1,3-butadiene exposure and provides strong evidence to support NIH policy on including both sexes in experimental animal studies. Additional follow up experiments that evaluate the chromatin landscape and gene expression profiles through ATAC-seq and RNA-seq may provide additional insight to sex-dependent toxicant induced responses. Furthermore, miRNA are also key epigenetic regulators that have been shown to have sex-dependent expression. Investigating the interplay between the miRNome and epigenetic machinery could provide further mechanistic insights.

Acknowledgements

This work was supported, in part, by grants from National Institutes of Health (R01 ES023195, R01 CA095039 and P30 ES025128). The views expressed in this article are those of the authors and do not necessarily reflect the views of NIH.

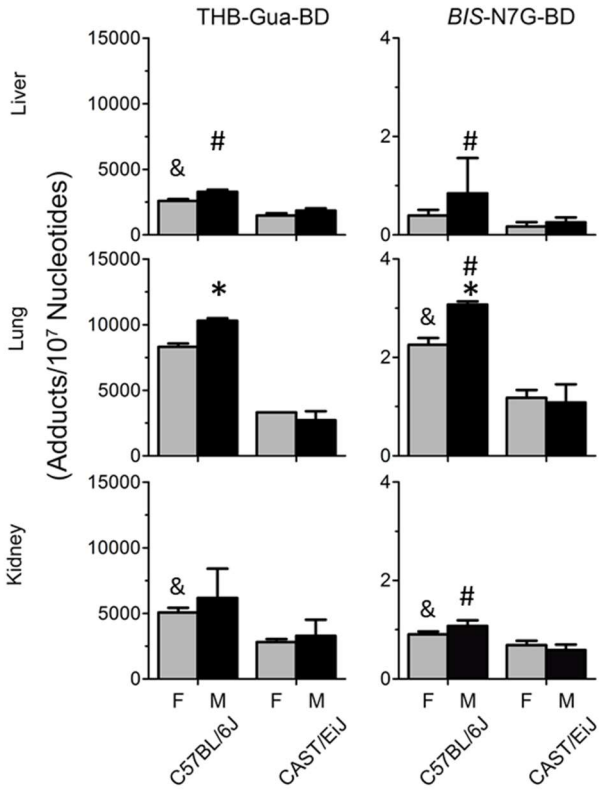

Figure 3.1 Levels of THB-Gua-butadiene adducts (left panel) and *bis*-N7G-butadiene crosslinks (right panel) in tissues from female (gray bars) and male (black bars) mice exposed to 425 ppm of 1,3-butadiene. Data are presented as mean +/-SD. Asterisk, pound, and ampersand (*, #, and &) denote significant ($p<0.05$) differences in the levels of adducts or crosslinks between C57BL/6J or CAST/EiJ male and female mice, C57BL/6J and CAST/EiJ male mice, or C57BL/6J and CAST/EiJ female mice, respectively.

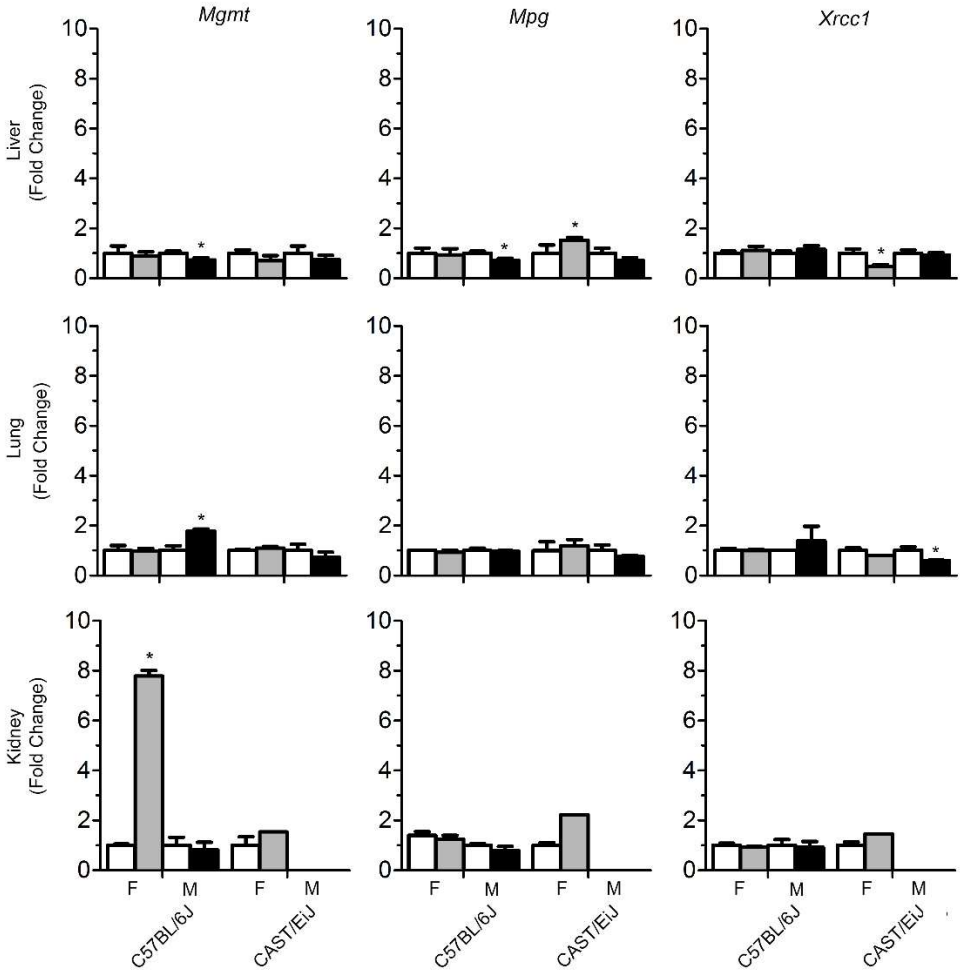

Figure 3.2 Effects of 1,3-butadiene exposure on the expression of DNA repair genes across strains and tissues (liver – top panel, lung – middle panel, kidney – bottom panel). White bars are controls, gray bars are treated females and black bars are treated males. Results are presented as the average fold change relative to the control values for each strain and sex. Data are expressed as mean +/-SD. Asterisks (*) denote significant ($p<0.05$) differences from corresponding strain and sex controls. Missing samples (male kidney, CAST/EiJ) have no bars.

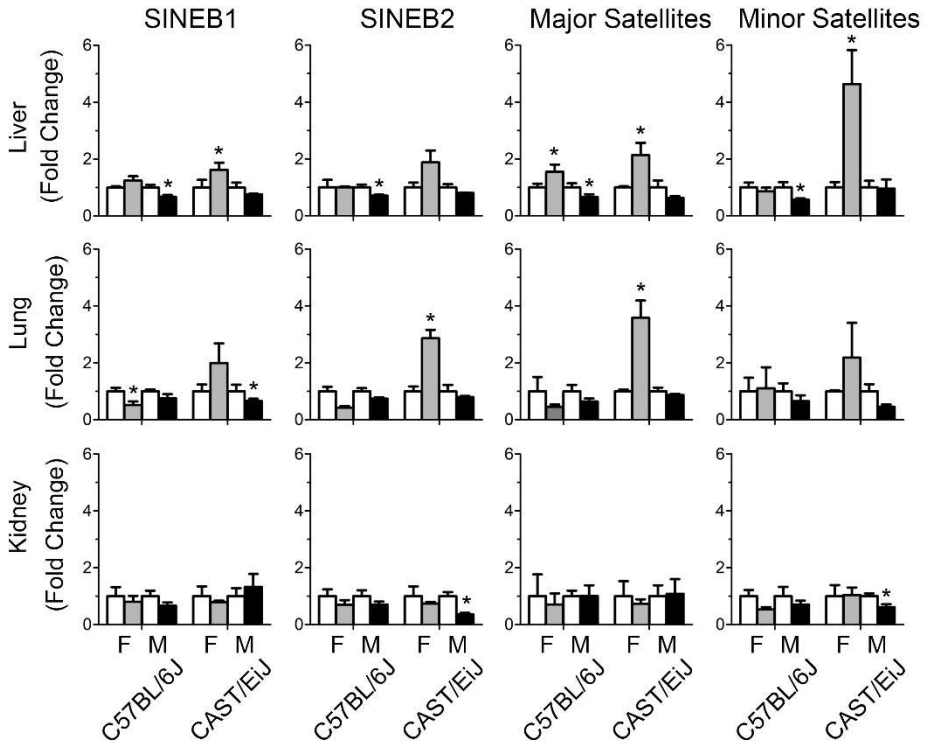

Figure 3.3 Effects of 1,3-butadiene exposure on the extent in DNA methylation across strains and tissues (liver – top panel, lung – middle panel, kidney – bottom panel). White bars are controls, gray bars are treated females, and black bars are treated males. The results are presented as fold change relative to the control values for each strain and sex. Data are presented as mean +/-SD. Asterisks (*) denote significant ($p<0.05$) difference from the corresponding strain and sex controls.

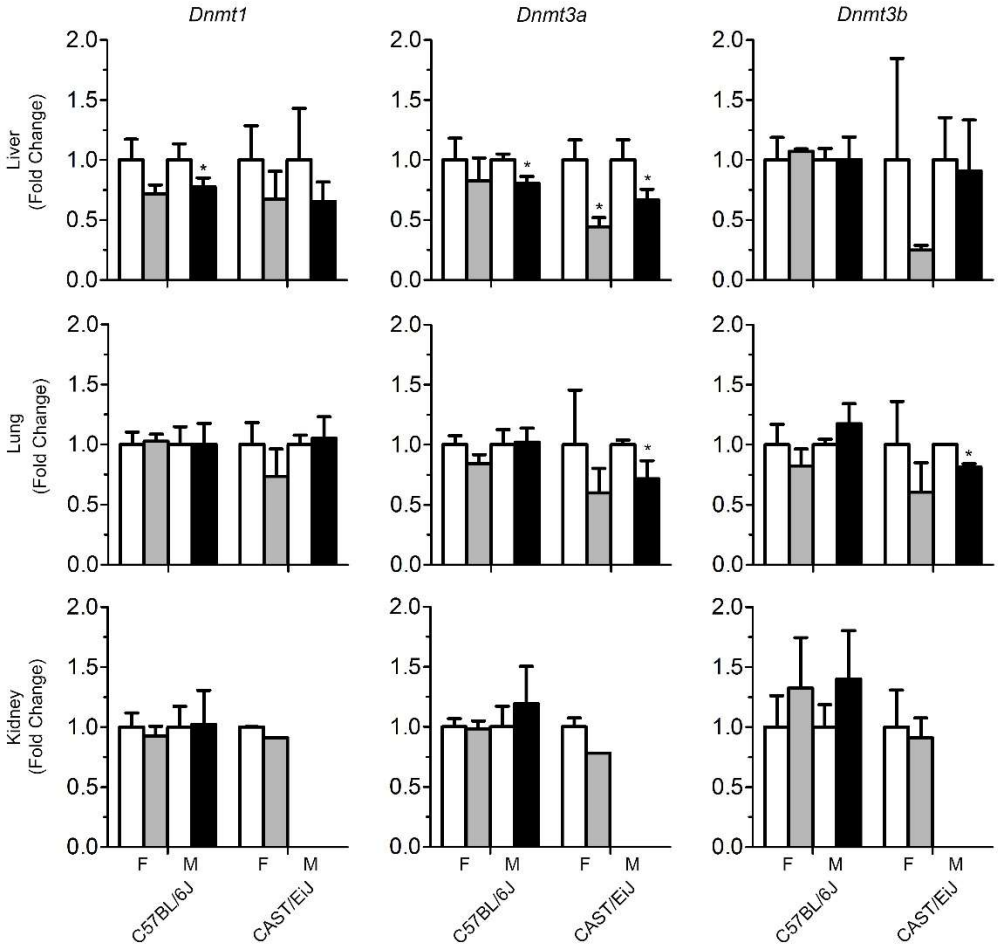

Figure 3.4 Effects of 1,3-butadiene exposure on the expression of DNA methyltransferase genes across strains and tissues (liver – top panel, lung – middle panel, kidney – bottom panel). White bars are controls, gray bars are treated females and black bars are treated males. The results are presented as fold change relative to the control values for each strain and sex. Data are presented as mean +/-SD. Asterisks (*) denote significant ($p<0.05$) differences from the corresponding strain and sex controls.

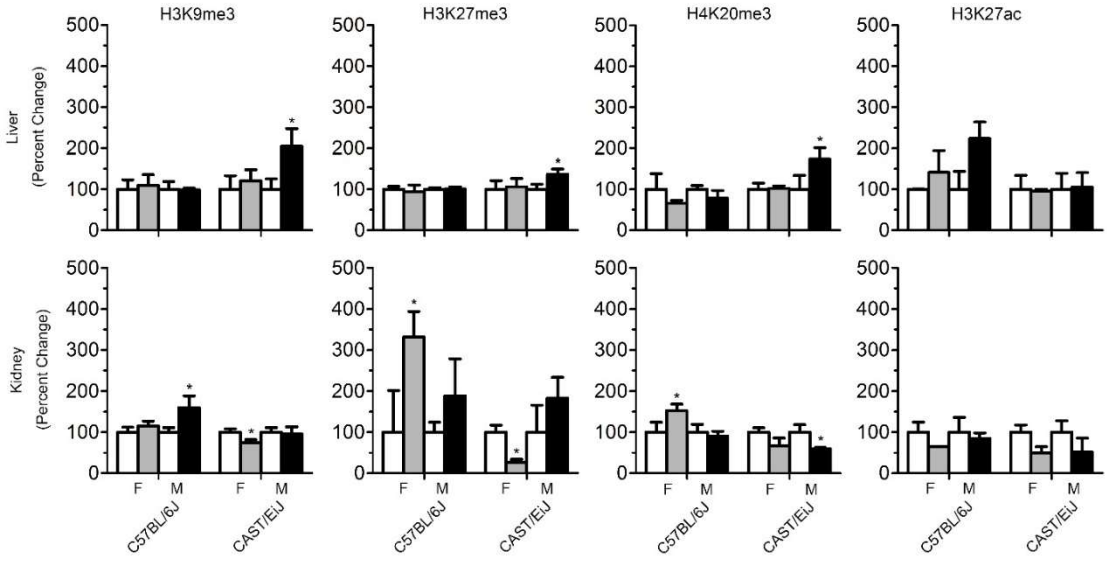

Figure 3.5 Effects of 1,3-butadiene exposure on histone trimethylation and acetylation across strains and tissues (liver – top panel, kidney – bottom panel). All histone levels were evaluated by immunostaining using specific antibodies against trimethylated or acetylated histones. Equal sample loading was confirmed by immunostaining against total H3 or H4. Densitometry analysis of the immunostaining results is shown as percent change in methylation levels relative to control after correction for the total histone levels in each sample. White bars are controls, gray bars are treated females and black bars are treated males. The results are presented as fold change relative to the control values for each strain and sex in mouse tissues. Data are presented as mean +/-SD. Asterisks (*) denote significant ($p<0.05$) differences from the corresponding strain and sex controls.

CHAPTER IV

MICRORNA AS REGULATORS OF 1,3-BUTADIENE-INDUCED STRAIN- AND TISSUE-SPECIFIC EFFECTS IN MICE

4.1 Introduction

microRNA (miRNA) are short, noncoding RNA that act as post-transcriptional repressors through translational inhibition or degradation of mRNA. miRNA can regulate numerous genes or one gene can be targeted by multiple miRNA. In addition, miRNA are involved in diverse biological processes such as apoptosis, cell proliferation, and development[153-155]. Furthermore, aberrant expression of miRNA has been implicated in various diseases including carcinogenesis[156].

In recent years, research focusing on miRNA in the field of toxicology has rapidly expanded. Accumulating evidence shows dysregulation of miRNA expression occurs in response to environmental toxicants such as heavy metals, air pollution, and cigarette smoke[156-158]. In humans and rodents, miRNA have also been identified as biomarkers of chemical exposure and tissue-specific injury[159]. However, the underlying mechanisms of miRNA expression in chemical-induced carcinogenesis is still undergoing investigation.

Exposure to 1,3-butadiene a model genotoxic chemical, results in DNA damage and epigenetic effects. In previous studies, we have observed 1,3-butadiene-induced strain-specific DNA damage and epigenetic alterations[14, 58]. Population-based models have demonstrated inter-strain variability in the chromatin remodeling response which may represent a mechanism for inter-strain differences in DNA damage[14, 160]. In addition,

tissue-specific epigenetic modifications in response to 1,3-butadiene exposure have been observed[84]. Alterations in global DNA methylation and histone modifications associated with genomic instability were observed in lung and liver which are target organs of 1,3-butadiene carcinogenesis but not in the kidney, a non-target organ.

In this study, we expanded upon our previous work which focused on 1,3-butadiene-induced global histone modifications and DNA methylation changes by investigating miRNA expression in response to 1,3-butadiene exposure. We hypothesized that miRNA regulate strain- and tissue-dependent transcriptional and epigenetic responses to 1,3-butadiene exposure in CAST/EiJ and C57BL/6J mice. These mice were exposed to clean air or 625ppm 1,3-butadiene (6 hr/day, 5 days/week) for 2 weeks. Distinct miRNA expression profiles were observed between strains and tissues as a result of 1,3-butadiene exposure. In addition, we identified miRNA as candidate master regulators of 1,3-butadiene-altered gene expression. Our results indicate that miRNA may influence strain- and tissue-dependent chemical-induced carcinogenesis.

4.2 Materials and Methods

Animals and exposures

The *in vivo* portion of this study and tissue collection was detailed in *Chappell et al*[78]. 1,3-butadiene exposure results in tumorigenesis at doses from 6.25ppm to 8000ppm[99]. In brief, male CAST/EiJ and C57BL/6J mice (Jackson Laboratory, Bar Harbor, ME; 9-13 weeks old) were exposed to filtered air or 1,3-butadiene for 6h/day, 5 days/week, Monday-Friday, over a 2-week period as previously described *Chappell et al*[78]. In this study, the

average concentration of 1,3-butadiene in the exposure chamber was 593 +/- 61 ppm. Animals were treated humanely and with regard for alleviation of suffering. The procedures were approved by the Institutional Animal Care and Use Committee at the University of North Carolina at Chapel Hill.

RNA and small RNA sequencing, data processing, and differential analysis

Total RNA was isolated from flash-frozen tissues with the Qiagen miRNeasy Kit. RNA and small RNA libraries were prepared for sequencing as described in *Chappell et al*[78]. Libraries were sequenced on the Illumina Hiseq 2500. miRNAs were annotated and quantified using the bioinformatics pipeline miRquant 2.0 as described by *Kanke et al* [161]. RNA-seq data was processed as described in *Chappell et al*[78]. Differentially expressed mRNAs and miRNAs were identified by using the DESeq2 version 1.24.0 in R version 3.6[162]. A minimum threshold of 10 reads in at least five mice from one strain was required.

miRNA pathway enrichment analysis

In order to determine the pathways targeted by miRNA that were significantly enriched in response to 1,3-butadiene exposure, differentially expressed miRNA (adjp<0.1) identified in each tissue from each strain were uploaded into DIANA-miRPath[163]. Analyses were conducted under the following settings: Mouse, Tarbase, and genes union. Results were filtered by biological relevance and significance ($p<0.05$).

Identification of miRNA regulatory hubs

Candidate miRNA regulatory hubs of 1,3-butadiene-induced expression were identified by Monte Carlo simulation as previously described[78, 164]. In this analysis, we used differentially expressed genes (padj <0.1) in 1,3-butadiene-exposed mice relative to control mice for each strain and tissue. Gene sets were separated out and run by expression directionality. Predicted miRNA targets were required to be conserved only in mouse. Significant candidate miRNA (p-value <0.1) that were predicted by miRhub were cross-referenced with significantly differentially expressed miRNA in 1,3-butadiene-exposed mice relative to control mice for each strain and tissue. Our final list of candidate miRNA was selected based on the directionality of miRNA and mRNA expression.

4.3 Results

In this study, we characterized strain- and tissue-specific miRNA expression in response to 1,3-butadiene, a model genotoxic carcinogen. In order to investigate the role of miRNA in chemical-induced carcinogenesis and potentially identify biomarkers of exposure, we used two inbred strains with established inter-strain differences in 1,3-butadiene-induced DNA damage and epigenetic effects.

Strain-specific miRNA expression at baseline across strains and tissues

In order to investigate if baseline miRNA expression profiles influence responses to 1,3-butaidene exposure, we compared miRNA expression in the lung, liver, and kidney from

CAST/EiJ and C57BL/6J control mice which were exposed to clean air. **Figure 1** shows the average reads per million mapped for each miRNA there was expressed in both strains at baseline. We identified 263 miRNA in lung, 172 miRNA in liver, and 176 miRNA in kidney that were differentially expressed between control CAST/EiJ and C57BL/6J (padj <0.1). We identified miRNA that are recognized as biomarkers for tissue-specific toxicity and disease; 3 in the lung, 3 in the liver, and 5 in the kidney (**Figure 1**). **Figure 2A** shows differentially expressed miRNA identified from the baseline inter-strain comparison (**Supplemental Table 1**). There were 22 differentially expressed miRNA common among lung, liver, and kidney. The lung had the highest number of tissue-specific differentially expressed miRNA. The liver and kidney were similar with 83 and 89 differentially expressed miRNA. Next, we used differentially expressed miRNA and their validated mRNA targets to identify biological networks present at baseline between strains and across tissues. **Figure 2B** shows the pathways (p-value <0.05) that were significantly enriched in CAST/EiJ and C57BL/6J control mice (**Supplemental Table 2**). Tissue-specific pathways are listed in **Figure 2C**. Each tissue presented pathways that were involved in general biological processes as well as pathways specific to carcinogenesis. The liver had the most tissue-specific pathways followed by lung, and kidney.

Strain-specific miRNA expression in response to 1,3-butadiene across strains and tissues

We investigated if 1,3-butadiene-induced miRNA expression profiles differed between strains and across tissues. **Table 1** shows differentially expressed miRNA and isomiRs

detected from control verse 1,3-butadiene exposure contrasts for each strain and tissue. There were more differentially expressed miRNA in 1,3-butadiene-exposed C57BL/6J mice to 1,3-butadiene-exposed CAST/EiJ across tissues. In both strains, the lung had the most differentially expressed miRNA followed by the kidney and liver. There were no differentially expressed miRNA identified in the liver of CAST/EiJ. Differentially expressed isomiRs presented similar findings. **Figure 3A** shows the common and unique miRNA across strains and tissues in response to 1,3-butadiene exposure (**Supplemental Table 3**). The lung and kidney of 1,3-butadiene-exposed C57BL/6J mice had the highest number of tissue-specific differentially expressed miRNA. There were 75 differentially expressed miRNA in common between the lung and kidney in 1,3-butadiene-exposed C57BL/6J mice compared to 1,3-butadiene exposed CAST/EiJ mice which had zero differentially expressed miRNA in common. Between 1,3-butadiene exposed CAST/EiJ and C57BL/6J lung, there were 4 differentially expressed miRNA in common and between 1,3-butadiene CAST/EiJ and C57BL/6J kidney, there was 1 differentially expressed miRNA in common.

Next, we explored miRNA targeted pathways in response to 1,3-butadiene exposure. **Figure 3B** shows enriched pathways targeted by significant miRNA for 1,3-butadiene-exposed CAST/EiJ and C57BL/6J mice in lung and kidney. There was twofold more strain-specific pathways identified for C57BL/6J mice in the lung and eightfold more in the kidney compared to CAST/EiJ mice (**Supplemental Table 4**). **Figure 3C** shows the pathways that were common between CAST/EiJ and C57BL/6J mice in lung. We identified several pathways including metabolism of xenobiotics by cytochrome P450,

chemical carcinogenesis and glutathione metabolism that were relevant to 1,3-butadiene exposure. We also detected pathways related to chemical exposure in the kidney in CAST/EiJ which are shown in **Figure 3D**.

Candidate drivers of 1,3-butadiene-induced differential gene expression

We identified 9 candidate miRNA regulatory hubs across strains and tissues (**Table 4.1**).

4.4 Discussion

1,3-Butadiene is a known rodent and human carcinogen that is both an occupational and environmental health hazard. Genotoxicity is an established mechanism of 1,3-butadiene carcinogenicity; however, it does not explain the tissue-specific tumor development observed in mice. Our previous work demonstrated strain- and tissue-specific alterations in epigenetic effects in response to 1,3-butadiene exposure which may contribute to tissue-specific toxicity. In the present study, we aimed to extend our findings by evaluating miRNA expression. miRNA represent another epigenetic mechanism for regulating gene expression and have been implicated in carcinogenesis. Our results show that 1,3-butadiene-induced miRNA expression in C57BL/6J and CAST/EiJ mice occurs in a strain- and tissue-dependent manner and may influence the development of carcinogenicity in the target organs of 1,3-butadiene carcinogenicity.

We observed marked strain-specific effects on miRNA expression between C57BL/6J and CAST/EiJ mice. The effect of 1,3-butadiene had a minor effect on miRNA expression in CAST/EiJ mice in comparison to C57BL/6J mice. This observation is

concordant with 1,3-butadiene-induced mRNA expression which was previously evaluated in CAST/EiJ and C57BL/6J mice[77]. Although there is sufficient evidence that miRNA expression is affected by toxicant exposure, few studies have addressed inter-strain differences in miRNA expression in response to chemical exposure. Inter-strain differences were reported in miRNA expression in the liver of mice that were fed a methyl-deficient diet in order to induce nonalcoholic steatohepatitis[165]. These strain-specific differences were implicated in the susceptibility to disease development. Two studies used a panel of inbred mouse strains to evaluate population variability in miRNA expression. First, exposure to dust mite allergen resulted in variability in miRNA expression between strains in the lung[166]. A second study identified inter-strain differences in plasma miRNA expression along with a significant correlation with miRNA expression and strain-specific liver injury as a result of cholate deficient diet[167].

With respect to tissue-specific effects on miRNA expression, we observed similarities between C57BL/6J and CAST/EiJ mice across tissues. In both strains, the most differentially expressed miRNA were identified in the lung, followed by the kidney. Interestingly, there was almost no effect of 1,3-butadiene exposure on miRNA expression in the liver of both strains. Observed differentially expressed miRNA may serve as potential biomarkers of 1,3-butadiene exposure. However, they will not serve as markers of 1,3-butadiene-induced DNA damage which was present in all tissues. Exploring additional markers for 1,3-butaidene-induced DNA damage may offer further insight. Increasing our knowledge of miRNA in response to chemical exposure will help with exposure assessment as well as hazard characterization.

In this study, we explored an additional epigenetic mechanism, miRNA in response to 1,3-butadiene exposure. We observed distinct miRNA expression profiles across strains and tissues. Our results reinforce previously described 1,3-butadiene-induced strain- and tissue-specific epigenetic effects. In addition, our findings emphasize the importance of considering genetic differences in experimental animal studies. Interestingly, we identified miRNA as candidate master regulators of 1,3-butadiene-induced gene expression. Collectively these findings indicate that miRNA may influence strain- and tissue-susceptibility to 1,3-butadiene-induced carcinogenesis.

Table 4.1 The number of differentially expressed miRNA and isomiRs in response to 1,3-butadiene exposure for each strain and tissue.

Strain	Tissue	Total DE genes (padj<0.1)	miRNA	isomiR
C57BL/6J	Lung	210	142	68
	Liver	0	0	0
	Kidney	142	94	48
CAST/EiJ	Lung	27	15	12
	Liver	1	1	0
	Kidney	15	14	68

Table 4.2 Candidate miRNA identified as master regulators of mRNA expression.

Strain	Tissue	miRNA family	miRhub p-value
C57BL/6J	Lung	miR-126-5p	0.009980
		miR-142-5p	0.073852
	Liver	miR-324-5p	0.007984
		miR-10abc/10a-5p	0.009980
CAST/EiJ	Lung	miR-125b-2-3p	0.059880
		miR-344a-5p/484/3155/3155b	0.021956
		miR-151-5p/151b	0.098802
		miR-3057-5p	0.062874
	Kidney	miR-486-5p/3107	0.059880

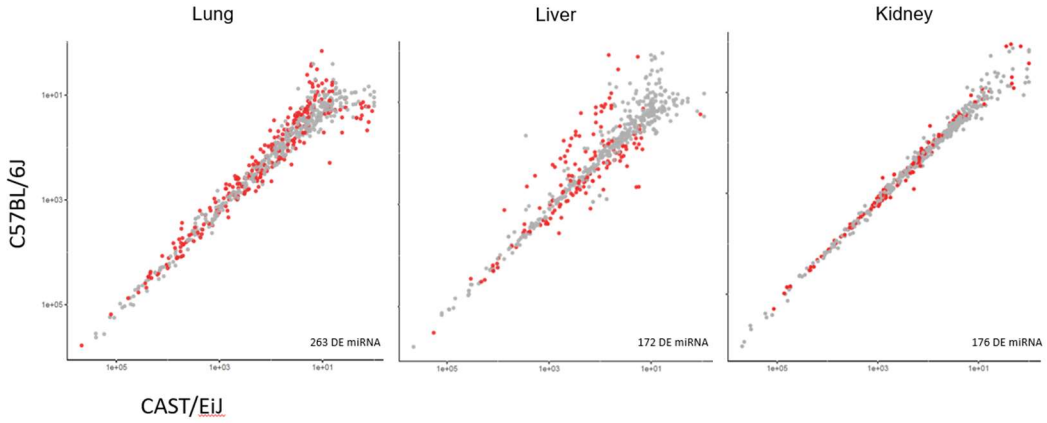

Figure 4.1 Baseline miRNA expression across strains and tissues. Scatterplots represent the average reads per million mapped miRNAs (RPMM) for each miRNA expressed in both control C57BL/6J and CAST/EiJ mice across tissues. Circles are colored according to significance (red, padj < 0.1: gray, not significant).

A. DE miRNA at baseline

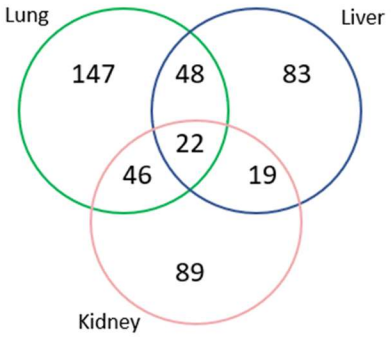

B. Tissue-specific miRNA Pathways

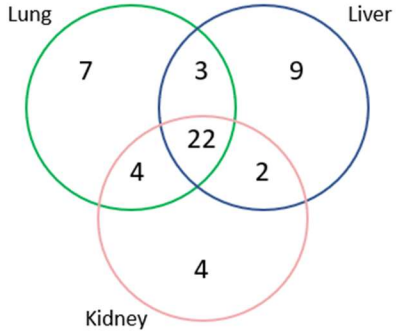

C.

Tissue	Pathway	P-value (<0.05)	#genes	#miRNA
Lung	Glycosphingolipid biosynthesis - ganglio series	6.83E-05	9	12
	Vitamin B6 metabolism	0.0008162		7
	Glyoxylate and dicarboxylate metabolism	0.00915792	16	19
	Peroxisome	0.01107254	46	27
	Small cell lung cancer	0.01967028	46	33
	Carbon metabolism	0.01967028	59	31
	Gap junction	0.02545381	44	28
Liver	Adipocytokine signaling pathway	0.04788674	32	15
	Biosynthesis of unsaturated fatty acids	0.03008566	13	14
	Central carbon metabolism in cancer	0.04059314	28	15
	Circadian rhythm	0.01878786	16	11
	Fatty acid elongation	0.01455008	13	12
	Galactose metabolism	0.02718691	14	9
	Glycosaminoglycan biosynthesis - chondroitin sulfate / dermatan sulfate	0.00113597	10	7
	Inositol phosphate metabolism	0.03397717	27	16
	Insulin signaling pathway	0.00071896	69	21
Kidney	Other types of O-glycan biosynthesis	0.03220975	11	11
	p53 signaling pathway	0.03483094	30	10
	Renal cell carcinoma	4.38E-08	42	13
	Sphingolipid signaling pathway	0.00074511	61	11

Figure 4.2 Pathway analysis of baseline miRNA expression across strains and tissues. A. Venn diagrams represent differentially expressed miRNA identified from the baseline inter-strain comparison for each tissue (padj < 0.1). Numbers within each sector of circles represent either unique or common differentially expressed miRNA. B. Tissue-specific pathways (p-value <0.05) using the differentially expressed tissue-specific miRNA (padj <0.1). C. Table shows the tissue-specific pathways. The p-value is the enrichment value derived from the DIANA-miRPATH analysis using the DIANA-tarbase (experimentally validated). Second and third column show the number of genes targeted by miRNA within the pathway and number of miRNA in pathway.

A.

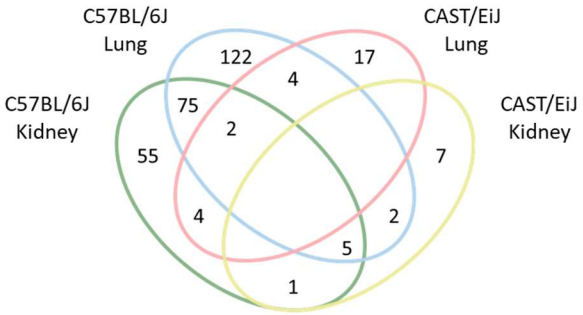

B.

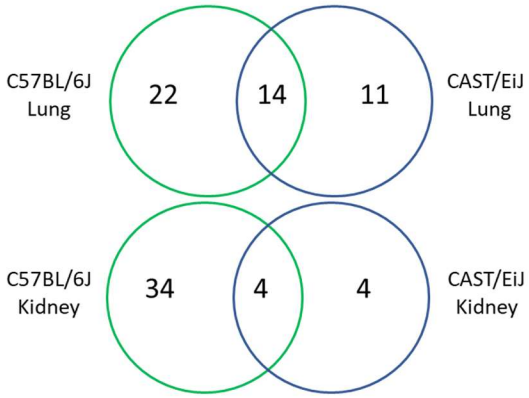

C.

Pathway	P-value (<0.05)	#genes	#miRNA
Metabolism of xenobiotics by cytochrome P450	1.96E-21	3	1
Steroid biosynthesis	3.44E-07	1	1
Mucin type O-Glycan biosynthesis	3.31E-03	1	1
Chemical carcinogenesis	1.19E-03	3	1
Lysine degradation	2.16E-02	2	1
Glutathione metabolism	2.16E-02	4	1

Pathway	P-value (<0.05)	#genes	#miRNA
Lysine degradation	9.56E-07	8	2
Biosynthesis of unsaturated fatty acids	8.17E-04	4	1
Adherens junction	8.17E-04	10	3
Transcriptional misregulation in cancer	2.17E-03	11	1
Wnt signaling pathway	4.55E-03	13	3
Proteoglycans in cancer	1.03E-02	13	2
Drug metabolism - other enzymes	2.03E-02	4	1
FoxO signaling pathway	4.56E-02	13	1

Figure 4.3 Strain-specific miRNA expression in response to 1,3-butadiene across strains and tissues. A. Venn diagrams represent differentially expressed miRNA in response to 1,3-butadiene exposure for each strain and tissue (padj < 0.1). Numbers within each sector of circles represent either unique or common differentially expressed miRNA. B. Venn diagrams show strain-specific pathways in response to 1,3-butadiene exposure. Panel C shows 1,3-butadiene-induced pathways that are shared between C57BL/6J and CAST mice in the lung. Panel D shows 1,3-butadiene-induced pathways that were identified in the kidney of CAST mice.

CHAPTER V

SUMMARY

5.1 Significance

DNA damage occurs as a result of exposure to environmental and occupational chemicals and can lead to cancer. Toxicant exposure can also alter the state of the epigenome, creating genome instability which is an enabling characteristic of cancer[30]. Epigenetic modifications are recognized as being equally important in the development of carcinogenesis as genotoxic events such as DNA damage[31, 50]. In addition, it is well established that crosstalk between these two types of molecular perturbations occurs during the carcinogenic process[101]. Epigenetic events may facilitate carcinogenesis or they may occur as a result of genotoxicity. Therefore, it is critical to understand the role of epigenetic modifications in chemical-induced carcinogenesis. In this dissertation, we address genotoxicity and epigenetic events in response to chemical exposure in order to understand the interplay between these molecular initiating events. Furthermore, we sought to understand mechanisms and biological drivers for inter-individual susceptibility to chemical exposure.

In **specific aim 1**, we investigated inter-individual variability in the effects of 1,3-butadiene exposure using the Collaborative Cross population-based mouse model. We were the first to use this population-wide approach to characterize epigenetic determinants of population variability in response to chemical exposure. We observed marked inter-strain differences in DNA damage and global epigenetic modifications which emphasizes the need to use population-based models in toxicological studies in order to account for

population variability in response to chemical exposure. Importantly, this study also identified tissue-specific epigenetic alterations, providing mechanistic insight for 1,3-butadiene carcinogenesis in target organs. Although there were no significant population changes in global DNA methylation changes, we identified an inverse correlation between THB-Gua adduct levels and SINE B1 methylation in the liver. Evidence shows that exposure to genotoxic chemicals can result in altered DNA methylation leading to transcriptional activation[14, 81, 84]. In addition, we identified four candidate genes related to chromatin remodeling that may act as drivers of inter-strain variability in the modifications of H3K9me3, H3K9ac, and H4K16ac in response to 1,3-butadiene exposure. Furthermore, our study quantified the inter-individual variability in phenotypes allowing for application in human health risk assessment. This approach addresses a critical gap in cancer risk assessment. Overall, our work in **specific aim 1** demonstrates how the Collaborative Cross mouse population can be used to explore mechanistic linkages as well as quantify the degree of inter-individual variability in tissue-specific effects that are relevant to toxicant-induced carcinogenesis.

In **specific aim 2**, we evaluated sex-differences in DNA damage and epigenetic effects in response to 1,3-butadiene exposure. Sex-specific differences in 1,3-butadiene-induced genotoxicity and carcinogenicity are well established; however, it remained unknown whether 1,3-butadiene-associated epigenetic alterations are also sex-dependent. Importantly, our results indicate that 1,3-butadiene-induced DNA damage and epigenome disruption is sex dependent. Furthermore, we also observed that sex-specific effects occur in a strain-specific manner. Our study highlights the importance of understanding the

interplay between strain and sex-specific molecular initiating events. Specifically, DNA repair enzymes and changes in chromatin structure could be driving significant differences in DNA damage between C57BL/6J male and female mice. In addition, our findings suggest that strain and sex-specific effects of 1,3-butadiene on the epigenome may contribute to the known differences in cancer susceptibility. Specific aim 2 also emphasizes the importance of supporting the NIH policy on including both sexes in experimental animal studies.

In **specific aim 3**, we expanded our investigation of epigenetic alterations in response to chemical exposure to include miRNA, an additional epigenetic endpoint. We observed marked differences in 1,3-butadiene-induced miRNA expression between strains and tissues. We also identified several differentially expressed miRNA in the lung of C57BL/6J mice which may explain strain- and tissue-specific sensitivity to 1,3-butadiene exposure in comparison to CAST/EiJ mice. Our results support another epigenetic mark that acts in strain- and tissue-specific manner. These findings are also important for the application of miRNA as biomarkers of exposure to human carcinogens. The results of this study indicate that miRNA may mediate strain- and tissue-dependent variability of 1,3-butadiene-induced epigenetic effects and potentially greater tissue susceptibility to carcinogenesis.

Overall, this dissertation emphasizes the importance of characterizing epigenetic marks as a result of exposure to a human carcinogen. Each specific aim contributed to a better understanding of the molecular events associated with chemical exposure. Our findings reinforce previous work that demonstrates epigenetic events in response to 1,3-

butadiene exposure occur in a strain- and tissue-specific manner. We also show the importance of investigating sex-specific chemical-induced epigenetic and genotoxic effects. In addition, we showed the utility of a population-based mouse model to explore inter-individual variability in epigenetic alterations and DNA damage. Together, our findings increase the knowledge of toxicant-induced epigenetic effects in order to effectively incorporate epigenetic endpoints into human health risk assessment.

5.2 Limitations

Several limitations can be identified with our study designs. We conducted exposures at one concentration of 1,3-butadiene and one time point for each animal study. Additional information may be obtained from investigating the relationship between multiple time points, concentrations, and epigenetic endpoints. Furthermore, the sample size of our animal studies were limited by the size of the exposure chamber. In Chapter II, in order to maximize the number of Collaborative Cross strains used in the experiment, we used a sample size of one mouse per strain. Lastly, in our 2 week exposure design, mice do not develop tumors in response to 1,3-butadiene exposure. Therefore, to validate that strain- and tissue-specific epigenetic alterations may influence individual and target organ susceptibility to carcinogenesis, long term studies should be conducted.

The studies in this dissertation could be enhanced by incorporating several additional experiments. First, conducting ATAC-seq, RNA-seq, and small RNA-seq could help evaluate the chromatin landscape, transcriptome, and miRnome and provide additional insight to individual (Chapter II) and sex-specific chemical-induced responses

(Chapter III). Global epigenetic experiments are informative however including next generation sequencing technologies would allow for the integration of ATAC-seq and RNA-seq data to identify potential gene regulatory regions. Second, we could investigate the protein levels of genes of interest identified in our studies. In Chapter II, we identified four candidate genes as drivers of inter-individual variability of 1,3-butadiene-induced chromatin structure alterations. In Chapter III, we evaluated the gene expression of DNA repair enzymes and DNA methyltransferases. Finally, in Chapter IV, we identified target genes of miRNA who may act as regulators of 1,3-butadiene-induced mRNA expression. Therefore, in these studies we could evaluate the levels of protein for each gene to better understand these genes and their relevant biological processes.

5.3 Future directions

We have shown that exposure to 1,3-butadiene, a model genotoxic chemical, results in DNA damage and epigenetic effects. In addition, we have demonstrated that epigenetic and chromatin effects may be a key driver of tissue-specific susceptibility to genotoxic effects of butadiene [58, 77, 84]. However, we have yet to explore the persistence of epigenetic modifications after cessation of exposure to an environmental toxicant such as 1,3-butadiene. Although the persistence of effects from exposure to environmental chemicals are of great interest, they are not well characterized. Few studies address the lasting effects chemical exposure has on both the epigenome and the transcriptome. The available data is conflicting, indicating that DNA damage and epigenetic effects from

chemical exposures could be transient yet other studies show that there could be irreversible aberrant gene expression[168-170].

In future studies, we plan to evaluate the persistence of 1,3-butadiene-induced epigenetic alterations including miRNA expression in target and non-target tissues. In addition, we will also assess genotoxicity and transcriptional alterations. Male CAST/EiJ and C57BL/6J mice will be exposed to 1,3-butadiene for 1 or 2 weeks followed by a "washout" of 1 or 2 weeks of clean air. We will evaluate the persistence of 1,3-butadiene-induced epigenetic effects by evaluating global histone modifications and changes in global DNA methylation. In addition, we will also use ATAC-sequencing to look at changes in the chromatin landscape. Transcriptional effects will be assessed by RNA-sequencing and miRNA expression will be evaluated by small RNA sequencing.

Our work in mice has also shown that inter-individual differences in both genotoxic and epigenetic effects of butadiene exist and can be modeled using a mouse population approach [14, 78]. While these data from an *in vivo* mouse model are important, they require species extrapolation and also were conducted using concentrations far exceeding human exposures. In the future, we aim to transition our previous work from a mouse population model to an *in vitro* human population model and our overall objective will be to investigate population variability in epigenetic alterations and DNA damage in response to butadiene using a human in vitro population-based model.

Previous analysis from our lab shows that with up to 100 individual cell lines it is possible to accurately predict whether the extent of inter-individual variability in response to a chemical is greater than a default uncertainty factor [171]. Thus, population size in both

human lymphoblast and PSC models will be up to 100. Lymphoblasts cell lines will be selected from our library of 1100+ cell lines from 9 populations of European, African, and Asian admixed ancestry, population used in several previous studies [172-175]. The human PSC lines will be ones previously used by Cellular Dynamics International to derive iCell and myCell cardiomyocytes [176]. A concentration-response of butadiene metabolites (1,2-epoxybutene, 1,2,3,4-diepoxybutane and 3,4-epoxy-1,2-butanediol) will be evaluated and include human exposure-relevant doses [177]. We will evaluate cell viability [172], as well as DNA damage and DNA repair kinetics with the high-throughput comet chip assay [178]. Next, we will select 10 PSC and 10 human lymphoblast cell lines based on the variability in responses to DNA damage and cytotoxicity and will evaluate N-7-(2,3,4-trihydroxybut-1-yl)-guanine (THB-Gua) adducts, gene expression [179, 180] and chromatin remodeling [181]. Overall this work will evaluate the use of a novel human *in vitro* population-based model, which could serve as a valuable tool for high-throughput chemical screening to assess human risks of chemical exposure.

REFERENCES

(1) National Research Council. (2009) *Science and Decisions: Advancing Risk Assessment*. National Academies Press, Washington, DC.

(2) Hirschhorn, J. N. (2009) Genomewide association studies--illuminating biologic pathways. *N Engl J Med 360*, 1699-1701.

(3) Wheeler, H. E., Maitland, M. L., Dolan, M. E., Cox, N. J., and Ratain, M. J. (2013) Cancer pharmacogenomics: strategies and challenges. *Nat Rev Genet 14*, 23-34.

(4) Ashley, E. A. (2016) Towards precision medicine. *Nat Rev Genet 17*, 507-522.

(5) Simonds, N. I., Ghazarian, A. A., Pimentel, C. B., Schully, S. D., Ellison, G. L., Gillanders, E. M., and Mechanic, L. E. (2016) Review of the Gene-Environment Interaction Literature in Cancer: What Do We Know? *Genet Epidemiol 40*, 356-365.

(6) Rusyn, I., Gatti, D. M., Wiltshire, T., Kleeberger, S. R., and Threadgill, D. W. (2010) Toxicogenetics: population-based testing of drug and chemical safety in mouse models. *Pharmacogenomics 11*, 1127-1136.

(7) Frazer, K. A., Eskin, E., Kang, H. M., Bogue, M. A., Hinds, D. A., Beilharz, E. J., Gupta, R. V., Montgomery, J., Morenzoni, M. M., Nilsen, G. B., Pethiyagoda, C. L., Stuve, L. L., Johnson, F. M., Daly, M. J., Wade, C. M., and Cox, D. R. (2007) A sequence-based variation map of 8.27 million SNPs in inbred mouse strains. *Nature 448*, 1050-1053.

(8) Threadgill, D. W., and Churchill, G. A. (2012) Ten years of the Collaborative Cross. *Genetics 190*, 291-294.

(9) Zeise, L., Bois, F. Y., Chiu, W. A., Hattis, D., Rusyn, I., and Guyton, K. Z. (2013) Addressing human variability in next-generation human health risk assessments of environmental chemicals. *Environ Health Perspect 121*, 23-31.

(10) Cichocki, J. A., Furuya, S., Venkatratnam, A., McDonald, T. J., Knap, A. H., Wade, T., Sweet, S., Chiu, W. A., Threadgill, D. W., and Rusyn, I. (2017) Characterization of Variability in Toxicokinetics and Toxicodynamics of Tetrachloroethylene Using the Collaborative Cross Mouse Population. *Environ Health Perspect 125*, 057006.

(11) Venkatratnam, A., Furuya, S., Kosyk, O., Gold, A., Bodnar, W., Konganti, K., Threadgill, D. W., Gillespie, K. M., Aylor, D. L., Wright, F. A., Chiu, W. A., and Rusyn, I. (2017) Collaborative Cross mouse population enables refinements to characterization of the variability in toxicokinetics of trichloroethylene and provides genetic evidence for the role of PPAR pathway in its oxidative metabolism. *Toxicological sciences : an official journal of the Society of Toxicology*.

(12) Tsuchiya, M., Ji, C., Kosyk, O., Shymonyak, S., Melnyk, S., Kono, H., Tryndyak, V., Muskhelishvili, L., Pogribny, I. P., Kaplowitz, N., and Rusyn, I. (2012) Interstrain differences in liver injury and one-carbon metabolism in alcohol-fed mice. *Hepatology 56*, 130-139.

(13) Gatti, D. M., Lu, L., Williams, R. W., Sun, W., Wright, F. A., Threadgill, D. W., and Rusyn, I. (2011) MicroRNA expression in the livers of inbred mice. *Mutation research 714*, 126-133.

(14) Koturbash, I., Scherhag, A., Sorrentino, J., Sexton, K., Bodnar, W., Swenberg, J. A., Beland, F. A., Pardo-Manuel Devillena, F., Rusyn, I., and Pogribny, I. P. (2011) Epigenetic mechanisms of mouse interstrain variability in genotoxicity of the environmental toxicant 1,3-butadiene. *Toxicol Sci 122*, 448-456.

(15) Bradford, B. U., Lock, E. F., Kosyk, O., Kim, S., Uehara, T., Harbourt, D., DeSimone, M., Threadgill, D. W., Tryndyak, V., Pogribny, I. P., Bleyle, L., Koop, D. R., and Rusyn, I. (2011) Interstrain differences in the liver effects of trichloroethylene in a multistrain panel of inbred mice. *Toxicol Sci 120*, 206-217.

(16) Gatti, D. M., Zhao, N., Chesler, E. J., Bradford, B. U., Shabalin, A. A., Yordanova, R., Lu, L., and Rusyn, I. (2010) Sex-specific gene expression in the BXD mouse liver. *Physiological genomics 42*, 456-468.

(17) Gatti, D. M., Harrill, A. H., Wright, F. A., Threadgill, D. W., and Rusyn, I. (2009) Replication and narrowing of gene expression quantitative trait loci using inbred mice. *Mammalian genome : official journal of the International Mammalian Genome Society 20*, 437-446.

(18) Pogribny, I. P., Tryndyak, V. P., Bagnyukova, T. V., Melnyk, S., Montgomery, B., Ross, S. A., Latendresse, J. R., Rusyn, I., and Beland, F. A. (2009) Hepatic epigenetic phenotype predetermines individual susceptibility to hepatic steatosis in mice fed a lipogenic methyl-deficient diet. *Journal of hepatology 51*, 176-186.

(19) Harrill, A. H., Watkins, P. B., Su, S., Ross, P. K., Harbourt, D. E., Stylianou, I. M., Boorman, G. A., Russo, M. W., Sackler, R. S., Harris, S. C., Smith, P. C., Tennant, R., Bogue, M., Paigen, K., Harris, C., Contractor, T., Wiltshire, T., Rusyn, I., and Threadgill, D. W. (2009) Mouse population-guided resequencing reveals that variants in CD44 contribute to acetaminophen-induced liver injury in humans. *Genome research 19*, 1507-1515.

(20) Gatti, D., Maki, A., Chesler, E. J., Kirova, R., Kosyk, O., Lu, L., Manly, K. F., Williams, R. W., Perkins, A., Langston, M. A., Threadgill, D. W., and Rusyn, I. (2007) Genome-level analysis of genetic regulation of liver gene expression networks. *Hepatology 46*, 548-557.

(21) Chiu, W. A., Campbell, J. L., Clewell, H. J., Zhou, Y. H., Wright, F. A., Guyton, K. Z., and Rusyn, I. (2014) Physiologically-Based Pharmacokinetic (PBPK) Modeling of Inter-strain Variability in Trichloroethylene Metabolism in the Mouse. *Environ Health Perspect 122*, 456-463.

(22) Aylor, D. L., Valdar, W., Foulds-Mathes, W., Buus, R. J., Verdugo, R. A., Baric, R. S., Ferris, M. T., Frelinger, J. A., Heise, M., Frieman, M. B., Gralinski, L. E., Bell, T. A., Didion, J. D., Hua, K., Nehrenberg, D. L., Powell, C. L., Steigerwalt, J., Xie, Y., Kelada, S. N., Collins, F. S., Yang, I. V., Schwartz, D. A., Branstetter, L. A., Chesler, E. J., Miller, D. R., Spence, J., Liu, E. Y., McMillan, L., Sarkar, A., Wang, J., Wang, W., Zhang, Q., Broman, K. W., Korstanje, R., Durrant, C., Mott, R., Iraqi, F. A., Pomp, D., Threadgill, D., Pardo-Manuel, d. V., and

Churchill, G. A. (2011) Genetic analysis of complex traits in the emerging collaborative cross. *Genome research 21*, 1213-1222.

(23) Phillippi, J., Xie, Y., Miller, D. R., Bell, T. A., Zhang, Z., Lenarcic, A. B., Aylor, D. L., Krovi, S. H., Threadgill, D. W., de Villena, F. P., Wang, W., Valdar, W., and Frelinger, J. A. (2014) Using the emerging Collaborative Cross to probe the immune system. *Genes Immun 15*, 38-46.

(24) French, J. E., Gatti, D. M., Morgan, D. L., Kissling, G. E., Shockley, K. R., Knudsen, G. A., Shepard, K. G., Price, H. C., King, D., Witt, K. L., Pedersen, L. C., Munger, S. C., Svenson, K. L., and Churchill, G. A. (2015) Diversity Outbred Mice Identify Population-Based Exposure Thresholds and Genetic Factors that Influence Benzene-Induced Genotoxicity. *Environ Health Perspect 123*, 237-245.

(25) Harrill, A. H., Desmet, K. D., Wolf, K. K., Bridges, A. S., Eaddy, J. S., Kurtz, C. L., Hall, J. E., Paine, M. F., Tidwell, R. R., and Watkins, P. B. (2012) A mouse diversity panel approach reveals the potential for clinical kidney injury due to DB289 not predicted by classical rodent models. *Toxicol Sci 130*, 416-426.

(26) Keane, T. M., Wong, K., Adams, D. J., Flint, J., Reymond, A., and Yalcin, B. (2014) Identification of structural variation in mouse genomes. *Front Genet 5*, 192.

(27) Watkins-Chow, D. E., and Pavan, W. J. (2008) Genomic copy number and expression variation within the C57BL/6J inbred mouse strain. *Genome research 18*, 60-66.

(28) Mahajan, V. S., Demissie, E., Mattoo, H., Viswanadham, V., Varki, A., Morris, R., and Pillai, S. (2016) Striking Immune Phenotypes in Gene-Targeted Mice Are Driven by a Copy-Number Variant Originating from a Commercially Available C57BL/6 Strain. *Cell Rep 15*, 1901-1909.

(29) Cardon, L. R., and Harris, T. (2016) Precision medicine, genomics and drug discovery. *Hum Mol Genet 25*, R166-R172.

(30) Hanahan, D., and Weinberg, R. A. (2011) Hallmarks of cancer: the next generation. *Cell 144*, 646-674.

(31) Smith, M. T., Guyton, K. Z., Gibbons, C. F., Fritz, J. M., Portier, C. J., Rusyn, I., DeMarini, D. M., Caldwell, J. C., Kavlock, R. J., Lambert, P. F., Hecht, S. S., Bucher, J. R., Stewart, B. W., Baan, R. A., Cogliano, V. J., and Straif, K. (2016) Key Characteristics of Carcinogens as a Basis for Organizing Data on Mechanisms of Carcinogenesis. *Environ Health Perspect 124*, 713-721.

(32) Marlowe, J., Teo, S. S., Chibout, S. D., Pognan, F., and Moggs, J. (2009) Mapping the epigenome--impact for toxicology. *EXS 99*, 259-288.

(33) Pogribny, I. P., and Rusyn, I. (2013) Environmental toxicants, epigenetics, and cancer. *Advances in experimental medicine and biology 754*, 215-232.

(34) LeBaron, M. J., Rasoulpour, R. J., Klapacz, J., Ellis-Hutchings, R. G., Hollnagel, H. M., and Gollapudi, B. B. (2010) Epigenetics and chemical safety assessment. *Mutation research 705*, 83-95.

(35) Dolinoy, D. C. (2008) The agouti mouse model: an epigenetic biosensor for nutritional and environmental alterations on the fetal epigenome. *Nutr Rev 66 Suppl 1*, S7-11.

(36) Dolinoy, D. C., Huang, D., and Jirtle, R. L. (2007) Maternal nutrient supplementation counteracts bisphenol A-induced DNA hypomethylation in early development. *Proc Natl Acad Sci U S A 104*, 13056-13061.

(37) Dolinoy, D. C., Weinhouse, C., Jones, T. R., Rozek, L. S., and Jirtle, R. L. (2010) Variable histone modifications at the A(vy) metastable epiallele. *Epigenetics 5*, 637-644.

(38) Arita, A., and Costa, M. (2009) Epigenetics in metal carcinogenesis: nickel, arsenic, chromium and cadmium. *Metallomics 1*, 222-228.

(39) Brocato, J., and Costa, M. (2013) Basic mechanics of DNA methylation and the unique landscape of the DNA methylome in metal-induced carcinogenesis. *Crit Rev Toxicol 43*, 493-514.

(40) Brocato, J., and Costa, M. (2015) 10th NTES Conference: Nickel and Arsenic Compounds Alter the Epigenome of Peripheral Blood Mononuclear Cells. *J Trace Elem Med Biol 31*, 209-213.

(41) Zhou, X., Li, Q., Arita, A., Sun, H., and Costa, M. (2009) Effects of nickel, chromate, and arsenite on histone 3 lysine methylation. *Toxicol Appl Pharmacol 236*, 78-84.

(42) Chervona, Y., Hall, M. N., Arita, A., Wu, F., Sun, H., Tseng, H. C., Ali, E., Uddin, M. N., Liu, X., Zoroddu, M. A., Gamble, M. V., and Costa, M. (2012)

Associations between arsenic exposure and global posttranslational histone modifications among adults in Bangladesh. *Cancer Epidemiol Biomarkers Prev 21*, 2252-2260.

(43) Wang, Q., Trevino, L. S., Wong, R. L., Medvedovic, M., Chen, J., Ho, S. M., Shen, J., Foulds, C. E., Coarfa, C., O'Malley, B. W., Shilatifard, A., and Walker, C. L. (2016) Reprogramming of the Epigenome by MLL1 Links Early-Life Environmental Exposures to Prostate Cancer Risk. *Mol Endocrinol 30*, 856-871.

(44) Wong, R. L., Wang, Q., Trevino, L. S., Bosland, M. C., Chen, J., Medvedovic, M., Prins, G. S., Kannan, K., Ho, S. M., and Walker, C. L. (2015) Identification of secretaglobin Scgb2a1 as a target for developmental reprogramming by BPA in the rat prostate. *Epigenetics 10*, 127-134.

(45) Khobta, A., and Epe, B. (2012) Interactions between DNA damage, repair, and transcription. *Mutation research 736*, 5-14.

(46) Pogribny, I. P., and Rusyn, I. (2014) Role of epigenetic aberrations in the development and progression of human hepatocellular carcinoma. *Cancer letters 342*, 223-230.

(47) Zhu, Q., and Wani, A. A. (2010) Histone modifications: crucial elements for damage response and chromatin restoration. *Journal of cellular physiology 223*, 283-288.

(48) Shanbhag, N. M., Rafalska-Metcalf, I. U., Balane-Bolivar, C., Janicki, S. M., and Greenberg, R. A. (2010) ATM-dependent chromatin changes silence transcription in cis to DNA double-strand breaks. *Cell 141*, 970-981.

(49) Schuster-Bockler, B., and Lehner, B. (2012) Chromatin organization is a major influence on regional mutation rates in human cancer cells. *Nature 488*, 504-507.

(50) Chappell, G., Pogribny, I. P., Guyton, K. Z., and Rusyn, I. (2016) Epigenetic alterations induced by genotoxic occupational and environmental human chemical carcinogens: A systematic literature review. *Mutat Res Rev Mutat Res 768*, 27-45.

(51) Varley, K. E., Gertz, J., Bowling, K. M., Parker, S. L., Reddy, T. E., Pauli-Behn, F., Cross, M. K., Williams, B. A., Stamatoyannopoulos, J. A., Crawford, G. E., Absher, D. M., Wold, B. J., and Myers, R. M. (2013) Dynamic DNA methylation across diverse human cell lines and tissues. *Genome research 23*, 555-567.

(52) Bonder, M. J., Luijk, R., Zhernakova, D. V., Moed, M., Deelen, P., Vermaat, M., van Iterson, M., van Dijk, F., van Galen, M., Bot, J., Slieker, R. C., Jhamai, P. M., Verbiest, M., Suchiman, H. E., Verkerk, M., van der Breggen, R., van Rooij, J., Lakenberg, N., Arindrarto, W., Kielbasa, S. M., Jonkers, I., van 't Hof, P., Nooren, I., Beekman, M., Deelen, J., van Heemst, D., Zhernakova, A., Tigchelaar, E. F., Swertz, M. A., Hofman, A., Uitterlinden, A. G., Pool, R., van Dongen, J., Hottenga, J. J., Stehouwer, C. D., van der Kallen, C. J., Schalkwijk, C. G., van den Berg, L. H., van Zwet, E. W., Mei, H., Li, Y., Lemire, M., Hudson, T. J., Consortium, B., Slagboom, P. E., Wijmenga, C., Veldink, J. H., van Greevenbroek, M. M., van Duijn, C. M., Boomsma, D. I., Isaacs, A., Jansen, R., van Meurs, J. B., t Hoen, P. A., Franke, L., and Heijmans, B. T. (2017)

Disease variants alter transcription factor levels and methylation of their binding sites. *Nature genetics 49*, 131-138.

(53) Bollati, V., Baccarelli, A., Hou, L., Bonzini, M., Fustinoni, S., Cavallo, D., Byun, H. M., Jiang, J., Marinelli, B., Pesatori, A. C., Bertazzi, P. A., and Yang, A. S. (2007) Changes in DNA methylation patterns in subjects exposed to low-dose benzene. *Cancer research 67*, 876-880.

(54) Baccarelli, A., Wright, R. O., Bollati, V., Tarantini, L., Litonjua, A. A., Suh, H. H., Zanobetti, A., Sparrow, D., Vokonas, P. S., and Schwartz, J. (2009) Rapid DNA methylation changes after exposure to traffic particles. *Am J Respir Crit Care Med 179*, 572-578.

(55) Reichard, J. F., Schnekenburger, M., and Puga, A. (2007) Long term low-dose arsenic exposure induces loss of DNA methylation. *Biochem Biophys Res Commun 352*, 188-192.

(56) Takiguchi, M., Achanzar, W. E., Qu, W., Li, G., and Waalkes, M. P. (2003) Effects of cadmium on DNA-(Cytosine-5) methyltransferase activity and DNA methylation status during cadmium-induced cellular transformation. *Exp Cell Res 286*, 355-365.

(57) IARC. (2008) IARC monographs on the evaluation of carcinogenic risks to humans. Volume 97. 1,3-butadiene, ethylene oxide and vinyl halides (vinyl fluoride, vinyl chloride and vinyl bromide). *IARC Monogr Eval Carcinog Risks Hum 97*, 3-471.

(58) Koturbash, I., Scherhag, A., Sorrentino, J., Sexton, K., Bodnar, W., Tryndyak, V., Latendresse, J. R., Swenberg, J. A., Beland, F. A., Pogribny, I. P., and Rusyn, I. (2011) Epigenetic alterations in liver of C57BL/6J mice after short-term inhalational exposure to 1,3-butadiene. *Environ Health Perspect 119*, 635-640.

(59) Faulk, C., Barks, A., Liu, K., Goodrich, J. M., and Dolinoy, D. C. (2013) Early-life lead exposure results in dose- and sex-specific effects on weight and epigenetic gene regulation in weanling mice. *Epigenomics 5*, 487-500.

(60) Chiu, W. A., and Rusyn, I. (2018) Advancing chemical risk assessment decision-making with population variability data: challenges and opportunities. *Mammalian genome : official journal of the International Mammalian Genome Society 29*, 182-189.

(61) Harrill, A. H., and McAllister, K. A. (2017) New Rodent Population Models May Inform Human Health Risk Assessment and Identification of Genetic Susceptibility to Environmental Exposures. *Environ Health Perspect 125*, 086002.

(62) Dornbos, P., and LaPres, J. J. (2018) Incorporating population-level genetic variability within laboratory models in toxicology: From the individual to the population. *Toxicology 395*, 1-8.

(63) Churchill, G. A., Airey, D. C., Allayee, H., Angel, J. M., Attie, A. D., Beatty, J., Beavis, W. D., Belknap, J. K., Bennett, B., Berrettini, W., Bleich, A., Bogue, M., Broman, K. W., Buck, K. J., Buckler, E., Burmeister, M., Chesler, E. J., Cheverud, J. M., Clapcote, S., Cook, M. N., Cox, R. D., Crabbe, J. C., Crusio, W.

E., Darvasi, A., Deschepper, C. F., Doerge, R. W., Farber, C. R., Forejt, J., Gaile, D., Garlow, S. J., Geiger, H., Gershenfeld, H., Gordon, T., Gu, J., Gu, W., de Haan, G., Hayes, N. L., Heller, C., Himmelbauer, H., Hitzemann, R., Hunter, K., Hsu, H. C., Iraqi, F. A., Ivandic, B., Jacob, H. J., Jansen, R. C., Jepsen, K. J., Johnson, D. K., Johnson, T. E., Kempermann, G., Kendziorski, C., Kotb, M., Kooy, R. F., Llamas, B., Lammert, F., Lassalle, J. M., Lowenstein, P. R., Lu, L., Lusis, A., Manly, K. F., Marcucio, R., Matthews, D., Medrano, J. F., Miller, D. R., Mittleman, G., Mock, B. A., Mogil, J. S., Montagutelli, X., Morahan, G., Morris, D. G., Mott, R., Nadeau, J. H., Nagase, H., Nowakowski, R. S., O'Hara, B. F., Osadchuk, A. V., Page, G. P., Paigen, B., Paigen, K., Palmer, A. A., Pan, H. J., Peltonen-Palotie, L., Peirce, J., Pomp, D., Pravenec, M., Prows, D. R., Qi, Z., Reeves, R. H., Roder, J., Rosen, G. D., Schadt, E. E., Schalkwyk, L. C., Seltzer, Z., Shimomura, K., Shou, S., Sillanpaa, M. J., Siracusa, L. D., Snoeck, H. W., Spearow, J. L., Svenson, K., Tarantino, L. M., Threadgill, D., Toth, L. A., Valdar, W., de Villena, F. P., Warden, C., Whatley, S., Williams, R. W., Wiltshire, T., Yi, N., Zhang, D., Zhang, M., and Zou, F. (2004) The Collaborative Cross, a community resource for the genetic analysis of complex traits. *Nat Genet 36*, 1133-1137.

(64) Bogue, M. A., Churchill, G. A., and Chesler, E. J. (2015) Collaborative Cross and Diversity Outbred data resources in the Mouse Phenome Database. *Mammalian genome : official journal of the International Mammalian Genome Society 26*, 511-520.

(65) Collaborative Cross Consortium. (2012) The genome architecture of the Collaborative Cross mouse genetic reference population. *Genetics 190*, 389-401.

(66) Threadgill, D. W., Miller, D. R., Churchill, G. A., and de Villena, F. P. M. (2011) The Collaborative Cross: A Recombinant Inbred Mouse Population for the Systems Genetic Era. *Ilar J 52*, 24-31.

(67) Zhang, J., Malo, D., Mott, R., Panthier, J. J., Montagutelli, X., and Jaubert, J. (2018) Identification of new loci involved in the host susceptibility to Salmonella Typhimurium in collaborative cross mice. *BMC genomics 19*, 303.

(68) Gralinski, L. E., Ferris, M. T., Aylor, D. L., Whitmore, A. C., Green, R., Frieman, M. B., Deming, D., Menachery, V. D., Miller, D. R., and Buus, R. J. J. P. g. (2015) Genome wide identification of SARS-CoV susceptibility loci using the Collaborative Cross. *11*, e1005504.

(69) Graham, J. B., Swarts, J. L., Mooney, M., Choonoo, G., Jeng, S., Miller, D. R., Ferris, M. T., McWeeney, S., and Lund, J. M. J. C. r. (2017) Extensive homeostatic T cell phenotypic variation within the Collaborative Cross. *21*, 2313-2325.

(70) Collin, R., Balmer, L., Morahan, G., and Lesage, S. (2019) Common Heritable Immunological Variations Revealed in Genetically Diverse Inbred Mouse Strains of the Collaborative Cross. *J Immunol 202*, 777-786.

(71) Venkatratnam, A., Furuya, S., Kosyk, O., Gold, A., Bodnar, W., Konganti, K., Threadgill, D. W., Gillespie, K. M., Aylor, D. L., Wright, F. A., Chiu, W. A., and Rusyn, I. (2017) Collaborative Cross Mouse Population Enables Refinements to

Characterization of the Variability in Toxicokinetics of Trichloroethylene and Provides Genetic Evidence for the Role of PPAR Pathway in Its Oxidative Metabolism. *Toxicol Sci 158*, 48-62.

(72) Mosedale, M., Kim, Y., Brock, W. J., Roth, S. E., Wiltshire, T., Eaddy, J. S., Keele, G. R., Corty, R. W., Xie, Y., Valdar, W., and Watkins, P. B. (2017) Candidate Risk Factors and Mechanisms for Tolvaptan-Induced Liver Injury Are Identified Using a Collaborative Cross Approach. *Toxicol Sci 156*, 438-454.

(73) Hartman, J. H., Miller, G. P., Caro, A. A., Byrum, S. D., Orr, L. M., Mackintosh, S. G., Tackett, A. J., MacMillan-Crow, L. A., Hallberg, L. M., Ameredes, B. T., and Boysen, G. (2017) 1,3-Butadiene-induced mitochondrial dysfunction is correlated with mitochondrial CYP2E1 activity in Collaborative Cross mice. *Toxicology 378*, 114-124.

(74) Venkatratnam, A., House, J. S., Konganti, K., McKenney, C., Threadgill, D. W., Chiu, W. A., Aylor, D. L., Wright, F. A., and Rusyn, I. (2018) Population-based dose-response analysis of liver transcriptional response to trichloroethylene in mouse. *Mammalian genome : official journal of the International Mammalian Genome Society 29*, 168-181.

(75) Luo, Y. S., Furuya, S., Chiu, W., and Rusyn, I. (2018) Characterization of inter-tissue and inter-strain variability of TCE glutathione conjugation metabolites DCVG, DCVC, and NAcDCVC in the mouse. *J Toxicol Environ Health A 81*, 37-52.

(76) Lewis, L., Crawford, G. E., Furey, T. S., and Rusyn, I. (2017) Genetic and epigenetic determinants of inter-individual variability in responses to toxicants. *Curr Opin Toxicol 6*, 50-59.

(77) Israel, J. W., Chappell, G. A., Simon, J. M., Pott, S., Safi, A., Lewis, L., Cotney, P., Boulos, H. S., Bodnar, W., Lieb, J. D., Crawford, G. E., Furey, T. S., and Rusyn, I. (2018) Tissue- and strain-specific effects of a genotoxic carcinogen 1,3-butadiene on chromatin and transcription. *Mammalian genome : official journal of the International Mammalian Genome Society 29*, 153-167.

(78) Chappell, G. A., Israel, J. W., Simon, J. M., Pott, S., Safi, A., Eklund, K., Sexton, K. G., Bodnar, W., Lieb, J. D., Crawford, G. E., Rusyn, I., and Furey, T. S. (2017) Variation in DNA-Damage Responses to an Inhalational Carcinogen (1,3-Butadiene) in Relation to Strain-Specific Differences in Chromatin Accessibility and Gene Transcription Profiles in C57BL/6J and CAST/EiJ Mice. *Environ Health Perspect 125*, 107006.

(79) Chiu, W. A., and Slob, W. (2015) A Unified Probabilistic Framework for Dose-Response Assessment of Human Health Effects. *Environ Health Perspect 123*, 1241-1254.

(80) Kaeppler, S. M. (1997) Quantitative trait locus mapping using sets of near-isogenic lines: relative power comparisons and technical considerations. *Theor Appl Genet 95*, 384-392.

(81) Lewis, L., Chappell, G. A., Kobets, T., O'Brian, B. E., Sangaraju, D., Kosyk, O., Bodnar, W., Tretyakova, N. Y., Pogribny, I. P., and Rusyn, I. (2019) Sex-specific

differences in genotoxic and epigenetic effects of 1,3-butadiene among mouse tissues. *Arch Toxicol*.

(82) National Toxicology Program. (1993) NTP Toxicology and Carcinogenesis Studies of 1,3-Butadiene (CAS No. 106-99-0) in B6C3F1 Mice (Inhalation Studies). *Natl.Toxicol Program Tech.Rep.Ser. 434*, 1-389.

(83) Goggin, M., Swenberg, J. A., Walker, V. E., and Tretyakova, N. (2009) Molecular dosimetry of 1,2,3,4-diepoxybutane-induced DNA-DNA cross-links in B6C3F1 mice and F344 rats exposed to 1,3-butadiene by inhalation. *Cancer research 69*, 2479-2486.

(84) Chappell, G., Kobets, T., O'Brien, B., Tretyakova, N., Sangaraju, D., Kosyk, O., Sexton, K. G., Bodnar, W., Pogribny, I. P., and Rusyn, I. (2014) Epigenetic events determine tissue-specific toxicity of inhalational exposure to the genotoxic chemical 1,3-butadiene in male C57BL/6J mice. *Toxicol Sci 142*, 375-384.

(85) U.S. EPA. (2011) Toxicological Review of Trichloroethylene (CAS No. 79-01-6): In Support of Summary Information on the Integrated Risk Information System (IRIS).

(86) U.S. EPA. (2011) Toxicological Review of Dichloromethane (Methylene Chloride) (CAS No. 75-09-2): In Support of Summary Information on the Integrated Risk Information System (IRIS).

(87) Konganti, K., Ehrlich, A., Rusyn, I., and Threadgill, D. W. (2018) gQTL: A Web Application for QTL Analysis Using the Collaborative Cross Mouse Genetic Reference Population. *G3 (Bethesda) 8*, 2559-2562.

(88) Swenberg, J. A., Bordeerat, N. K., Boysen, G., Carro, S., Georgieva, N. I., Nakamura, J., Troutman, J. M., Upton, P. B., Albertini, R. J., Vacek, P. M., Walker, V. E., Sram, R. J., Goggin, M., and Tretyakova, N. (2011) 1,3-Butadiene: Biomarkers and application to risk assessment. *Chem Biol Interact. 24*, 809-817.

(89) Tretyakova, N. Y., Lin, Y. P., Upton, P. B., Sangaiah, R., and Swenberg, J. A. (1996) Macromolecular adducts of butadiene. *Toxicology 113*, 70-76.

(90) Bae, J. M., Shin, S. H., Kwon, H. J., Park, S. Y., Kook, M. C., Kim, Y. W., Cho, N. Y., Kim, N., Kim, T. Y., Kim, D., and Kang, G. H. (2012) ALU and LINE-1 hypomethylations in multistep gastric carcinogenesis and their prognostic implications. *International journal of cancer. Journal international du cancer 131*, 1323-1331.

(91) Baccarelli, A., and Bollati, V. (2009) Epigenetics and environmental chemicals. *Curr Opin Pediatr 21*, 243-251.

(92) Thomson, J. P., Moggs, J. G., Wolf, C. R., and Meehan, R. R. (2014) Epigenetic profiles as defined signatures of xenobiotic exposure. *Mutation research 764-765*, 3-9.

(93) Dillon, N. (2004) Heterochromatin structure and function. *Biol Cell 96*, 631-637.

(94) Martin, C., and Zhang, Y. (2005) The diverse functions of histone lysine methylation. *Nat Rev Mol Cell Biol 6*, 838-849.

(95) Melnick, R. L., and Huff, J. (1992) 1,3-butadiene: Toxicity and carcinogenicity in laboratory animals and in humans. *Reviews in Environmental Contamination & Toxicology 124*, 111-144.

(96) Boldry, E. J., Patel, Y. M., Kotapati, S., Esades, A., Park, S. L., Tiirikainen, M., Stram, D. O., Le Marchand, L., and Tretyakova, N. (2017) Genetic Determinants of 1,3-Butadiene Metabolism and Detoxification in Three Populations of Smokers with Different Risks of Lung Cancer. *Cancer epidemiology, biomarkers & prevention : a publication of the American Association for Cancer Research, cosponsored by the American Society of Preventive Oncology 26*, 1034-1042.

(97) Sram, R. J., Rossner, P., Peltonen, K., Podrazilova, K., Mrackova, G., Demopoulos, N. A., Stephanou, G., Vlachodimitropoulos, D., Darroudi, F., and Tates, A. D. (1998) Chromosomal aberrations, sister-chromatid exchanges, cells with high frequency of SCE, micronuclei and comet assay parameters in 1, 3-butadiene-exposed workers. *Mutation research 419*, 145-154.

(98) Koturbash, I., Beland, F. A., and Pogribny, I. P. (2011) Role of epigenetic events in chemical carcinogenesis--a justification for incorporating epigenetic evaluations in cancer risk assessment. *Toxicology mechanisms and methods 21*, 289-297.

(99) Melnick, R. L., and Huff, J. E. (1993) 1,3-Butadiene induces cancer in experimental animals at all concentrations from 6.25 to 8000 parts per million. *IARC Sci Publ*, 309-322.

(100) Koc, H., Tretyakova, N. Y., Walker, V. E., Henderson, R. F., and Swenberg, J. A. (1999) Molecular dosimetry of N-7 guanine adduct formation in mice and rats exposed to 1,3-butadiene. *Chemical research in toxicology 12*, 566-574.

(101) Rudin, C. M., and Thompson, C. B. (2001) Transcriptional activation of short interspersed elements by DNA-damaging agents. *Genes Chromosomes Cancer 30*, 64-71.

(102) Richardson, S. R., Doucet, A. J., Kopera, H. C., Moldovan, J. B., Garcia-Perez, J. L., and Moran, J. V. (2015) The Influence of LINE-1 and SINE Retrotransposons on Mammalian Genomes. *Microbiol Spectr 3*, MDNA3-0061-2014.

(103) Carnell, A. N., and Goodman, J. I. (2003) The long (LINEs) and the short (SINEs) of it: altered methylation as a precursor to toxicity. *Toxicol Sci 75*, 229-235.

(104) Klutstein, M., Moss, J., Kaplan, T., and Cedar, H. (2017) Contribution of epigenetic mechanisms to variation in cancer risk among tissues. *Proc Natl Acad Sci U S A 114*, 2230-2234.

(105) Jenuwein, T. (2006) The epigenetic magic of histone lysine methylation. *FEBS J 273*, 3121-3135.

(106) Zhao, Q. Y., Lei, P. J., Zhang, X., Zheng, J. Y., Wang, H. Y., Zhao, J., Li, Y. M., Ye, M., Li, L., Wei, G., and Wu, M. (2016) Global histone modification profiling reveals the epigenomic dynamics during malignant transformation in a four-stage breast cancer model. *Clin Epigenetics 8*, 34.

(107) He, Y., Zhao, Y., Wang, L., Bohrer, L. R., Pan, Y., Wang, L., and Huang, H. (2018) LSD1 promotes S-phase entry and tumorigenesis via chromatin co-occupation with E2F1 and selective H3K9 demethylation. *Oncogene 37*, 534-543.

(108) Wang, G. G., Song, J., Wang, Z., Dormann, H. L., Casadio, F., Li, H., Luo, J. L., Patel, D. J., and Allis, C. D. (2009) Haematopoietic malignancies caused by dysregulation of a chromatin-binding PHD finger. *Nature 459*, 847-851.

(109) Li, L., Greer, C., Eisenman, R. N., and Secombe, J. (2010) Essential functions of the histone demethylase lid. *PLoS Genet 6*, e1001221.

(110) Iwase, S., Lan, F., Bayliss, P., de la Torre-Ubieta, L., Huarte, M., Qi, H. H., Whetstine, J. R., Bonni, A., Roberts, T. M., and Shi, Y. (2007) The X-linked mental retardation gene SMCX/JARID1C defines a family of histone H3 lysine 4 demethylases. *Cell 128*, 1077-1088.

(111) Shahbazian, M. D., and Grunstein, M. (2007) Functions of site-specific histone acetylation and deacetylation. *Annu Rev Biochem 76*, 75-100.

(112) Fraga, M. F., Ballestar, E., Villar-Garea, A., Boix-Chornet, M., Espada, J., Schotta, G., Bonaldi, T., Haydon, C., Ropero, S., Petrie, K., Iyer, N. G., Perez-Rosado, A., Calvo, E., Lopez, J. A., Cano, A., Calasanz, M. J., Colomer, D., Piris, M. A., Ahn, N., Imhof, A., Caldas, C., Jenuwein, T., and Esteller, M. (2005) Loss of acetylation at Lys16 and trimethylation at Lys20 of histone H4 is a common hallmark of human cancer. *Nature Genetics 37*, 391-400.

(113) Nasrin, N., Kaushik, V. K., Fortier, E., Wall, D., Pearson, K. J., de Cabo, R., and Bordone, L. (2009) JNK1 phosphorylates SIRT1 and promotes its enzymatic activity. *PloS one 4*, e8414.

(114) Greeson, N. T., Sengupta, R., Arida, A. R., Jenuwein, T., and Sanders, S. L. (2008) Di-methyl H4 lysine 20 targets the checkpoint protein Crb2 to sites of DNA damage. *J Biol Chem 283*, 33168-33174.

(115) Sanders, S. L., Portoso, M., Mata, J., Bahler, J., Allshire, R. C., and Kouzarides, T. (2004) Methylation of histone H4 lysine 20 controls recruitment of Crb2 to sites of DNA damage. *Cell 119*, 603-614.

(116) O'Regan, L., Blot, J., and Fry, A. M. (2007) Mitotic regulation by NIMA-related kinases. *Cell Div 2*, 25.

(117) Hashimoto, Y., Akita, H., Hibino, M., Kohri, K., and Nakanishi, M. (2002) Identification and characterization of Nek6 protein kinase, a potential human homolog of NIMA histone H3 kinase. *Biochemical and biophysical research communications 293*, 753-758.

(118) Rusyn, I., and Pogribny, I. P. (2017) Editorial overview of the special issue on genomic toxicology epigenetics. *Curr Opin Toxicol 6*, i-iii.

(119) Rusyn, I., Kleeberger, S. R., McAllister, K. A., French, J. E., and Svenson, K. L. (2018) Introduction to mammalian genome special issue: the combined role of genetics and environment relevant to human disease outcomes. *Mammalian genome : official journal of the International Mammalian Genome Society 29*, 1-4.

(120) Kundakovic, M., Gudsnuk, K., Franks, B., Madrid, J., Miller, R. L., Perera, F. P., and Champagne, F. A. (2013) Sex-specific epigenetic disruption and behavioral changes following low-dose in utero bisphenol A exposure. *Proc Natl Acad Sci U S A 110*, 9956-9961.

(121) Kippler, M., Engstrom, K., Mlakar, S. J., Bottai, M., Ahmed, S., Hossain, M. B., Raqib, R., Vahter, M., and Broberg, K. (2013) Sex-specific effects of early life cadmium exposure on DNA methylation and implications for birth weight. *Epigenetics 8*, 494-503.

(122) Clayton, J. A., and Collins, F. S. (2014) Policy: NIH to balance sex in cell and animal studies. *Nature 509*, 282-283.

(123) IARC. (2009) *1,3-Butadiene, ethylene oxide and vinyl halides (vinyl fluoride and vinyl bromide)*. WHO, Lyon, France.

(124) Cogliano, V. J., Baan, R., Straif, K., Grosse, Y., Lauby-Secretan, B., El Ghissassi, F., Bouvard, V., Benbrahim-Tallaa, L., Guha, N., Freeman, C., Galichet, L., and Wild, C. P. (2011) Preventable exposures associated with human cancers. *J Natl Cancer Inst 103*, 1827-1839.

(125) Melnick, R. L., Huff, J., and Matanoski, G. M. (1992) Carcinogenicity of 1,3-butadiene. *Lancet 340*, 724-725.

(126) Goggin, M., Swenberg, J. A., Walker, V. E., and Tretyakova, N. (2009) Molecular dosimetry of 1,2,3,4-diepoxybutane-induced DNA-DNA cross-links in B6C3F1 mice and F344 rats exposed to 1,3-butadiene by inhalation. *Cancer Res 69*, 2479-2486.

(127) Meng, Q., Walker, D. M., McDonald, J. D., Henderson, R. F., Carter, M. M., Cook, D. L., Jr., McCash, C. L., Torres, S. M., Bauer, M. J., Seilkop, S. K., Upton, P. B., Georgieva, N. I., Boysen, G., Swenberg, J. A., and Walker, V. E. (2007) Age-, gender-, and species-dependent mutagenicity in T cells of mice and rats exposed by inhalation to 1,3-butadiene. *Chem Biol Interact 166*, 121-131.

(128) Vacek, P. M., Albertini, R. J., Sram, R. J., Upton, P., and Swenberg, J. A. (2010) Hemoglobin adducts in 1,3-butadiene exposed Czech workers: female-male comparisons. *Chem Biol Interact 188*, 668-676.

(129) Owen, P. E., Glaister, J. R., Gaunt, I. F., and Pullinger, D. H. (1987) Inhalation toxicity studies with 1,3-butadiene. 3. Two year toxicity/carcinogenicity study in rats. *Am Ind Hyg Assoc J 48*, 407-413.

(130) Sangaraju, D., Goggin, M., Walker, V., Swenberg, J., and Tretyakova, N. (2012) NanoHPLC-nanoESI(+)-MS/MS quantitation of bis-N7-guanine DNA-DNA cross-links in tissues of B6C3F1 mice exposed to subppm levels of 1,3-butadiene. *Anal Chem 84*, 1732-1739.

(131) Martens, J. H., O'Sullivan, R. J., Braunschweig, U., Opravil, S., Radolf, M., Steinlein, P., and Jenuwein, T. (2005) The profile of repeat-associated histone lysine methylation states in the mouse epigenome. *EMBO J 24*, 800-812.

(132) Pogribny, I. P., Ross, S. A., Tryndyak, V. P., Pogribna, M., Poirier, L. A., and Karpinets, T. V. (2006) Histone H3 lysine 9 and H4 lysine 20 trimethylation and the expression of Suv4-20h2 and Suv-39h1 histone methyltransferases in

hepatocarcinogenesis induced by methyl deficiency in rats. *Carcinogenesis 27*, 1180-1186.

(133) Robertson, K. D. (2005) DNA methylation and human disease. *Nat Rev Genet 6*, 597-610.

(134) Yoder, J. A., Walsh, C. P., and Bestor, T. H. (1997) Cytosine methylation and the ecology of intragenomic parasites. *Trends in Genetics 13*, 335-340.

(135) Thomson, J. P., Moggs, J. G., Wolf, C. R., and Meehan, R. R. (2014) Epigenetic profiles as defined signatures of xenobiotic exposure. *Mutat Res Genet Toxicol Environ Mutagen 764-765*, 3-9.

(136) Swenberg, J. A., Ham, A. J., Koc, H., Morinello, E., Ranasinghe, A., Tretyakova, N., Upton, P. B., and Wu, K. Y. (2000) DNA adducts: effects of low exposure to ethylene oxide, vinyl chloride and butadiene. *Mutation research 464*, 77-86.

(137) Rusyn, I., Asakura, S., Pachkowski, B., Bradford, B. U., Denissenko, M. F., Peters, J. M., Holland, S. M., Reddy, J. K., Cunningham, M. L., and Swenberg, J. A. (2004) Expression of base excision DNA repair genes is a sensitive biomarker for in vivo detection of chemical-induced chronic oxidative stress: identification of the molecular source of radicals responsible for DNA damage by peroxisome proliferators. *Cancer research 64*, 1050-1057.

(138) Arif, J. M., Dresler, C., Clapper, M. L., Gairola, C. G., Srinivasan, C., Lubet, R. A., and Gupta, R. C. (2006) Lung DNA adducts detected in human smokers are unrelated to typical polyaromatic carcinogens. *Chemical research in toxicology 19*, 295-299.

(139) Tubbs, J. L., Pegg, A. E., and Tainer, J. A. (2007) DNA binding, nucleotide flipping, and the helix-turn-helix motif in base repair by O6-alkylguanine-DNA alkyltransferase and its implications for cancer chemotherapy. *DNA repair 6*, 1100-1115.

(140) Kovalchuk, O., Burke, P., Besplug, J., Slovack, M., Filkowski, J., and Pogribny, I. (2004) Methylation changes in muscle and liver tissues of male and female mice exposed to acute and chronic low-dose X-ray-irradiation. *Mutat Res 548*, 75-84.

(141) Dumenco, L. L., Allay, E., Norton, K., and Gerson, S. L. (1993) The prevention of thymic lymphomas in transgenic mice by human O6-alkylguanine-DNA alkyltransferase. *Science 259*, 219-222.

(142) Hossain, K., Suzuki, T., Hasibuzzaman, M. M., Islam, M. S., Rahman, A., Paul, S. K., Tanu, T., Hossain, S., Saud, Z. A., Rahman, M., Nikkon, F., Miyataka, H., Himeno, S., and Nohara, K. (2017) Chronic exposure to arsenic, LINE-1 hypomethylation, and blood pressure: a cross-sectional study in Bangladesh. *Environ Health-Glob 16*.

(143) Pogribny, I., Raiche, J., Slovack, M., and Kovalchuk, O. (2004) Dose-dependence, sex- and tissue-specificity, and persistence of radiation-induced genomic DNA methylation changes. *Biochem Bioph Res Co 320*, 1253-1261.

(144) Zuo, J., Brewer, D. S., Arlt, V. M., Cooper, C. S., and Phillips, D. H. (2014) Benzo pyrene-induced DNA adducts and gene expression profiles in target and non-target organs for carcinogenesis in mice. *BMC genomics 15*, 880.

(145) Tryndyak, V., Kindrat, I., Dreval, K., Churchwell, M. I., Beland, F. A., and Pogribny, I. P. (2018) Effect of aflatoxin B1, benzo[a]pyrene, and methapyrilene on transcriptomic and epigenetic alterations in human liver HepaRG cells. *Food Chem Toxicol 121*, 214-223.

(146) Pogribny, I. P., and Beland, F. A. (2009) DNA hypomethylation in the origin and pathogenesis of human diseases. *Cellular and molecular life sciences : CMLS 66*, 2249-2261.

(147) Primavera, A., Fustinoni, S., Biroccio, A., Ballerini, S., Urbani, A., Bernardini, S., Federici, G., Capucci, E., Manno, M., and Lo Bello, M. (2008) Glutathione transferases and glutathionylated hemoglobin in workers exposed to low doses of 1,3-butadiene. *Cancer epidemiology, biomarkers & prevention : a publication of the American Association for Cancer Research, cosponsored by the American Society of Preventive Oncology 17*, 3004-3012.

(148) Zhang, X., Hou, H., Chen, H., Liu, Y., Wang, A., and Hu, Q. (2015) A column-switching LC-MS/MS method for simultaneous quantification of biomarkers for 1,3-butadiene exposure and oxidative damage in human urine. *J Chromatogr B Analyt Technol Biomed Life Sci 1002*, 123-129.

(149) Valinluck, V., Tsai, H. H., Rogstad, D. K., Burdzy, A., Bird, A., and Sowers, L. C. (2004) Oxidative damage to methyl-CpG sequences inhibits the binding of the methyl-CpG binding domain (MBD) of methyl-CpG binding protein 2 (MeCP2). *Nucleic Acids Res 32*, 4100-4108.

(150) Baylin, S. B., and Herman, J. G. (2000) DNA hypermethylation in tumorigenesis: epigenetics joins genetics. *Trends in Genetics 16*, 168-174.

(151) Patchsung, M., Settayanon, S., Pongpanich, M., Mutirangura, D., Jintarith, P., and Mutirangura, A. (2018) Alu siRNA to increase Alu element methylation and prevent DNA damage. *Epigenomics 10*, 175-185.

(152) Liu, E. Y., Russ, J., Wu, K., Neal, D., Suh, E., McNally, A. G., Irwin, D. J., Van Deerlin, V. M., and Lee, E. B. (2014) C9orf72 hypermethylation protects against repeat expansion-associated pathology in ALS/FTD. *Acta Neuropathol 128*, 525-541.

(153) Hwang, H. W., and Mendell, J. T. (2006) MicroRNAs in cell proliferation, cell death, and tumorigenesis. *Br J Cancer 94*, 776-780.

(154) Cheng, A. M., Byrom, M. W., Shelton, J., and Ford, L. P. (2005) Antisense inhibition of human miRNAs and indications for an involvement of miRNA in cell growth and apoptosis. *Nucleic Acids Res 33*, 1290-1297.

(155) Alvarez-Garcia, I., and Miska, E. A. (2005) MicroRNA functions in animal development and human disease. *Development 132*, 4653-4662.

(156) Izzotti, A., and Pulliero, A. (2014) The effects of environmental chemical carcinogens on the microRNA machinery. *Int J Hyg Environ Health 217*, 601-627.

(157) Rager, J. E., Smeester, L., Jaspers, I., Sexton, K. G., and Fry, R. C. (2011) Epigenetic changes induced by air toxics: formaldehyde exposure alters miRNA expression profiles in human lung cells. *Environ Health Perspect 119*, 494-500.

(158) Hou, L., Wang, D., and Baccarelli, A. (2011) Environmental chemicals and microRNAs. *Mutation research 714*, 105-112.

(159) Harrill, A. H., McCullough, S. D., Wood, C. E., Kahle, J. J., and Chorley, B. N. (2016) MicroRNA Biomarkers of Toxicity in Biological Matrices. *Toxicol Sci 152*, 264-272.

(160) Lewis, L., Borowa-Mazgaj, B., de Conti, A., Chappell, G. A., Luo, Y. S., Bodnar, W., Konganti, K., Wright, F. A., Threadgill, D. W., Chiu, W. A., Pogribny, I. P., and Rusyn, I. (2019) Population-Based Analysis of DNA Damage and Epigenetic Effects of 1,3-Butadiene in the Mouse. *Chemical research in toxicology 32*, 887-898.

(161) Kanke, M., Baran-Gale, J., Villanueva, J., and Sethupathy, P. (2016) miRquant 2.0: an Expanded Tool for Accurate Annotation and Quantification of MicroRNAs and their isomiRs from Small RNA-Sequencing Data. *J Integr Bioinform 13*, 307.

(162) Love, M. I., Huber, W., and Anders, S. (2014) Moderated estimation of fold change and dispersion for RNA-seq data with DESeq2. *Genome Biol 15*, 550.

(163) Vlachos, I. S., Zagganas, K., Paraskevopoulou, M. D., Georgakilas, G., Karagkouni, D., Vergoulis, T., Dalamagas, T., and Hatzigeorgiou, A. G. (2015) DIANA-miRPath v3.0: deciphering microRNA function with experimental support. *Nucleic Acids Res 43*, W460-466.

(164) Baran-Gale, J., Fannin, E. E., Kurtz, C. L., and Sethupathy, P. (2013) Beta cell 5'-shifted isomiRs are candidate regulatory hubs in type 2 diabetes. *PloS one 8*, e73240.

(165) Pogribny, I. P., Starlard-Davenport, A., Tryndyak, V. P., Han, T., Ross, S. A., Rusyn, I., and Beland, F. A. (2010) Difference in expression of hepatic microRNAs miR-29c, miR-34a, miR-155, and miR-200b is associated with strain-specific susceptibility to dietary nonalcoholic steatohepatitis in mice. *Laboratory investigation; a journal of technical methods and pathology 90*, 1437-1446.

(166) Rutledge, H., Baran-Gale, J., de Villena, F. P., Chesler, E. J., Churchill, G. A., Sethupathy, P., and Kelada, S. N. (2015) Identification of microRNAs associated with allergic airway disease using a genetically diverse mouse population. *BMC genomics 16*, 633.

(167) Tryndyak, V. P., Latendresse, J. R., Montgomery, B., Ross, S. A., Beland, F. A., Rusyn, I., and Pogribny, I. P. (2012) Plasma microRNAs are sensitive indicators of inter-strain differences in the severity of liver injury induced in mice by a choline- and folate-deficient diet. *Toxicol Appl Pharmacol 262*, 52-59.

(168) de Conti, A., Kobets, T., Tryndyak, V., Burnett, S. D., Han, T., Fuscoe, J. C., Beland, F. A., Doerge, D. R., and Pogribny, I. P. (2015) Persistence of furan-induced epigenetic aberrations in the livers of F344 rats. *Toxicol Sci 144*, 217-226.

(169) de Conti, A., Tryndyak, V., Doerge, D. R., Beland, F. A., and Pogribny, I. P. (2016) Irreversible down-regulation of miR-375 in the livers of Fischer 344 rats after chronic furan exposure. *Food Chem Toxicol 98*, 2-10.

(170) Rieswijk, L., Claessen, S. M., Bekers, O., van Herwijnen, M., Theunissen, D. H., Jennen, D. G., de Kok, T. M., Kleinjans, J. C., and van Breda, S. G. (2016) Aflatoxin B1 induces persistent epigenomic effects in primary human hepatocytes associated with hepatocellular carcinoma. *Toxicology 350-352*, 31-39.

(171) Chiu, W. A., Wright, F. A., and Rusyn, I. (2017) A tiered, Bayesian approach to estimating of population variability for regulatory decision-making. *ALTEX 34*, 377-388.

(172) Abdo, N., Xia, M., Brown, C. C., Kosyk, O., Huang, R., Sakamuru, S., Zhou, Y. H., Jack, J. R., Gallins, P., Xia, K., Li, Y., Chiu, W. A., Motsinger-Reif, A. A., Austin, C. P., Tice, R. R., Rusyn, I., and Wright, F. A. (2015) Population-based in vitro hazard and concentration-response assessment of chemicals: the 1000 genomes high-throughput screening study. *Environ Health Perspect 123*, 458-466.

(173) Abdo, N., Wetmore, B. A., Chappell, G. A., Shea, D., Wright, F. A., and Rusyn, I. (2015) In vitro screening for population variability in toxicity of pesticide-containing mixtures. *Environ Int 85*, 147-155.

(174) Eduati, F., Mangravite, L. M., Wang, T., Tang, H., Bare, J. C., Huang, R., Norman, T., Kellen, M., Menden, M. P., Yang, J., Zhan, X., Zhong, R., Xiao, G.,

Xia, M., Abdo, N., Kosyk, O., Collaboration, N.-N.-U. D. T., Friend, S., Dearry, A., Simeonov, A., Tice, R. R., Rusyn, I., Wright, F. A., Stolovitzky, G., Xie, Y., and Saez-Rodriguez, J. (2015) Prediction of human population responses to toxic compounds by a collaborative competition. *Nat Biotechnol 33*, 933-940.

(175) Lock, E. F., Abdo, N., Huang, R., Xia, M., Kosyk, O., O'Shea, S. H., Zhou, Y. H., Sedykh, A., Tropsha, A., Austin, C. P., Tice, R. R., Wright, F. A., and Rusyn, I. (2012) Quantitative high-throughput screening for chemical toxicity in a population-based in vitro model. *Toxicol Sci 126*, 578-588.

(176) Grimm, F. A., Blanchette, A., House, J. S., Ferguson, K., Hsieh, N. H., Dalaijamts, C., Wright, A. A., Anson, B., Wright, F. A., Chiu, W. A., and Rusyn, I. (2018) A human population-based organotypic in vitro model for cardiotoxicity screening. *ALTEX*.

(177) Cochrane, J. E., and Skopek, T. R. (1994) Mutagenicity of butadiene and its epoxide metabolites: I. Mutagenic potential of 1,2-epoxybutene, 1,2,3,4-diepoxybutane and 3,4-epoxy-1,2-butanediol in cultured human lymphoblasts. *Carcinogenesis 15*, 713-717.

(178) Ge, J., Prasongtanakij, S., Wood, D. K., Weingeist, D. M., Fessler, J., Navasummrit, P., Ruchirawat, M., and Engelward, B. P. (2014) CometChip: a high-throughput 96-well platform for measuring DNA damage in microarrayed human cells. *J Vis Exp*, e50607.

(179) Yeakley, J. M., Shepard, P. J., Goyena, D. E., VanSteenhouse, H. C., McComb, J. D., and Seligmann, B. E. (2017) A trichostatin A expression signature

identified by TempO-Seq targeted whole transcriptome profiling. *PloS one 12*, e0178302.

(180) Grimm, F. A., Iwata, Y., Sirenko, O., Chappell, G. A., Wright, F. A., Reif, D. M., Braisted, J., Gerhold, D. L., Yeakley, J. M., Shepard, P., Seligmann, B., Roy, T., Boogaard, P. J., Ketelslegers, H. B., Rohde, A. M., and Rusyn, I. (2016) A chemical-biological similarity-based grouping of complex substances as a prototype approach for evaluating chemical alternatives. *Green Chem 18*, 4407-4419.

(181) Mahony, S., and Pugh, B. F. (2015) Protein-DNA binding in high-resolution. *Crit Rev Biochem Mol Biol 50*, 269-283.

APPENDIX A

FIGURES

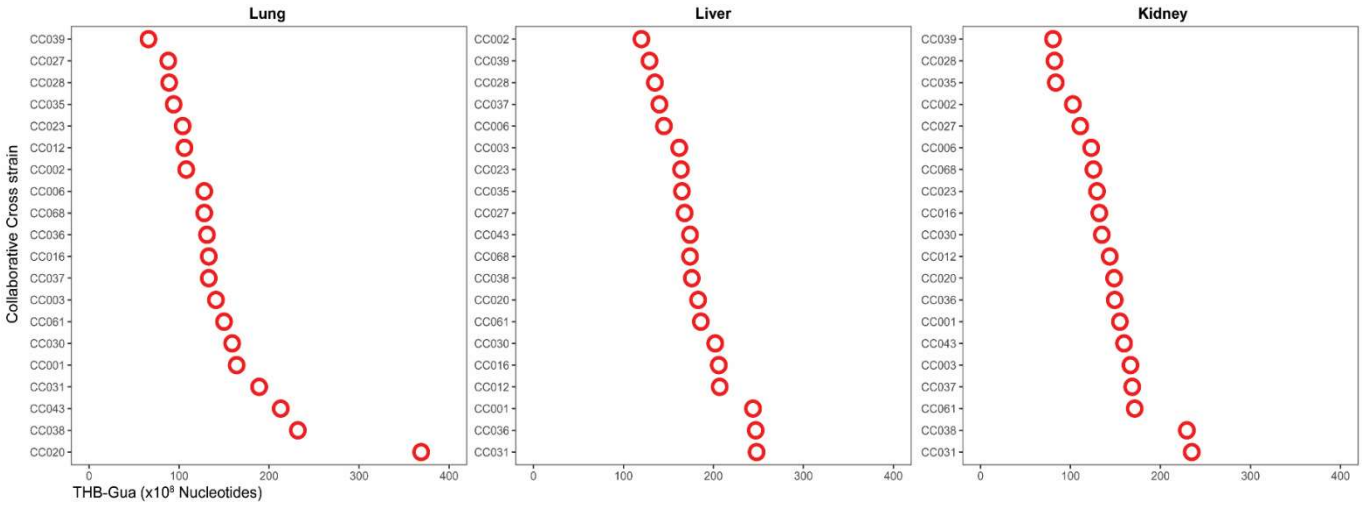

Figure S2.1. Strain variability in genotoxicity of 1,3-butadiene across mouse tissues. Inter-strain differences in levels of THB-Gua adducts in lung, liver, and kidney of mice exposed to 625 ppm of 1,3-butadiene for 2 weeks. Each red circle represents DNA adduct levels for a Collaborative Cross strain.

APPENDIX B

TABLES

Table S2.1. Primers used for methylated DNA immunoprecipitation qPCR analysis.

Gene Name	Primer	Sequence
SINEB1	Forward	$^{5'}$GTGGCGCACGCCTTTAATC$^{3'}$
	Reverse	$^{5'}$GACAGGGTTTCTCTGTGTAG$^{3'}$
LINE1	Forward	$^{5'}$TTTGGGACACAATGAAAGCA$^{3'}$
	Reverse	$^{5'}$CTGCCGTCTACTCCTCTTGG$^{3'}$

Table S2.2. Primary antibodies used for western blotting.

Target modification	Dilution	Catalog Number	Supplier
H3K9me3	1:1000	ab8898	Abcam
H3K27me3	1:1000	ab6002	Abcam
H4K20me3	1:1000	ab9053	Abcam
H3K9ac	1:1000	ab10812	Abcam
H3K27ac	1:1000	ab4729	Abcam
H4K16ac	1:1000	ab109463	Abcam

Table S2.3. Phenotype data used for genome-wide quantitative trait loci (QTL) mapping. Data are expressed as the number of adducts per 10^8 nucleotides (for DNA adduct data) or fold change relative to control (for other data).

Strain	CC001	CC002	CC003	CC006	CC012	CC016	CC020	CC023	CC027	CC028	CC030	CC031	CC035	CC036	CC037	CC038	CC039	CC043	CC061	CC068
Lung DNA adducts	163.95	107.71	141.22	127.57	105.70	133.19	369.28	103.82	87.68	89.48	158.85	188.51	93.67	131.12	133.35	231.88	66.42	212.59	149.67	128.17
Liver DNA adducts	243.65	120.17	162.30	145.48	206.62	206.35	183.20	163.74	167.97	135.24	202.14	247.59	164.99	247.01	139.79	176.21	129.42	173.69	186.48	173.91
Kidney DNA adducts	154.90	102.68	166.66	123.04	143.60	132.03	148.52	129.46	110.89	82.28	134.85	234.75	83.65	149.19	168.62	229.33	80.60	159.56	171.37	125.50
H3K9me3 Lung	1.47	0.72	1.07	0.71	0.80	0.80	0.91	1.20	0.60	1.37	0.88	0.79	0.74	0.89	0.76	0.71	0.68	0.92	0.72	1.51
H3K9me3 Liver	1.17	0.96	1.08	2.11	0.71	0.68	0.85	1.74	0.85	0.91	1.52	1.31	0.89	0.74	1.45	0.77	0.78	0.86	0.75	1.50
H3K9me3 Kidney	1.13	1.02	1.23	1.07	1.23	0.98	1.06	1.33	1.28	1.33	1.10	1.28	0.77	0.62	1.11	1.22	1.23	1.88	1.10	0.90
H3K27me3 Lung	1.31	1.01	1.12	0.51	1.26	1.45	1.10	1.08	0.76	1.52	0.82	0.96	1.09	0.78	0.81	0.75	0.82	1.23	0.71	1.41
H3K27me3 Liver	1.58	1.30	1.06	1.87	0.89	1.34	0.92	1.21	1.04	0.83	0.98	1.40	1.22	0.78	1.35	0.92	1.50	0.66	0.52	1.13
H3K27me3 Kidney	1.36	1.58	1.30	0.85	0.64	2.28	1.64	0.68	1.10	0.67	1.14	0.50	0.73	0.83	1.70	1.58	7.41	0.89	2.06	1.56
H4K20me3 Lung	1.29	1.07	1.17	0.71	1.33	0.87	1.31	0.88	0.52	1.38	0.50	0.83	1.30	0.88	0.91	0.76	1.04	0.99	0.76	1.50
H4K20me3 Liver	1.57	1.57	1.24	1.71	1.21	2.15	0.88	1.20	1.06	1.08	0.98	1.12	1.13	2.11	1.54	0.93	1.28	1.09	0.82	1.43
H4K20me3 Kidney	1.76	1.05	0.62	0.89	1.13	0.71	0.44	1.24	0.73	1.05	0.76	0.83	1.10	0.80	1.00	1.09	1.31	1.34	0.87	1.14
H3K9ac Lung	0.57	0.64	1.17	0.79	1.06	0.83	2.82	1.61	1.58	1.99	1.17	0.58	2.41	0.80	0.69	0.57	0.91	0.91	1.17	0.77
H3K9ac Liver	0.97	0.67	0.87	1.43	1.54	0.89	0.73	1.30	0.76	1.47	0.84	1.24	0.97	0.82	0.76	0.80	0.85	0.92	0.73	0.93
H3K9ac Kidney	1.16	0.93	1.00	0.78	1.13	0.99	0.96	1.05	0.93	1.34	0.95	1.06	1.18	1.21	0.94	1.28	1.09	1.11	1.10	0.81
H3K27ac Lung	1.06	1.00	1.09	0.47	1.15	0.50	0.88	1.27	0.44	1.70	0.60	0.68	1.04	0.69	0.62	0.61	0.62	0.92	0.75	2.16
H3K27ac Liver	1.13	0.76	0.74	1.74	1.42	1.36	0.73	1.57	0.90	1.27	1.21	1.72	1.44	0.87	0.78	0.76	0.96	0.81	0.58	0.83
H3K27ac Kidney	0.95	0.94	1.05	1.14	1.12	0.97	0.74	1.21	0.90	1.21	0.97	1.06	0.95	0.80	0.89	0.90	0.92	1.33	0.77	1.51
H4K16ac Lung	1.24	0.93	1.19	0.62	2.16	0.82	1.14	1.38	0.61	2.44	0.79	0.88	1.55	0.96	0.69	0.70	0.66	1.56	0.90	1.19
H4K16ac Liver	0.99	0.80	0.74	1.09	1.45	1.70	0.72	1.43	0.71	1.27	0.89	1.20	1.26	0.39	0.51	0.73	0.95	0.76	0.77	0.49
H4K16ac Kidney	2.45	0.90	1.50	0.48	1.01	0.85	1.02	1.69	1.01	1.08	1.35	1.00	1.47	1.37	1.15	1.36	1.56	1.21	1.16	0.96
SINEB1 Lung	1.03	3.93	0.84	0.61	1.02	0.57	1.40	0.52	0.91	0.43			0.90	2.08	1.18	2.47		0.64	0.41	0.95
SINEB1 Liver	0.24	1.81	0.57	1.04	0.43	0.98	0.33	1.63	1.34	1.21			1.01	0.69	0.44	0.61		0.50	0.52	1.17
SINEB1 Kidney	1.77	0.24	0.46	0.39	2.99	1.90	0.45	0.49	3.57	0.41	1.93	0.71	0.23	2.15	7.09		0.84	4.77	0.27	0.48
LINE1 Lung	1.79	0.60	0.64	1.72	3.18	0.64	1.42	0.50	0.80	0.16			0.81	0.81	1.19	12.14		0.48	0.18	0.98
LINE1 Liver	0.49	1.17	1.56	0.94	2.44	0.69	0.58	3.05	1.75	0.52			1.40	0.32	0.31	0.83		0.34	1.43	3.32
LINE1 Kidney	8.74	0.87	0.37	0.39	3.38	7.61	0.65	1.38	3.43	0.75	0.30	0.65	0.54	32.50	0.31		0.15	3.12	1.56	0.57

Table S2.4. P-values for Spearman correlation among phenotypes collected from all tissues.

	DNA adducts Lung	DNA adducts Liver	DNA adducts Kidney	H3K27me3 Kidney	H4K16ac Kidney	H3K9me3 Kidney	H4K20me3 Kidney	H3K9ac Kidney	H3K27ac Kidney	SINEB1 Kidney	LINE1 Kidney	LINE1 Liver	SINEB1 Liver	SINEB1 Lung	LINE1 Lung	H4k20me3 Lung	H3K27me3 Lung	H3K9me3 Lung	H4K16ac Lung	H3K27ac Lung	H3K9ac Lung	H4K20me3 Liver	H3K27me3 Liver	H3K9me3 Liver	H4K16ac Liver	H3K27ac Liver	H3K9ac Liver
DNA adducts Lung	1.00	0.01	0.00	0.38	0.89	0.81	0.33	0.76	0.48	0.56	0.75	0.95	0.00	0.32	0.30	0.43	0.83	0.36	0.92	0.51	0.69	0.26	0.45	0.96	0.24	0.09	0.26
DNA adducts Liver	0.01	1.00	0.01	0.43	0.96	0.54	0.46	0.23	0.67	0.15	0.02	0.95	0.02	0.57	0.14	0.43	0.78	0.32	0.64	0.67	0.36	0.77	0.33	0.17	0.88	0.58	0.64
DNA adducts Kidney	0.00	0.01	1.00	0.74	0.59	0.57	0.42	0.46	0.37	0.18	0.49	0.66	0.00	0.49	0.35	0.26	0.38	0.63	0.82	0.62	0.74	0.34	0.34	0.73	0.21	0.13	0.37
H3K27me3 Kidney	0.38	0.43	0.74	1.00	0.99	0.13	0.57	0.24	0.02	0.97	0.43	0.39	0.32	0.46	0.80	0.67	0.56	0.23	0.03	0.15	0.25	0.80	0.54	0.26	0.13	0.00	0.00
H4K16ac Kidney	0.89	0.96	0.59	0.99	1.00	0.39	0.11	0.01	0.49	0.67	0.79	0.92	0.22	0.99	0.82	0.68	0.97	0.31	0.27	0.25	0.83	0.57	0.68	0.98	0.86	0.66	0.93
H3K9me3 Kidney	0.81	0.54	0.57	0.13	0.39	1.00	0.24	0.35	0.11	0.18	0.81	0.16	0.84	0.17	0.31	0.87	0.63	0.71	0.45	0.54	0.95	0.08	0.48	0.68	0.31	0.58	0.14
H4K20me3 Kidney	0.33	0.46	0.42	0.57	0.11	0.24	1.00	0.13	0.07	0.84	0.81	0.28	0.98	0.94	0.76	0.10	0.30	0.43	0.08	0.04	0.51	0.57	0.58	0.52	0.34	0.35	0.06
H3K9ac Kidney	0.76	0.23	0.46	0.24	0.01	0.35	0.13	1.00	0.85	0.98	0.12	0.21	0.32	0.96	0.84	0.31	0.41	0.46	0.02	0.17	0.15	0.39	0.06	0.03	0.31	0.82	0.27
H3K27ac Kidney	0.48	0.67	0.37	0.02	0.49	0.11	0.07	0.85	1.00	1.00	0.89	0.24	0.24	0.08	0.44	0.22	0.01	0.02	0.03	0.04	0.09	0.43	0.67	0.05	0.04	0.02	0.00
SINEB1 Kidney	0.56	0.15	0.18	0.97	0.67	0.18	0.84	0.98	1.00	1.00	0.28	0.29	0.20	0.46	0.39	0.30	0.93	0.80	0.50	0.18	0.94	0.65	0.67	0.50	0.37	0.99	0.93
LINE1 Kidney	0.75	0.02	0.49	0.43	0.79	0.81	0.81	0.12	0.89	0.28	1.00	0.47	0.69	0.81	0.95	0.87	0.40	0.46	0.24	0.72	0.38	0.50	0.19	0.03	0.69	0.94	0.78
LINE1 Liver	0.95	0.95	0.66	0.39	0.92	0.16	0.28	0.21	0.24	0.29	0.47	1.00	0.52	0.25	0.71	0.52	0.08	0.33	0.11	0.74	0.36	0.81	0.91	0.67	0.01	0.07	0.06
SINEB1 Liver	0.00	0.02	0.00	0.32	0.22	0.84	0.98	0.32	0.24	0.20	0.69	0.52	1.00	0.42	0.07	0.48	0.63	0.47	0.63	0.84	0.22	0.72	0.57	0.25	0.62	0.21	0.83
SINEB1 Lung	0.32	0.57	0.49	0.46	0.99	0.17	0.94	0.96	0.08	0.46	0.81	0.25	0.42	1.00	0.01	0.60	0.51	0.47	0.40	0.57	0.54	0.52	0.63	0.69	0.03	0.18	0.10
LINE1 Lung	0.30	0.14	0.35	0.80	0.82	0.31	0.76	0.84	0.44	0.39	0.95	0.71	0.07	0.01	1.00	0.87	0.56	0.51	0.34	0.38	0.74	0.42	0.18	0.93	0.47	0.61	0.64
H4k20me3 Lung	0.43	0.43	0.26	0.67	0.68	0.87	0.10	0.31	0.22	0.30	0.87	0.52	0.48	0.60	0.87	1.00	0.00	0.01	0.00	0.00	0.00	0.54	0.86	0.83	0.74	0.67	0.20
H3K27me3 Lung	0.83	0.78	0.38	0.56	0.97	0.63	0.30	0.41	0.01	0.93	0.40	0.08	0.63	0.51	0.56	0.00	1.00	0.00	0.00	0.00	0.00	0.42	0.95	0.81	0.11	0.58	0.04
H3K9me3 Lung	0.36	0.32	0.63	0.23	0.31	0.71	0.43	0.46	0.02	0.80	0.46	0.33	0.47	0.47	0.51	0.01	0.00	1.00	0.00	0.00	0.00	0.66	0.41	0.24	0.87	0.94	0.07
H4K16ac Lung	0.92	0.64	0.82	0.03	0.27	0.45	0.08	0.02	0.03	0.50	0.24	0.11	0.63	0.40	0.34	0.00	0.00	0.00	1.00	0.00	0.00	0.78	0.09	0.85	0.19	0.74	0.03
H3K27ac Lung	0.51	0.67	0.62	0.15	0.25	0.54	0.04	0.17	0.04	0.18	0.72	0.74	0.84	0.57	0.38	0.00	0.00	0.00	0.00	1.00	0.00	0.99	0.35	0.56	0.51	0.85	0.08
H3K9ac Lung	0.69	0.36	0.74	0.25	0.83	0.95	0.51	0.15	0.09	0.94	0.38	0.36	0.22	0.54	0.74	0.00	0.00	0.00	0.00	0.00	1.00	0.89	0.07	0.58	0.86	0.80	0.10
H4K20me3 Liver	0.26	0.77	0.34	0.80	0.57	0.08	0.57	0.39	0.43	0.65	0.50	0.81	0.72	0.52	0.42	0.54	0.42	0.66	0.78	0.99	0.89	1.00	0.01	0.66	0.65	0.22	0.35
H3K27me3 Liver	0.45	0.33	0.34	0.54	0.68	0.48	0.58	0.06	0.67	0.67	0.19	0.91	0.57	0.63	0.18	0.86	0.95	0.41	0.09	0.35	0.07	0.01	1.00	0.03	0.24	0.05	0.39
H3K9me3 Liver	0.96	0.17	0.73	0.26	0.98	0.68	0.52	0.03	0.05	0.50	0.03	0.67	0.25	0.69	0.93	0.83	0.81	0.24	0.85	0.56	0.58	0.66	0.03	1.00	1.00	0.21	0.25
H4K16ac Liver	0.24	0.88	0.21	0.13	0.86	0.31	0.34	0.31	0.04	0.37	0.69	0.01	0.62	0.03	0.47	0.74	0.11	0.87	0.19	0.51	0.86	0.65	0.24	1.00	1.00	0.00	0.00
H3K27ac Liver	0.09	0.58	0.13	0.00	0.66	0.58	0.35	0.82	0.02	0.99	0.94	0.07	0.21	0.18	0.61	0.67	0.58	0.94	0.74	0.85	0.80	0.22	0.05	0.21	0.00	1.00	0.00
H3K9ac Liver	0.26	0.64	0.37	0.00	0.93	0.14	0.06	0.27	0.00	0.93	0.78	0.06	0.83	0.10	0.64	0.20	0.04	0.07	0.03	0.08	0.10	0.35	0.39	0.25	0.00	0.00	1.00

Supplemental Table 3.1. Selected primers and their assay numbers from Applied Biosystems.

Gene	Gene Expression Assay Number
Gusb	Mm00446953_m1
Dnmt1	Mm00599763_m1
Dnmt3a	Mm00432881_m1
Dnmt3b	Mm01240113_m1
Suv39h1	Mm00468952_m1
Suv420h2	Mm00525366_m1
Ezh2	Mm00468464_m1
Xrcc1	Mm00494222_m1
Mgmt	Mm00485014_m1
Mpg	Mm00447872_m1